

https://dspace.org/

Validation of the current support design methodology at mine A using keyblock analysis

Nkosi, Glorious Bongiwe Nsiki

2021

https://wiredspace.wits.ac.za/handle/10539/33420

Downloaded from a DSpace repository. https://dspace.org/

School of Mining Engineering



VALIDATION OF THE CURRENT SUPPORT DESIGN METHODOLOGY AT MINE A USING KEYBLOCK ANALYSIS

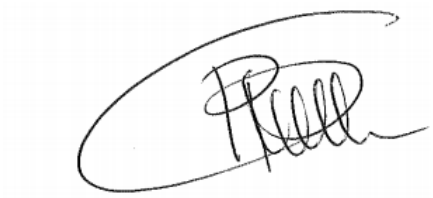
Student Name: Glorious Bongiwe Nsiki Nkosi

A research report submitted to the Faculty of Engineering and the Built Environment, University of the Witwatersrand, Johannesburg, in partial fulfilment of the requirements for the degree of Master of Science in Engineering.

Johannesburg, February 2020

DECLARATION

I declare that this report is my own, unaided work. I have read the University Policy on Plagiarism and hereby confirm that no plagiarism exists in this report. I also confirm that there is no copying nor is there any copyright infringement. I willingly submit to any investigation in this regard by the School of Mining Engineering and I undertake to abide by the decision of any such investigation.



28 February 2020

Signature of Candidate Date

ABSTRACT

Support is crucial for ensuring that Falls Of Ground (FOG) injuries are minimized. FOGs are the leading cause of fatalities and injuries in South African Mines. Not only do FOGs result in loss of life, but they also cause damages, which result in loss of revenue and loss of time (due to additional loading of waste material). Most FOGs are observed within the high risk zone, which is between the first line of support and the face. Most of these FOGs occur during face preparation and drilling activities. The falls at Mine A are mainly bound by geological discontinuities - structures such as joints, faults, pothole structures and sympathetic jointing associated with faults.

Various support design methodologies are being employed within the South African platinum industry. The current support design method used at Mine A is the fall out height method. It involves a statistical back analysis on past FOGs, and provides a thickness of hangingwall that corresponds to the height of 95.0 % of the FOGs. Several limitations of this method were observed during the research investigations. One major limitation is that it does not explicitly consider geological discontinuities, their properties, orientations and exposures with reference to the excavation. It is for this reason that further research on the support design was done at Mine A.

The research, described in this report, investigated the current support design at Mine A, and explored ways to optimize the design. A keyblock analysis method was found to be the most applicable to the shallow depth

environment at the Mine. The keyblock analysis was done using the JBlock modelling program (Esterhuizen, 2003), which is a statistical package that determines possible block sizes that can form as a result of geological discontinuities. The package considers the orientations of structures with respect to the excavations, the number of joint sets, the spacing of the joints within each set and the geomechanical properties of the discontinuities.

Several models were constructed for various support Scenarios and the results allowed the following conclusions to be made:

1. The current support design at Mine A will not reduce injuries occurring in the working areas to tolerable levels;
2. Injuries can be reduced to international standards/norms if 2.5 m long bolts are used on a 2.5 m X 2.5 m spacing (34 kN/m^2) with suitable Wire-mesh and Osro straps (45 kN); and
3. Bolts of a length of 1.5 m installed on a 2.0 m X 2.0 m spacing (30 kN/m^2), with Wire-mesh and suitable straps, will adequately reduce the current risk of FOG injury in most areas, provided it is accompanied by a Triggered Action Response Plan.

ACKNOWLEDGEMENTS

I would like to appreciate and thank my supervisor, Professor BP Watson for his guidance and for further pushing me to do more research in the project to get more insight and understanding.

Thanks to Jeanne Walls for her support and guidance in the understanding of the software program used in this research. Thank you to Mr Henry Chiwaye for his guidance and insight.

Lastly, I would like to appreciate my family and friends for their continuous support and motivation which helped me to finish this work.

TABLE OF CONTENTS

1. INTRODUCTION 1

1.1 Description of the Mine 5

1.2 Problem Statement 9

1.3 Research Objectives and Scope of Research 10

1.4 Research Methodology 11

1.5 Sources of Data 11

1.6 Content of the Dissertation 12

2. LITERATURE REVIEW 13

2.1 Introduction 13

2.2 Failure Mechanisms in Shallow Environments 14

2.3 Support Design Methods for Shallow Mining Environments . 15

2.3.1 Empirical methods 16

2.3.2 Analytical, statistical and numerical methods 22

2.3.3 Observational methods 32

2.4 Collection of Data for the Research 33

2.5 Description of Data Inputs for the Research 35

2.5.1 Orientation/Attitude 35

2.5.2 Spacing 36

2.5.3 Length 38

2.5.4 Shear strength 40

3. METHODOLOGY 44

3.1 Underground Joint Mapping 45

3.2 Joint Data Analysis 49

3.3 Description of JBlock input parameters 55

3.3.1 Geotechnical domain file 55

3.3.2 Excavation file 58

3.3.3 Support file 59

3.3.4 Summary 65

4. JBLOCK RESULTS AND ANALYSIS 66

4.1 Rock fall Distribution 69

4.1.1 Support using 1.5 m long bolts spaced at 1.5 m X 1.5 m with the Triplets horizon at 1.7 m above the hangingwall 69

4.1.2 Sensitivity analysis on the Triplets height for 1.5 m long bolts spaced at 1.5 m X 1.5 m 71

4.1.3 Sensitivity analysis on bolt length (bolt spaced at 1.5 m X 1.5 m and Triplets height of 1.7 m) 75

4.1.4 Sensitivity analysis of Triplets heights for a 1.8 m long bolt (spaced at 1.5 m X 1.5 m for Scenario 1 and 2) 77

4.1.5 Sensitivity analysis of Triplets heights for a 2.5 m long bolt (spaced at 1.5 m X 1.5 m for Scenarios 1 and 2) 78

4.1.6 Comparison of bolt spacings at 1.5 m X 1.5 m and 2.0 m X 2.0 m (1.7 m Triplet height for Scenario 1 and 2) 79

4.2 Statistics 80

4.2.1 Hazard and risk results for 1.5 m long bolts spaced at 1.5 m X 1.5 m for Scenarios 1 and 2 (Triplet height at 1.7 m)..... 81

4.2.2 Hazard and risk results for a support configuration of 1.5 m long bolts spaced at 1.5 m X 1.5 m for various Triplet heights 82

4.2.4 Hazard and risk results for a 2.5 m long bolts spaced at 1.5 m X 1.5 m for various Triplets heights 84

4.2.5 Hazard and risk results for 1.5 m long bolts spaced at 2.0 m X 2.0 m with Wire-mesh at various Triplets heights 85

4.2.6 Hazard and risk results for 2.5 m long bolts spaced at 2.5 m X 2.5 m with Wire-mesh at various Triplets heights 87

4.3 Comparison of JBlock Results with actual Fall of Ground Statistics..... 89

5. DISCUSSIONS..... 91

6. CONCLUSIONS AND RECOMMEDATIONS 97

7. REFERENCE LIST..... 100

APPENDIX A. Mine A FOGs Accidents 112

APPENDIX B. Mine A FOGs Incidents 113

APPENDIX C. Joint Mapping Data 114

APPENDIX D. Dips Information 135

APPENDIX E. Sort Encapsulation Test 136

APPENDIX F. Company Specifications 138

LIST OF TABLES

Table 1.1: Fall of ground summary sheet of Unki Mine (after Mponya, 2016). 2

Table 2.1: Guidelines for excavation and support of 10.0 m span rock tunnels in accordance with the RMR system (after Bieniawski, 1989). 21

Table 2.2: The recorded FOG statistics for Mine A 25

Table 2.3: The calculated FOS for the support at Mine A 27

Table 2.4: The discontinuity spacing classification (Brady and Brown, 1993, ISRM 1978)..... 37

Table 2.5: The discontinuity persistence classification (Brady and Brown, 1993, ISRM 1978)..... 40

Table 3.1: The scanline mapping log sheet (OHMS, 2019) 48

Table 3.2: Summary of joint properties. 54

Table 3.3: Summary of historical Rock fall data at Mine A Mine from 2012-2018..... 64

Table 4.1: The hazard and risk results for a support Scenario of 1.5 m long bolts spaced at 1.5 m X 1.5 m for Scenario 1 and 2 (Triplet height at 1.7 m) 81

Table 4.2: The hazard and risk results for a support Scenario of 1.5 m bolts spaced at 1.5 m X 1.5 m at different Triplet heights for Scenario 1 82

Table 4.3: The hazard and risk results for a support Scenario of 1.5 m bolts spaced at 1.5 m X 1.5 m at different Triplet heights for Scenario 2. 83

Table 4.4: The hazard and risk results for a 1.8 m bolt length spaced at 1.5 m x 1.5 m at different Triplet heights for Scenario 1..... 83

Table 4.5: The hazard and risk results for a 1.8 m bolt length spaced at 1.5 m x 1.5 m at different Triplet heights for Scenario 2. 84
Table 4.6: The hazard and risk results for a 2.5 m bolt length spaced at 1.5 m x 1.5 m at different Triplet heights for Scenario 1. 85
Table 4.7: The hazard and risk results for a 2.5 m bolt length spaced at 1.5 m x 1.5 m at different Triplet heights for Scenario 2 85
Table 4.8: The hazard and risk results for a 1.5 m bolt length spaced at 2.0 m X 2.0 m installed with Wire-mesh at different Triplet heights for Scenario 1……..…….86
Table 4.9: The hazard and risk results for a 1.5 m bolt length spaced at 2.0 m X 2.0 m installed with Wire-mesh at different Triplet heights for Scenario 2……..…….87
Table 4.10: The hazard and risk results for a 2.5 m bolt length spaced at 2.5 m X 2.5 m installed with Wire-mesh at different Triplet heights for Scenario 1……...88
Table 4.11: The hazard and risk results for a 2.5 m bolt length spaced at 2.5 m X 2.5 m installed with Wire-mesh at different Triplet heights for Scenario 2……..……..88
Table 4.12: Mine A yearly FOGs incidents ad accidents Vs JBlock results 90
Table 5.1: Mine A’s yearly JBlock results converted to accidents rates using Scenario 1..... 94
Table 5.2: Mine A’s yearly JBlock results converted to accidents rates using Scenario 2..... 95

Table 5.3: Mine A’s yearly JBlock results converted to accidents rates using Scenario 1 for support Scenario results shown in Table 4.8 96

LIST OF FIGURES

Figure 1.1: Mine A FOG Injury statistics; T&R (treat and return), LDI (lost day injury), SI (serious injury) 2

Figure 1.2: South African fatalities percentages by classifications (MOSH learning hub, 2019). 3

Figure 1.3: The number of South Africa FOG related injuries and fatalities (MOSH learning hub, 2019). 4

Figure 1.4: The mining lease area of Mine A -green fill (Sibanda, 2018) ... 5

Figure 1.5: A typical layout of the mining method used at Mine A 7

Figure 1.6: The support standard for the UG2 reef (Sibanda, 2018)..... 9

Figure 2.1: Tunnelling support guidelines (after Grimstad et al., 1993)…...18

Figure 2.2: Rock mass ratings across Mine A..... 20

Figure 2.3: Tunnelling support guidelines indicating different support requirements at zones where the red and blue lines coincide (after Grimstad et al., 1993). 22

Figure 2.4: Flowchart outlining the principal design steps of support design methodology (after Daehnke et al., 2001)..... 24

Figure 2.5: Cumulative fall out height graph for Mine A Mine (after Daehnke et al., 1998, 2001) 26

Figure 2.6: Discontinuity mapping in a scanline survey (after Priest and Hudson, 1981) 34

Figure 2.7: The illustration of the definition of dip and dip direction……..36

Figure 2.8: The illustration of joint spacing correction (Nezomba, 2012)…38

Figure 2.9: The illustration of the definition of persistence of discontinuity (Brady and Brown, 1993) 40
Figure 2.10: The illustration of Patton's experiment on shear strength of saw-tooth specimens (after Patton, 1966). 42
Figure 3.1: The Mine plan indicating mapped panel and the direction of the scanline tape..... 46
Figure 3.2: The Brunton TRUARCH 15 compass. 47
Figure 3.3: Lower hemisphere meridional stereonet projections of the mapped joint poles and the great circles of the manually evaluated sets using Dips 50
Figure 3.4: Lower hemisphere meridional stereonet projections showing the Dips contour plot of joint poles and the manually evaluated sets shown by the great circle 51
Figure 3.5: Joint spacing data of Joint set 1 indicating a negative exponential distribution……..53
Figure 3.6: Joint spacing data of Joint set 2 indicating a negative exponential distribution…….……53
Figure 3.7: Joint spacing data of the random joint set indicating a negative exponential distribution.. 53
Figure 3.8: JBlock image of the joint data 1 input 55
Figure 3.9: JBlock image of the joint data 2 input. 56
Figure 3.10: JBlock image of the large structures input. 57
Figure 3.11: UG2 to Triplets layer isopachs (Kekana, 2018) 57
Figure 3.12: JBlock image of the excavation file for a panel along strike. 58

Figure 3.13: JBlock image of the excavation file for a panel along dip 59
Figure 3.14: The support standard for the UG2 reef, (Sibanda, 2018)..... 60
Figure 3.15: JBlock image of the excavation and the delineated hazard zone 63
Figure 3.16: JBlock image of the keyblock release distance and probabilities 64
Figure 4.1: A plan view of a mining area indicating the trace of joints in the hangingwall with primary and secondary block formation (after Joughin et al., 2012b)..... 67
Figure 4.2: Event tree analysis for injuries (after Joughin et al., 2012a) .. 68
Figure 4.3: Rock fall distributions for both Scenarios..... 70
Figure 4.4: Contributing factors to bolt behaviours for both Scenarios..... 71
Figure 4.5: Rock fall distributions for the different Triplets heights for Scenario 1..... 72
Figure 4.6: Contributing factors to bolt behaviours at various Triplets heights for Scenario 1. 73
Figure 4.7: Rock fall distributions for the different Triplets heights for Scenario 2..... 74
Figure 4.8: Contributing factors to bolt behaviours at various Triplets heights for Scenario 2. 75
Figure 4.9: Rock fall distributions for various bolt lengths (1.5 m X 1.5 m spacing for Scenario 1,Triplets at 1.7 m) 76
Figure 4.10: Rock fall distributions for the different bolt lengths at 1.5 m X 1.5 m spacing for Scenario 2, 1.7 m Triplet height..... 76

Figure 4.11: Rock fall distributions for the 1.8 m bolt length spaced at 1.5 m X 1.5 m for Scenario 77
Figure 4.12: Rock fall distributions for the 1.8 m bolt length spaced at 1.5 m X 1.5 m for Scenario 2. 78
Figure 4.13: Rock fall distributions for the 2.5 m bolt length spaced at 1.5 m X 1.5 m for Scenario 1.. 78
Figure 4.14: Rock fall distributions for the 2.5 m bolt length spaced at 1.5 m X 1.5 m for Scenario 2 79
Figure 4.15: Rock fall distributions for three bolt lengths at different spacings for Scenario 1, (1.7 m Triplet height)..... 80
Figure 4.16: Rock fall distributions for three bolt lengths at different spacings for Scenario 2, (1.7 m Triplet height)..... 80
Figure 4.17: Mine A yearly FOGs accident frequencies. T&R (Treat and Return), LDI (Lost Day Injury) 90
Figure 5.1: F-N graph for bench marking safety impact (Joughin et al., 2012a)..... 92
Figure 5.2: Heinrich's accidents triangle (Kuder, 2017) 93

LIST OF SYMBOLS AND ABBREVIATIONS

Fall of ground	FOG
Code of practice	COP
Ground control district	GCD
Uniaxial compressive strength	UCS
Treat and return	T&R
Lost day injury	LDI
Serious Injury	SI
Mineral counsel of South Africa	MCSA
Upper group	UG2
Factor of safety	FOS
Excavation support ratio	ESR
Load carried by support unit	F
Tributary area	A
Rock density	ρ
Acceleration due to gravity	g
Height of the fall	h
Frequency of a given discontinuity spacing value	$f(x)$
Average number of discontinuities per meter	λ
Number of joint that would have been mapped	$\mathrm{N'}$
Standard length	$\mathrm{L_s}$

Actual sampling length	L
Peak shear strength	τ_p
Normal stress	σ_n
Cohesive strength	C
Friction angle	ϕ
Basic friction is angle of the surface.	ϕ_b
Angle of the saw-tooth face	i
Joint roughness coefficient	JRC
Joint wall compressive strength	JCS
Joint roughness condition	Jr
Joint alteration number	Ja

CHAPTER 1

1. INTRODUCTION

The number of fall of ground (FOG) injuries in the past 5 years at Mine A are relatively high (Figure 1.1), when compared to other Mines in other countries such as Zimbabwe Unki Mine (Table 1.1). The numbers shown in Figure 1.1 do not project a downward trend of FOGs because the root cause has not been properly mitigated, there will therefore be fluctuations in accidents from year to year, as shown in the figure. Approximatey 67.0 % of FOGs still occur in the area between the face and the first line of permanent support. This zone remains a high-risk zone as it is the area of exposure before support is to be installed for the next shift. FOGs do not only result in loss of life and damage to equipment, but they also largely contribute to the loss of business production therefore affecting the stability of the business at large. The Mine's database of FOGs showed that 88.0 % of FOGs, which caused lost time injuries, were related to geological discontinuities - structures such as joints, faults, potholes and sympathetic jointing associated with the faults.

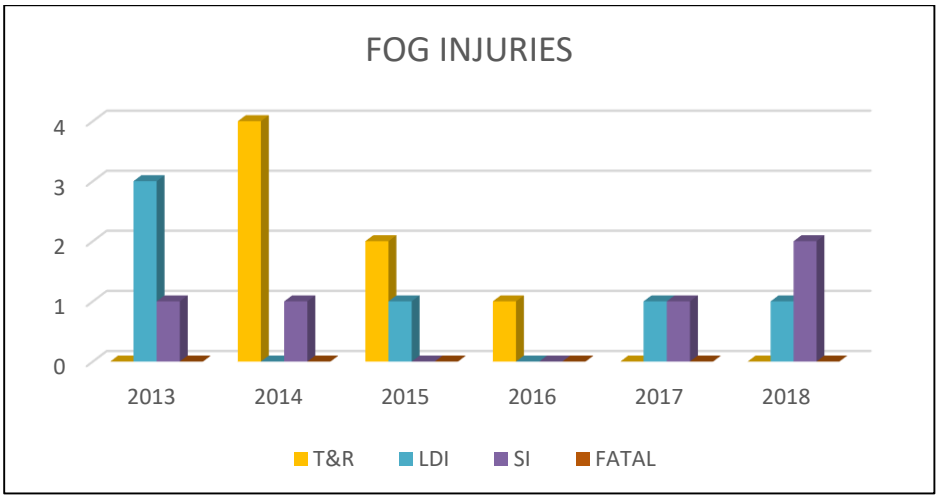


Figure 1.1: Mine A FOG Injury statistics; T&R (treat and return), LDI (lost day injury), SI (serious injury).

Table 1.1: Fall of ground summary sheet of Unki Mine (after Mponya, 2016).

Date	Working Place	Width (m)	Length (m)	Thick (m)	Size	Damage	Injury	Comments
01-Feb-10	LDN	0.17	0.35	0.12	L	N	Y	MTC involving Lazarus Nyika while removing barricade
04-May-10	1SB1	0.1	0.25	0.1	S	N	Y	MTC involving Bland Zulu, Head and hand injury
25-Nov-10	1NB4	1.1	2.3	0.45	L	Y	N	LHD Mud guard damaged during lashing
01-Feb-11	3NB2	0.25	0.65	0.5	L	N	N	No Injuries or damage to property
08-Mar-11	2NS	1.4	2.16	0.98	L	N	N	FOG after blast
07-Apr-11	4NB1	0.52	0.77	0.15	L	N	Y	Fatality Involving Tainos Shumba while barring down
03-May-11	2SB6	0.66	1.1	0.24	L	Y	N	Autorock damaged
23-Oct-11	5NB1	0.41	0.08	0.06	L	N	Y	MTC involving Kundai Burayayi, Head and Shoulder injury
16-Nov-11	3NB5	4.5	2.5	0.6	L	N	N	FOG after blast
16-Dec-11	1NS	4.2	3.2	8	L	N	N	FOG after blast
20-Mar-12	3NB3	0.38	0.225	0.12	L	N	N	Near miss involving Lawrence Mzizi
04-Apr-12	2SB1	0.54	0.39	0.11	L	Y	N	MTC involving Prosper Masuku's right hand
15-May-12	6NB6	0.92	3.6	0.33	L	Y	N	Damage to property LHD work light housing
16-Oct-12	7SB1	0.1	0.05	0.03	S	Y	N	Josiah Mawarire sustained soft tissue injury
17-Jan-13	2NB4	0.5	3.2	0.79	L	N	N	FOG occurred at face during rig drilling
01-Feb-13	4SB5	0.35	0.5	0.15	L	N	N	FOG occurred at face during face marking for rig drilling
14-Feb-13	1NB2	1.26	0.39	0.36	L	N	Y	Significant Incident involving K. Hwacha
15-Oct-13	1NB3	MSZ	1.64	1.97	0.82	N	N	
08-Jun-14	5SB5 V/H49	MSZ	6.00	7.00	0.85	N	N	FOG occurred during or after blast
06-Aug-14	4SB2	MSZ	1.26	0.39	0.36	N	Y	Significant Incident involving Prince Dindi
08-Sep-14	1SB2	MSZ	0.12	0.21	0.0525	N	Y	Significant Incident involving Alfred Manda
26-Feb-15	3NB2	MSZ	7	20	2.5	N	N	High Potential Incident
10-Apr-15	7NB1 V/H21	MSZ	0.5	1.4	0.3	N	Y	Significant Incident involving Zuze Nzerere
06-Nov-15	5NB3	MSZ	7	7.2	2.3	N	N	High Potential Incident

FOGs remain the leading cause of fatalities in South African Mines (MOSH Learning Hub, 2019). The recent statistics presented by the Mineral Counsel of South Africa (MCSA), shown in Figure 1.2, clearly demonstrate that the vast majority of fatalities in 2018 were FOG related, i.e. a total of 37.0 %. Rock falls are shown to be a major accident contributor in the South African mining industry, i.e. out of a total of 30 reported FOG related fatalities in 2018, only 5 were rock burst related. Although the FOG injuries have generally declined between 2003 and 2018 (Figure 1.3), the zero harm mandate is far from being achieved.

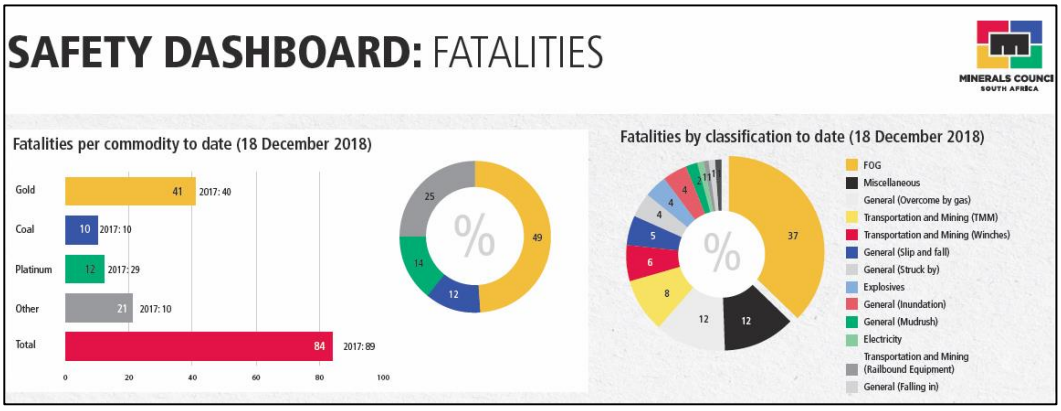


Figure 1.2: South African fatalities percentages by classifications (MOSH learning hub, 2019).

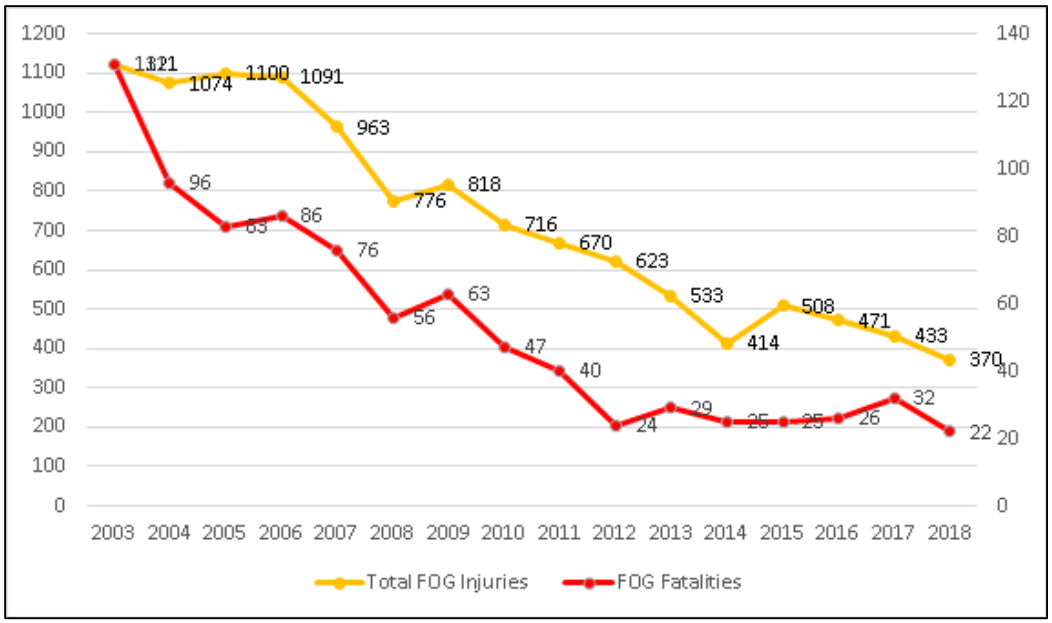


Figure 1.3: The number of South Africa FOG related injuries and fatalities (MOSH learning hub, 2019).

Several support design methods are used in the industry to ensure stability in underground Mines. The current support design at Mine A is done using the fall out height method. Given the number of FOG injuries occurring yearly at the Mine (Figure 1.1), the reliability of the design method needs to be questioned. This research will therefore investigate an alternative support design strategy for underground stability at Mine A, and will compare it to the current support design. The strategy was suggested by Walls (2018) in an internal report to the Mine. Walls (2018) stated that even though the current support design at Mine A is in line with the industry practice, meaningful and confident inputs need to be continuously applied in design validation of the current support design system. The study described in this research report focuses on the validation of the current stope support system at Mine A, and provides an improved alternative design.

The Mine preferred to remain anonymous and hence it is called Mine A for the purposes of the research report.

1.1 Description of the Mine

Mine A Shaft is located in the Western Limb of the Bushveld Complex, in the Kroondal area, approximately 120.0 km North West of Johannesburg in the North West province. This Shaft is a trackless Mine using the bord and pillar mining method for the extraction of ore. Mine A exploits only the UG2 (Upper Group) chromitite reef. The Mine A boundary is highlighted in Figure 1.4 below.

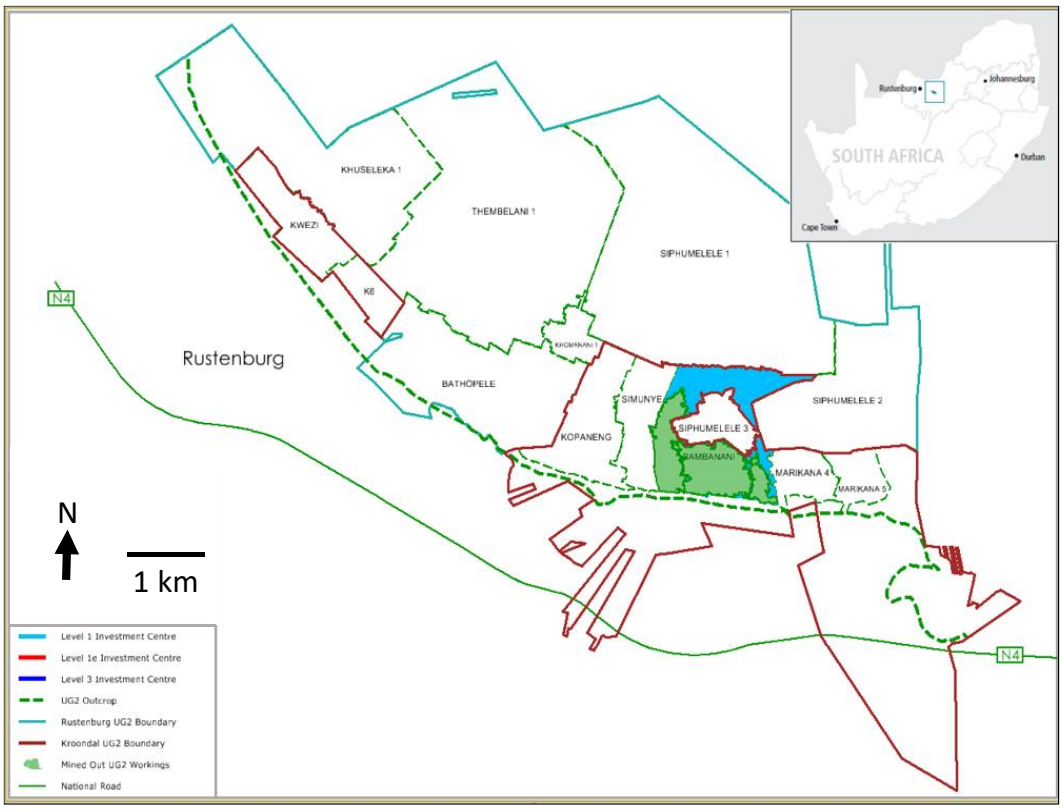


Figure 1.4: The mining lease area of Mine A - green fill, (Sibanda, 2018).

The current bord and pillar mining method at the Mine requires bords to be developed from the decline barrels along strike (Figure 1.5). Splits are developed as holings on dip in between the bords. The UG2 reef is located below the Merensky reef at a middling distance of 120.0 m (Schouwstra and Kinloch, 2000). At Mine A, the UG2 reef dips at approximately 9° towards the north. The mining of this reef is planned to extend from a depth of 386.0 m to 650.0 m below surface. Immediately overlying the UG2 main seam is a 0.6 m to 0.8 m thick chromitite layer named the leader-seam (Sibanda, 2018). This seam varies in height above the UG2 reef between 0.1 m and 1.5 m.

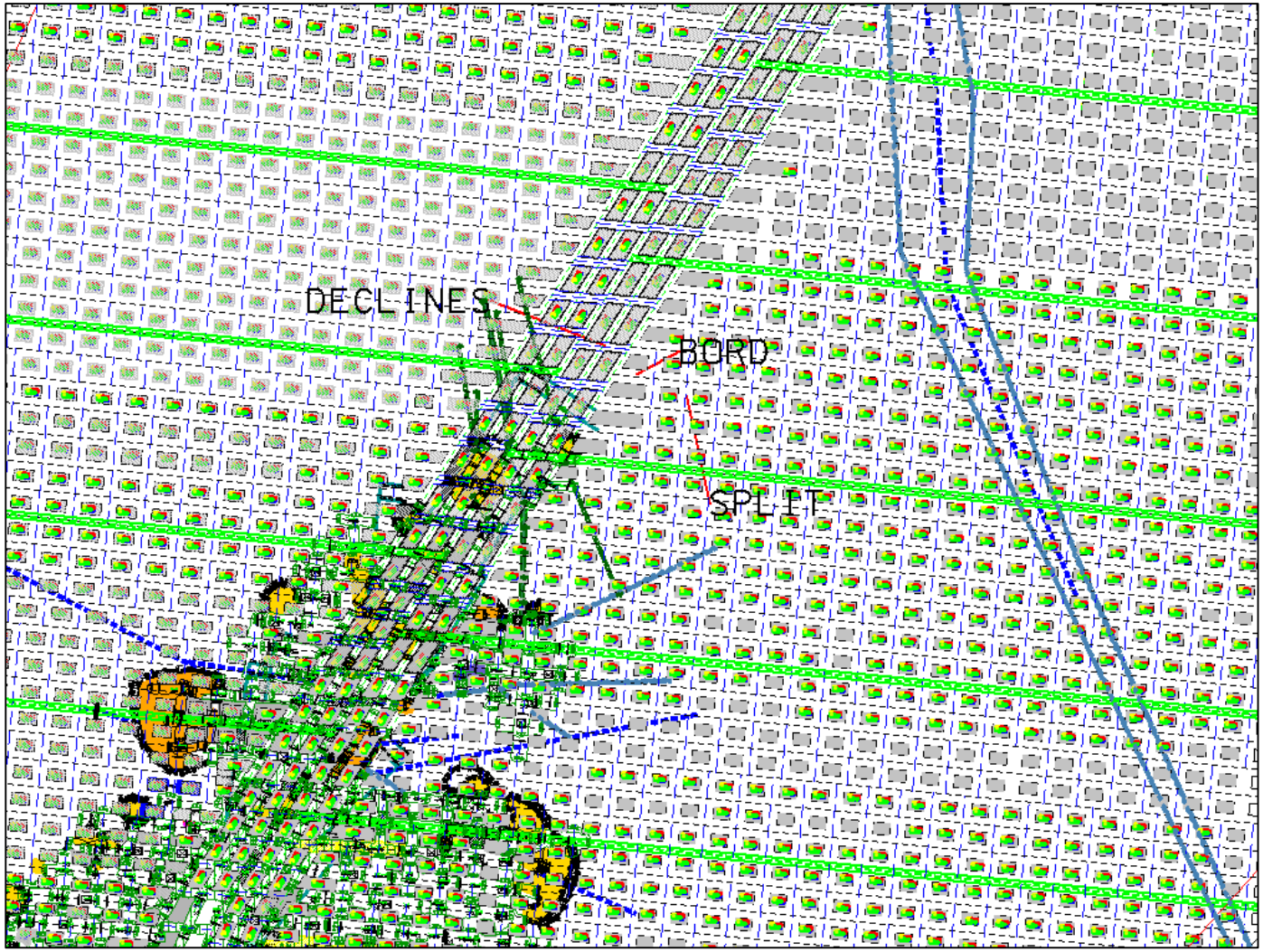


Figure 1.5: A typical layout of the mining method used at Mine A.

The middling rock between the UG2 main seam and the leader-seam is feldspathic pyroxenite. The mining cut in this Shaft includes both chromitite seams, which are mined simultaneously. The pillars, therefore, consist of chromitite and pyroxenite layers.

Panels and splits are designed both to have a span of 10.0 m. Stable pillars are left in between the splits and bords. These pillars are designed to carry the overburden to surface, for the life of the Mine. The mining method requires a minimum of 7 people per shift to be fully exposed at the panel face during mining activities, i.e. preparing the area for cleaning, supporting and blasting. These people are exposed to several hazards, FOGs being the main one. The support to face distances after the blast is designed to be a maximum of 3.1 m, resulting in an unsupported span within the face area.

Currently, the hangingwall is supported on 1.5 m long bolts spaced at 1.5 m along both strike and dip (Figure 1.6). According to the support standard, the area between the face of the panel and the first line of bolts should be at a maximum of 1.0 m (±10.0 cm) at all times before the blast. This area is temporarily supported with safety nets and Camlok props in order to protect the personnel drilling in the face area for the installation of the face-support before a new blast can be taken. Drilling of the face is done by hand-held rock drills, resulting in a maximum face advance of 2.1 m per blast, provided no disturbance in the ground conditions is present.

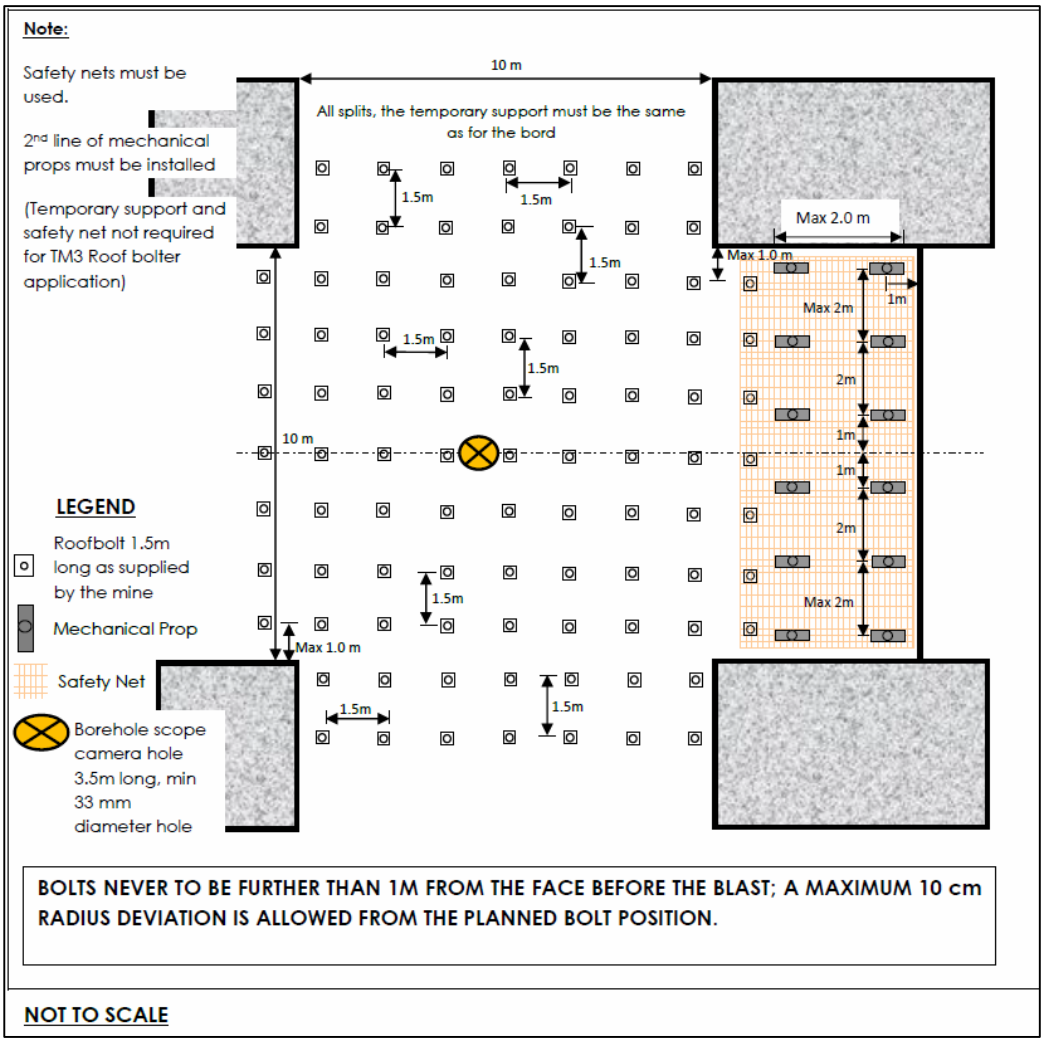


Figure 1.6: The support standard for the UG2 reef, (Sibanda, 2018).

According to the Mine A's mandatory code of practice (COP) to combat rock fall and rock burst accidents, the current support system at Mine A is designed for fair-ground conditions (RMR > 61) and mining the dual seam when the leader seam is less than 1.3 m above the main seam (Sibanda, 2018).

1.2 Problem Statement

The current traditional support design at Mine A is based purely on the 95.0 % fall out height, where the data used was collected from the FOG

statistics. This approach to support design has been shown by previous researchers to have limitations with regards to developing a robust support system to ensure safe mining operations (Joughin *et al.,* 2012a; Nezomba, 2012). In Chapter 2, the benefits of the keyblock analysis approach are described. This approach uses a software called JBlock. The software will be used to investigate the support design at the Mine, using a more rigorous, statistical analysis approach. The keyblock analysis was used to extend the knowledge and the understanding of the rock behaviour, and to optimize the current support design.

1.3 Research Objectives and Scope of Research

The research involved the following activities:

- Joints were mapped in the bords and splits across the entire Mine. The data collection concentrated on the joint geometrical properties (such as orientation, spacing, length/persistence);
- The shear strength was determined using an empirical method outlined in the Chapter 3.
- Joint sets were defined using poles generated from lower hemisphere, equal angle stereonet projections. Statistical analyses were used to determine the variability of joint sets across the Mine and the possible need to divide the Mine into geotechnical zones, i.e. Ground Control Districts (GCD).
- Validation of the current support system was done using JBlock analyses. The ultimate aim was to check the adequacy of the current support design and to optimize.

- The JBlock analyses focused on the face area, as this zone was found to be the highest risk area.
- The JBlock results were compared to the Mine A fall of ground statistics, and the injuries associated with them.
- The JBlock results were benchmarked to internationally acceptable risk.
- Support recommendations were made based on the research findings.

1.4 Research Methodology

The following methodology was employed to achieve the stated objectives:

- Collection of discontinuity data was done underground using the scanline mapping method.
- The Dips program was run to compute the mean, standard deviation, minimum and maximum.
- The JBlock model was done for panels advancing along strike and dip, and incorporated the current support configuration. Different support Scenarios were subsequently evaluated in the JBlock program. The modelled Scenarios included the variety of measured joint sets, parting plane heights, support unit lengths, and the strengths and spacings of the installed support units. The effects of areal coverage were also investigated.

1.5 Sources of Data

All data used in the program was obtained from underground mapping. The FOGs statistics of the Mine were observed from historical data found on the Mines data base from the Rock Engineering Department.

1.6 Content of the Dissertation

Chapter 2 will describe the various support design methods used by the industry and define their shortcomings. The data collection will also be explained. Chapter 3 describes the geotechnical data used in the analysis. Chapter 4 provides the JBlock results. Chapter 5 compares the results with international acceptable risks and converts the findings of Chapter 3 and 4 into meaningful data. The conclusion and recommendations will be provided in Chapter 6.

CHAPTER 2

2. LITERATURE REVIEW

2.1 Introduction

Currently the deepest level at Mine A is 510.0 m below surface, which means the whole Mine can be classified as operating within a shallow mining environment (Jager and Ryder, 1999), and the virgin stress is less than 14.3 MPa. The overburden rock type is both the pyroxenite and norite rock averaged to a density of 2850.0 kg/m^3 and uniaxial compressive strength of 160.0 MPa (Jager and Ryder, 1999). The literature review included the typical Rock Engineering related problems in shallow Mines and the failure mechanisms commonly encountered. The Chapter also includes some of the more popular support design approaches used in the shallow Bushveld Complex Mines. The advantages and limitations of each approach will be described. The research showed that the most applicable and useful tool for determining support requirements is the keyblock analysis method. A detailed literature review of the fall of ground height method (which is the basis of the current design on Mine A) and the probabilistic keyblock method was therefore made. The probabilistic approach was used for support optimization. The method used for the data collection and the required JBlock input parameters are also described in the Chapter.

2.2 Failure Mechanisms in Shallow Environments

Stacey and Swart (2001), summarized the different circumstances under which underground excavations can fail:

- Failure of rock material or mass around an opening as a result of high stress to strength ratios;
- Movement and collapse of rock blocks bounded by geological structures (structural instability);
- A combination of stress induced rock failure and structural instability.

In shallow mining environments, the high vertical stress driven failure modes are generally rare (except in cases where mining takes place in or near remnants). The reason for this is that the rocks in the Bushveld Complex area are strong and the vertical virgin stresses at Mine A are generally low. By far the most common problem is one where rock blocks, defined by geological structures, become unstable. As Jager and Ryder (1999) stated, there are 4 factors that tend to promote such structurally controlled failures in shallow Mines:

- The existence of relatively large vertical tensile zones in the hangingwall.
- Generally high virgin horizontal stresses which clamps vertical fractures therefore creating horizontal fractures.
- The absence of the face fracturing which is observed in deeper Mines which generates horizontal dilatational stresses that act to clamp the hangingwall blocks together.

- Relatively high tectonic stresses such as often observed in pothole structures and reef roles.

The structurally controlled failures are influenced by the presence of:

- Tensile stress or geological discontinuities opening up resulting in the failure of the hangingwall beam.
- Keyblock failure where geological discontinuities intersect each other, unravelling of the hangingwall.
- Wedge failure as a result of shallow dipping discontinuities intersecting with each other or intersecting other vertical discontinuities.
- And massive stope back breaks where the tensile zone is not sufficiently supported.

Massive back breaks can occur gradually or speedily where a large thickness of rock may fall from the hangingwall. It is due to such problems that Jager and Ryder (1999) said that the support systems in shallow mining environments should be robust and active.

2.3 Support Design Methods for Shallow Mining Environments

Support in underground Mines is classified as either regional or local support (Jager and Ryder, 1999). Regional support addresses issues of Mine-wide stability whereas local support deals with the support of localized individual excavations such as a tunnel or a stope between regional supports (Jager and Ryder, 1999). Regional support is achieved by means of pillars or backfill whereas local support uses elements such as roof bolts, cable bolts, elongates etc. The scope of this research will be on local

support and as such regional support issues will not be discussed further. The phrase “support design” will be taken to mean only local support unless otherwise explicitly stated.

There are various approaches to support design in underground Mines. These methods can be roughly classified as:

- Empirical methods
- Analytical/Numerical methods and
- Observational methods

A description of each approach will be given in this Section with more emphasis on the approaches that are more common in the shallow mining environments.

2.3.1 Empirical methods

Empirical methods are described as applications based on experience, experiments or past practices (Swart and Handley, 2005). Such knowledge is viewed to be obtained from historical testing of the Mine designs. Approaches of support design in a jointed rock mass mainly involve empirical methods (Dunn *et al.*, 2008).

Most empirical design methods are based on rock mass classification methods that have been calibrated to assist in estimating support requirements (Hutchinson and Diederichs, 1996). These classification methods are known to be successful because:

- They allow simple measurements to be taken for the use of characterizing the rock mass strength.
- They allow results of quantitative engineering data to be obtained based on geologic information.
- They create a platform of communication between Geologists and Rock Engineers.
- They allow the ease of ground control experiences to be compared between sites.

Hutchinson & Diederichs (1996) said, “Classification and its application to underground support design is primarily founded in civil engineering tunnel construction”. This is particularly true for RQD (Deere *et al.*, 1967), RMR (Bieniawski, 1976, 1989, 1993) and Q (Barton *et al.*, 1974; Barton, 1988; Grimstad and Barton, 1993). Laubscher and Taylor (1976) and Laubscher (1993) modified RMR for use in the design of block caving Mines. In addition, Mathews *et al*. (1981) and Potvin (1988) developed an extension of the Q system and applied it to open stope design. A modified Stability Graph system for conventional stope support in the Bushveld Merensky workings was later developed by Watson (2004). This system is used to determine panel stability by defining risk levels of collapse (Watson, 2004).

Watson and Gerber (2018) concluded the work assessed by Watson (2004) by stating that four out of the fourteen rock mass rating system considered by the author, were found fit to evaluate the stability in shallow dipping,

tabular stopes. Those were noted as the RMR system, the Q system, the MRMR system and the N' system.

Figure 2.1 shows how the Q classification system can be used to estimate tunnel support requirements (Barton *et al.*, 1974; Barton, 1988; Grimstad and Barton, 1993). ESR used in the below diagram is defined as the excavation support ratio. This ratio is used to describe the planned use of the excavation. It provides a higher value for temporary Mine openings and reduces as the degree of security or length of time in terms of the use of the excavation increases.

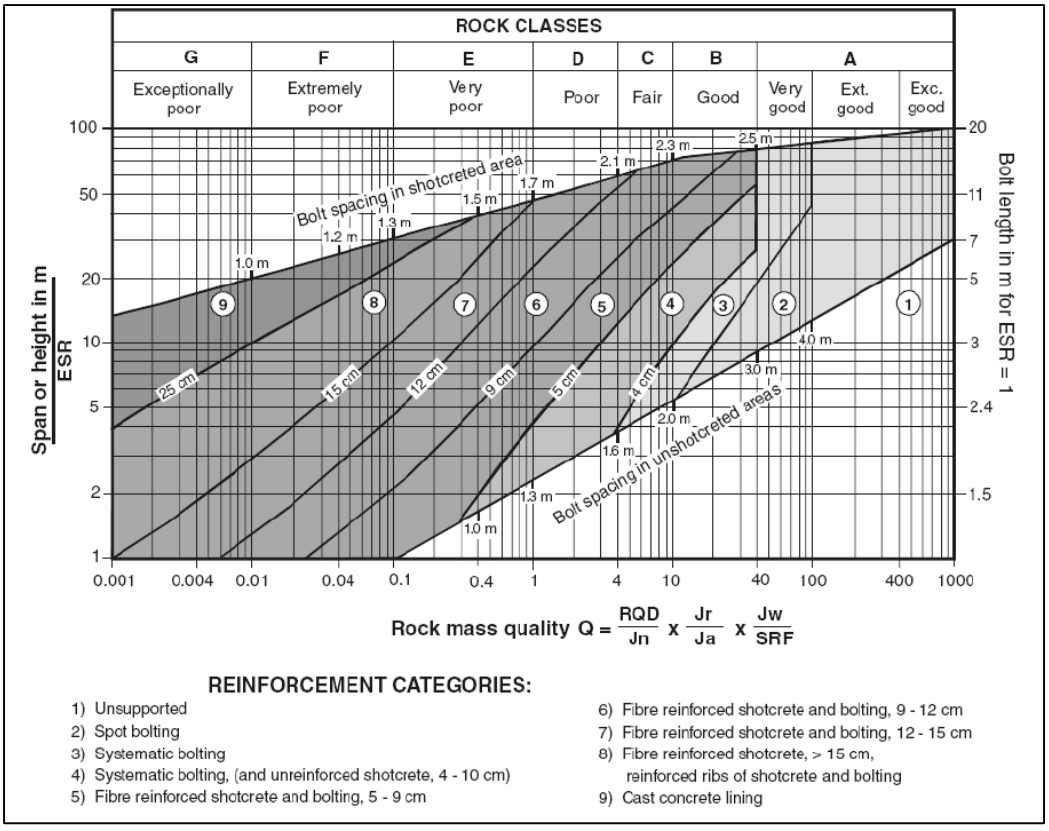


Figure 2.1: Tunnelling support guidelines (after Grimstad et al., 1993).

The major advantage of empirical methods is their ease of use. This is very crucial where quick decision making is needed and if properly validated for site specific conditions, can be used by Rock Engineering practitioners. Another major advantage is that these rating systems also give a numerical value to experience, which allows for experience to be transferred between different sites and people.

Although such methods are rarely used in the narrow reef stope support design, they are used in open stope design as well as design of tunnel support. According to Esterhuizen (2014) empirical methods have limitations, since they cannot be stretched beyond their databases or experiments at which they were assembled. It is therefore risky to apply the recommendations provided for shallow civil engineering excavations to deeper mining excavations, as it is outside their databases. Additionally, recommendations for civil structures are generally too conservative for mining applications. It is therefore necessary to adapt the recommendations to a specific mining Scenario, a task which is generally difficult to accomplish. Rock mass ratings were determined across Mine A and the results are plotted in Figure 2.2. The work shows the limitation of empirical methods and is described in the Sections below.

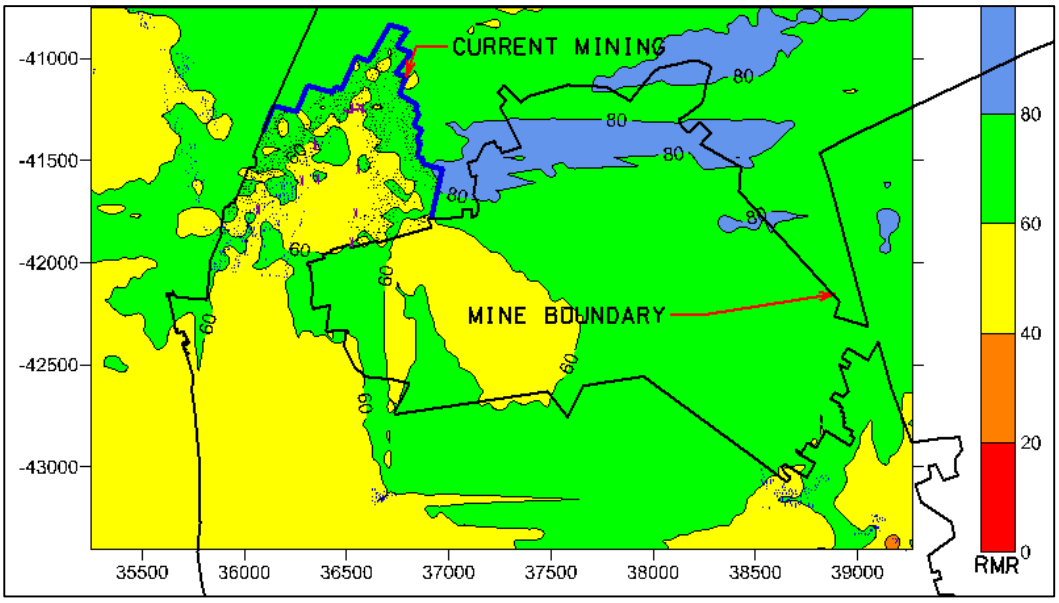


Figure 2.2: Rock mass ratings across Mine A.

The support guidelines provided by Bieniawski (1989) for RMR 41-60 and 61-80 indicating fair and good rock mass, respectively, are illustrated in Table 2.1. Based on the guidelines, 4.0 m long bolts accompanied by Wire-Wire-mesh and 50 mm-100 mm Shotcrete must be installed in fair rock mass conditions. Good rock mass requires 3.0 m long bolts with occasional Wire-mesh along with 50 mm Shotcrete. These support guidelines are significantly greater than the current support and are probably proposing an over support of the rock mass condition, due to the much shorter excavation life than the expected life of a civil excavation. A similar observation is made for the Q classification system (Figure 2.3). A Q-value of 3.3 (fair rock mass) was used to estimate the support requirements at a span of 10.0 m and ESR value of 1.6. In this case it is observed that the Q system requires the excavation to be supported with a 2.6 m bolt length installed systematically along with unreinforced Shotcrete (Figure 2.3). At fair ground conditions,

this system similarly suggest greater support requirements compared to the current support being installed. At good rock mass conditions, the Q system under estimates the support requirements observed at Mine A. The Q system suggests that no support is required when the Q-value is above 15 (Figure 2.3). However, FOGs have been observed at the Mine in such Scenarios.

Table 2.1: Guidelines for excavation and support of 10.0 m span rock tunnels in accordance with the RMR system (after Bieniawski, 1989).

Rock mass class	Excavation	Rock bolts (20 mm diameter, fully grouted)	Shotcrete	Steel sets
I - Very good rock *RMR*: 81-100	Full face, 3 m advance.	Generally no support required except spot bolting.		
II - Good rock *RMR*: 61-80	Full face , 1-1.5 m advance. Complete support 20 m from face.	Locally, bolts in crown 3 m long, spaced 2.5 m with occasional wire mesh.	50 mm in crown where required.	None.
III - Fair rock *RMR*: 41-60	Top heading and bench 1.5-3 m advance in top heading. Commence support after each blast. Complete support 10 m from face.	Systematic bolts 4 m long, spaced 1.5 - 2 m in crown and walls with wire mesh in crown.	50-100 mm in crown and 30 mm in sides.	None.
IV - Poor rock *RMR*: 21-40	Top heading and bench 1.0-1.5 m advance in top heading. Install support concurrently with excavation, 10 m from face.	Systematic bolts 4-5 m long, spaced 1-1.5 m in crown and walls with wire mesh.	100-150 mm in crown and 100 mm in sides.	Light to medium ribs spaced 1.5 m where required.
V – Very poor rock *RMR*: < 20	Multiple drifts 0.5-1.5 m advance in top heading. Install support concurrently with excavation. Shotcrete as soon as possible after blasting.	Systematic bolts 5-6 m long, spaced 1-1.5 m in crown and walls with wire mesh. Bolt invert.	150-200 mm in crown, 150 mm in sides, and 50 mm on face.	Medium to heavy ribs spaced 0.75 m with steel lagging and forepoling if required. Close invert.

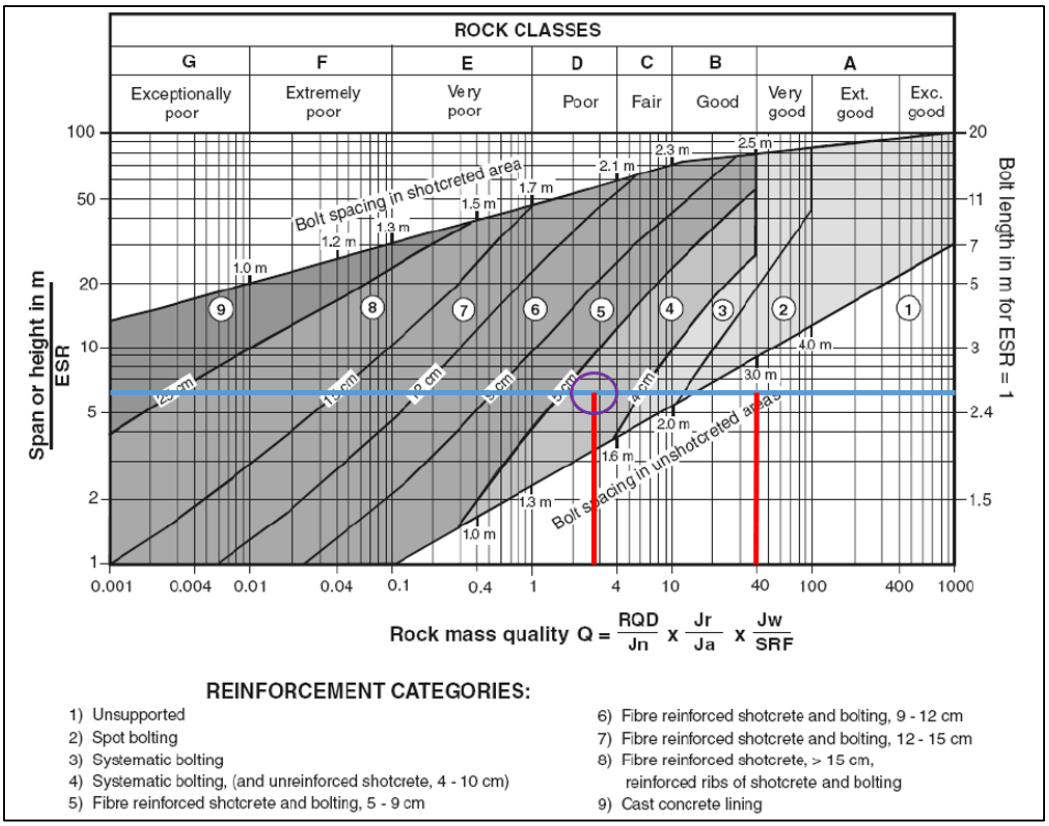


Figure 2.3: Tunnelling support guidelines indicating different support requirements at zones where the red and blue lines coincide (after Grimstad et al., 1993).

The Q and RMR ratings do not adequately cater for the geometry of the excavation or the dip orientation of joints (Nezomba, 2012).

2.3.2 Analytical, statistical and numerical methods

Analytical and numerical methods are the best design criteria. Such methods are generally either based on closed form solutions or approximate solutions derived from numerical analyses. In the Bushveld area, the most common approach to support design is the so called “fall out height” analysis. This approach uses statistical evaluation without necessarily understanding of the failure mechanism. Other methods employ beam and keyblock analyses.

The fall out height analysis

Explanation of the method. This is a support design methodology largely employed in the platinum and the gold Mines, where mining of narrow tabular reefs is taking place. Mining methods such as the scattered breast mining, the up-dip and down-dip mining, hybrid mining method and bord and pillar are being used. The support resistance requirement is based upon historical data of rock fall and rock bursts and the tributary area theory. The weight of the rock and height of the fall (fall out thickness) is divided by the weight that a support element can carry within the given area (Daehnke *et al.*, 2001; Brink *et al.*, 2002). The fall out height thickness is determined from historical data of rock fall and rock bursts, brow heights or from the height of prominent hangingwall discontinuities that are parallel to the reef plane (Jager and Ryder, 2002). In practice, most Rock Engineers use the 95^{th} percentile of the historic FOGs as the fall out height. The 5^{th} percentile is not catered for by the resulting support system, therefore these conditions must be recognized and supported separately. Both the quasi-static and the dynamic environments are incorporated where applicable in such a design method, where the energy absorption criteria and closure rates are considered in dynamic environments. However, in shallow Mines the dynamic component of support design is generally unnecessary due to the low stress regime and lack of seismicity.

Details on the implementation of the fall out height analysis. The implementation of the fall out height method that is discussed below, will focus on the current design at Mine A which was done using the flowchart

provided by Daehnke *et al.* (1998, 2001). The flowchart specifies the design steps that were followed in the support design (Figure 2.4)

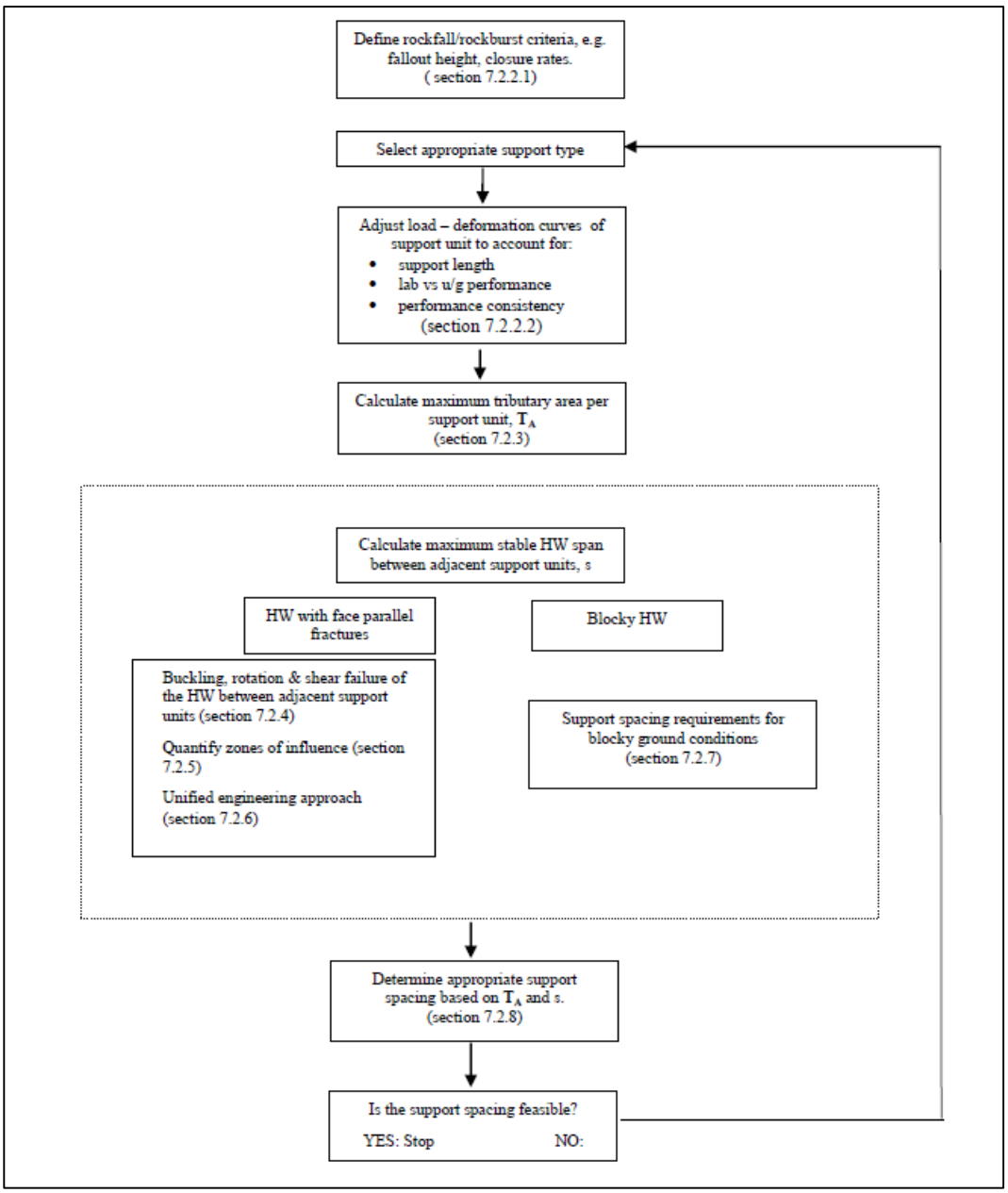


Figure 2.4: Flowchart outlining the principal design steps of support design methodology (after Daehnke et al., 2001).

The support design was done using FOG statistics from FOG incidents and accidents between the years 2012 and 2018 and is summarized in Table

2.2. Daehnke *et al.* (2001) suggested that the data should include both incidents and accidents resulting from FOGs to ensure the relevance of the statistics. The cumulative fall out height was determined to be 0.75 m as highlighted in Table 2.2 and shown in Figure 2.5.

Table 2.2: The recorded FOG statistics for Mine A.

Mine A	Include (Y/N)	If no why?	Fall out thickness (m)	Cumulative amount	Cumulative %
1	y		0.005	1	4.00
2	y		0.01	1	4.00
3	y		0.15	13	52.00
4	y		0.20	14	56.00
5	y		0.25	16	64.00
6	y		0.30	17	68.00
7	y		0.35	20	80.00
8	y		0.4	22	88.00
9	y		0.45	22	88.00
10	y		0.50	23	92.00
11	y		0.55	23	92.00
12	y		0.6	23	92.00
13	y		0.65	23	92.00
14	y		0.70	23	92.00
15	y		0.75	24	96.00
16	y		0.80	25	100.00
17	y		0.85	25	100.00
18	y		0.90	25	100.00
19	y		0.95	25	100.00
20	y		1.00	25	100.00
21	y		1.05	25	100.00

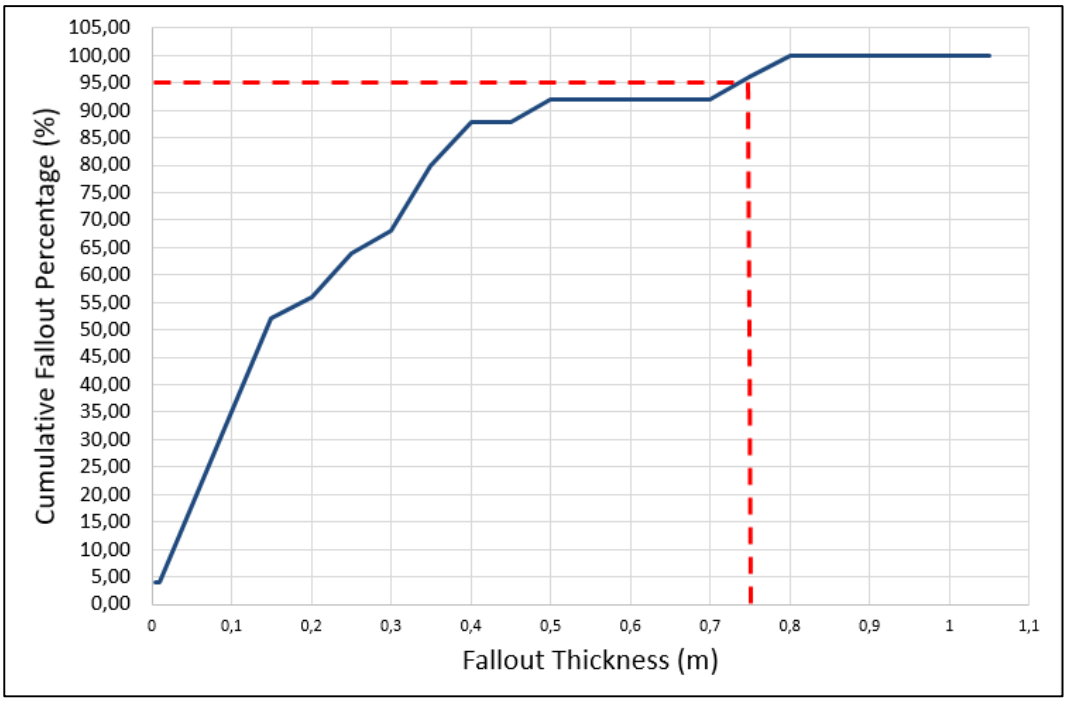


Figure 2.5: Cumulative fall out height graph for Mine A (after Daehnke et al., 1998, 2001).

Note the limited data, posing one of the limitations which are outlined in the Section below. Over the past 7 years, only 21 FOGs in the data sets were used in the calculation of the fall out thickness. A certain number of smaller FOGs may occur yearly but not all get to be recorded. The data collection is highly dependent on the mining personnel in that they need to report every FOGs to the Rock Engineering Department to ensure all necessary information is captured. Often FOGs that did not result in injury were not recorded.

The fall out height is incorporated in the design and used to calculate the required support resistance (expressed in KN/m^2) as follows:

$$\frac{F}{A} = \rho g h \left(\frac{kN}{m^2}\right) \quad [1]$$

Where:

F= Load carried by the support unit (N)

$A =$ Tributary area (m^2)

$\rho =$ Rock Density $\left(\frac{kg}{m^3}\right)$

$g =$ Acceleration due to gravity $\left(\frac{m}{s^2}\right)$

$h =$ Height of the fall (m)

The Factor of Safety (FOS) relating to the installed support system is calculated from the dividend of the actual support resistance of the support units obtained from the laboratory by the required support resistance obtained using the equation stated above and illustrated in Table 2.3 below.

Table 2.3: The calculated FOS for the support at Mine A.

MINE A	
Fall out thickness (m)	0.75
Density (kg/m³)	2850
Required support resistance (N/m²)	20969
Required support resistance (kN/m²)	20.96
18mm 1.5m bolt strength (kN)	117.80
Bolt spacing on strike (m)	1.50
Bolt spacing on Dip (m)	1.50
Actual support resistance (kN/m²)	52.40
FOS above the 95% FOG height requirement	**2.5**

Shortcomings of the method. Daehnke *et al.* (2001) outlines limitations of this method as not adequately catering for the fractured or jointed rock mass even though it may cater for equilibrium requirements. The fall out height analysis does not give an indication of the potential for unravelling of rock blocks from between support elements. In essence the method assumes that the rock mass is massive between the support elements.

Another downfall of this analysis is that the data used to obtain the fall out height is determined while using an existing support system, an underestimation of the percentage may be made when the existing support prevents/reduces the smaller height FOGs from taking place. The fall out height of the rock falls is usually not normally distributed, the larger sized falls tend to be discarded therefore not indicating a true value of the 95th percentile. The larger sized falls are discarded as they are said to be catered for in the remaining 5th percentile. Therefore, a system is introduced to deal with the 5th percentile separately, on a case by case basis. A Triggered Action Response Plan (TARP) system is used to cater for the 5th percentile across Sibanye Stillwater Mines. This is a trigger response system which allows high risk geological discontinuities/structures to be treated and supported differently, separate from the generally used support standard. The limitations of the system can be described as the inadequate data to obtain the fall out height, particularly when FOGs are not recorded. Additionally, the fall out height method does not consider the properties or orientations of geological discontinuities/structures with reference to the excavation.

Beam analyses

Beam analysis is popularly used for bord and pillar mining support design in stratified rock masses. The analyses are divided into elastic and voussoir beam (Swart and Handley, 2005). In both analyses, there are main critical components that must be present:

- The shear strength of the stratified layers is low compared to the shear strength of the intact rock.
- The tensile strengths of parting planes are low or zero (Swart and Handley, 2005).

The low tensile strength in the horizontal direction is the cause for voussoir beam development and the main difference between the two beam analyses. The two common failure modes expected in both beam analyses will be the parting along well defined and persistent, bedding planes/stratification and deflection of the beam with shear failure along the stratified layers during the beam bending.

When a thick weak roof is present and a strong beam is out of reach for suspension of the weak roof, elastic beam creation methods are considered for support design (Van Der Merve and Madden, 2002). The suspension of the weak layer will create an increased maximum stress in the upper layer, above abutments. Two options are open when designing support systems using the elastic beam analysis:

- Pinning the layers together to make up a thicker beam to reduce the deflection, or

- Adding a normal force perpendicular to the layers to increase the shear resistance so that slip may be prevented on the interfaces (Van der Merve, 2014).

Other factors such as controlling the span become very important when designs such as this are considered. Elastic beam analyses are not appropriate for a highly jointed rock mass.

Keyblock analysis

Explanation of the method. This method is usually employed in shallow environments, where the failure mechanism is largely controlled by structures occurring within the rock mass. In areas where these structures intersect each other, keyblocks may form resulting in instabilities. A keyblock is defined as a “finite block that is free to move into a free space (excavation) without displacing adjacent blocks” (Gumede, 2006), and will result in the subsequent unravelling of the adjacent surrounding blocks after it has fallen (Esterhuizen and Streuders, 1998). Once a keyblock is supported, the surrounding blocks will also be supported.

Several keyblock analysis programs have been designed in the past to do such analyses. A safety factor may be calculated for potentially unstable wedges incorporating support systems such as bolts, Shotcrete and support pressures using a deterministic analysis done by the Unwedge software (Hoek *et al.*, 1995). The Unwedge program (Rocscience, 2007) is however limited to the use of conditions where the *in-situ* stresses are low or in

conditions where the stress impact can be ignored without errors being introduced (Hoek *et al.*, 1995).

Another limitation of the Unwedge program, is that it only considers a single wedge at a time (Dunn *et al.*, 2008). This wedge has to be defined by three joints for the analysis. The approach does not give one an understanding of the likelihood of getting a particular wedge, neither does it consider the range of the sizes of the wedges (Dunn *et al.*, 2008)

A probabilistic approach of doing keyblock analysis, evaluating the risk associated with such instabilities using JBlock software (Rocscience, 2011) was developed and later modified by Esterhuizen (1996, 2003). The program provides the probability of a gravity driven FOG, potential keyblock dimensions and their reaction to the installed support system (Esterhuizen and Streuders 1998; Dunn *et al.*, 2008). The analysis also accounts for the joint properties. JBlock allows analyses of the distributions of the volume of possible keyblocks and the distribution of the probability of the keyblock failure (Nezomba, 2012). The modelling also allows the direct evaluation of expected rock fall injuries (Joughin *et al.,* 2012a, 2012b) and the economic losses associated with the injuries for a given support system.

Shortcomings of the method. The JBlock analysis is applicable for environments with low clamping stresses estimated between 1.0 kPa and 2.0 kPa (Joughin *et al.*, 2012b). There is a need for using this analysis with variable clamping stresses. This analysis only considers one failure modes

i.e. gravitation. It does not consider rock burst and seismically induced rock fall, pillar failure, unravelling, stress damage and time dependent deterioration. This program only considers a tensile state with no confining stresses.

The JBlock program was, however, considered to be suitable for use at Mine A, as the majority of the failure modes are gravity driven, mainly as a result of geological discontinuities/structures interacting together in a shallow environment where the clamping stresses are not significant.

2.3.3 Observational methods

This method is described by Swart and Handley (2005) as analysis based on daily monitoring to obtain visual outputs as mining advances. This daily monitoring entails underground geological mapping along with support quality and quantity evaluation in each working place. The underground inspections would also include records of layout and deviations from plan in each working place. Further additional support instructions are issued as per the observations.

During underground FOGs investigations, the volumes of the falls, including the fall out heights measurements are noted and kept within the database of the Mine. It is in these investigations where the failure mechanism in each FOG is described in detailed. Such data may be used to adjust the initial support design where the need arises. This becomes an ongoing process during the life of the Mine. The observational method in support design

forms part of the evaluation and optimization stages of the design methodology.

2.4 Collection of Data for the Research

Kemeny and Post (2003) recommend scanline mapping for the collection of the discontinuity data for keyblock analysis. The collected data must include measurements of the discontinuity properties, including orientation (dip, dip direction), rock type, length, joint roughness coefficient, moisture, wall hardness, wall alternation, separation and infill thickness.

Scanline mapping is defined as a collection of discontinuity data along a line. Only the discontinuities that intersect that particular line are measured, as shown in Figure 2.6 (Priest and Hudson, 1976; 1981). A discontinuity in this research is a collective term used to describe geological structures such as: joints, veins, bedding planes, faults, dykes stringers and other contacts (Signhal and Gupta, 2010).

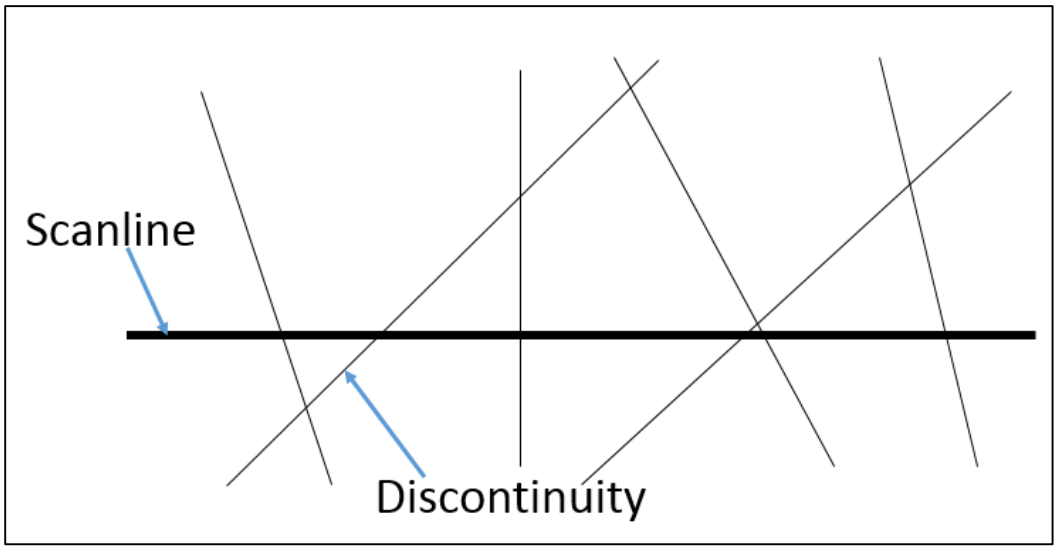


Figure 2.6: Discontinuity mapping in a scanline survey (after Priest and Hudson, 1981).

Gumede (2006) outlines the advantages of scanline mapping as follows:

- Easy processing and analyses of data.
- Proper organizing and controlling of the mapping and data.
- Good accuracy.

The disadvantages of scanline mapping are also described by Gumede (2006) as follows:

- Slowness in the measurements taken.
- Difficulty in detecting sparsely scattered/random discontinuities.

There are two main biases in this mapping method, i.e. the orientation and size bias (Baecher and Lanney, 1978; Baecher, 1983; Priest and Hudson, 1981). The orientation bias results in fewer measurements of discontinuities parallel to the scanline compared to those perpendicular to it. This bias is reduced in this research by taking measurements along three mutually

perpendicular, scanlines (along strike, along dip, across the stoping height). The size bias arises due to the length of the exposed discontinuity in the excavation (Gumede, 2006), therefore shorter joints are less likely to be to be picked up than longer joints (Gumede and Stacey, 2006).

2.5 Description of Data Inputs for the Research

Geological discontinuities such as joints, bedding planes, veins, faults, shear zones, dykes stringers and other geological structures form part of a rock mass. A discontinuity is defined by Priest (1993) as “a significant mechanical break or fracture of negligible tensile strength in a rock”. Although most structures influence the stability or strength of the rock mass, joints are the most commonly observed structures. When discontinuities interact they have an ability to form wedges and keyblocks that have a potential of falling. A Joint is defined by Carmichael (1988) as “a break of geological origin in the continuity of rock”, other authors such as Priest (1993) defines a joint as “fractures or cracks in the rock along which there been extremely little or no movement”.

2.5.1 Orientation/Attitude

The ISRM (1978) defines the orientation of a discontinuity as the “attitude in space”. In this report, the orientation is described by the dip and the dip direction. The maximum declination of a discontinuity surface measured from the horizontal is defined as a dip and the dip direction is the angle of the feature from true north (Figure 2.7). The dip angle is commonly expressed in two digits and the dip direction is expressed in three digits, e.g. 45°/230°. Parallel planes that have approximately the same orientation

are considered to be a set (Priest and Samaniego, 1983). The cut off variation of a set was limited to 20°. A variation of 20° was marked by Watson and Gerber (2018), stating that angles between 10° and 30° tend to have similar severity when modelled for instability.

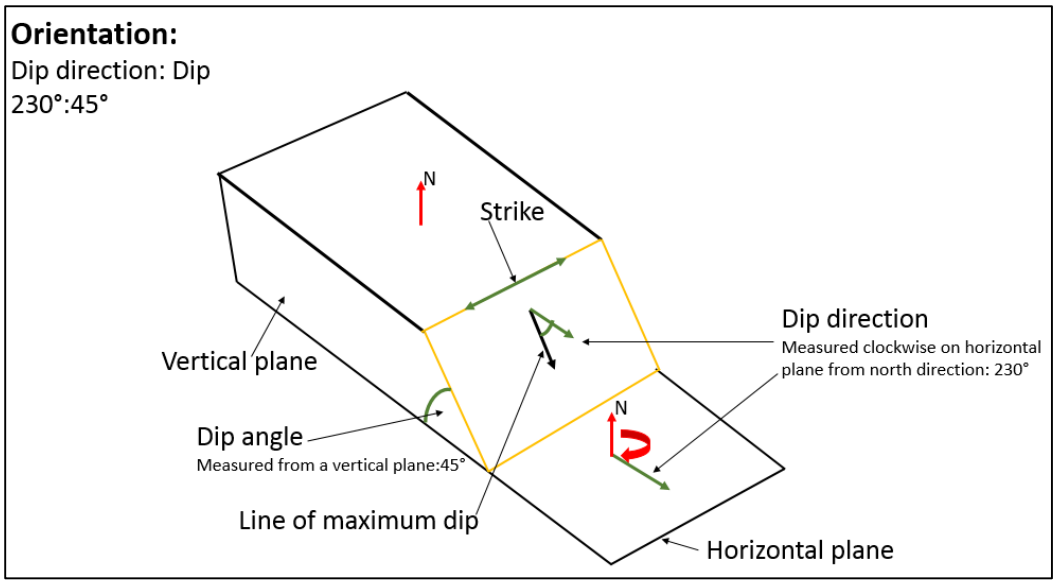


Figure 2.7: The illustration of the definition of dip and dip direction.

2.5.2 Spacing

The perpendicular distance between two parallel discontinuities is referred to as the spacing. The spacing is commonly denoted as modal or mean spacing joint sets (ISRM, 1978). The spacing of discontinuities in a rock mass influences the block sizes and are classified in Table 2.4 (Brady and Brown, 1993). Spacings can be even, clustered and random. Random discontinuities are considered to have a negative exponential distribution as described by Feng (1996). The correction for spacing bias is shown by:

$$f(x) = \lambda e^{-\lambda x} \ (0 \leq \mathrm{x} \leq \infty) \qquad [2]$$

Where:

$f(x) =$ Frequency of a given discontinuity spacing value x

$\lambda =$ Average number of discontinuities per meter

Table 2.4: The discontinuity spacing classification (Brady and Brown, 1993, ISRM 1978).

Description	Spacing (m)
Extremely close spacing	<0.02
Very close spacing	0.02-0.06
Close spacing	0.06-0.2
Moderate spacing	0.2-0.6
Wide spacing	0.6-2
Very wide spacing	2-6
Extremely wide spacing	> 6

A scanline of not less than 3.0 m and not greater than ten times the estimated spacing is recommended to ensure reliable results (Nezomba, 2012). Nezomba (2012) further states that the spacing in joints has an exponential or lognormal distribution. The spacing error, similarly defined by Terzaghi (1965) is illustrated in Figure 2.8 and corrected as follows:

$$d = l sin\theta \qquad [3]$$

Where:

$l =$ Distance between successive joints of the same set

d = True spacing distance

θ = The angle between the scanline and the mean orientation of the joint set

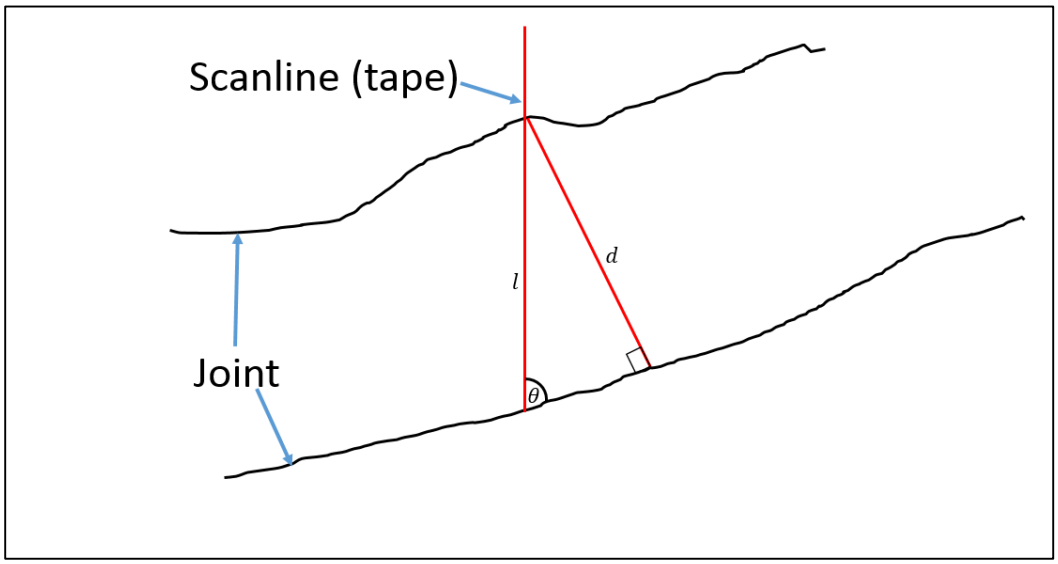


Figure 2.8: The illustration of joint spacing correction (Nezomba, 2012).

2.5.3 Length

Also known as trace, defined to be a line of a discontinuity that is exposed along excavations and therefore tracing the extent of the joint in the rock mass (Brady and Brown, 1993). Discontinuities form potential failure planes along the exposed length (Gumede and Stacey, 2006). The term trace length refers to the traceable/exposed portion of the discontinuity bearing in mind that the discontinuity may have the possibility of running into the rock mass further than the boundaries of exposure. For this reason two other biases, namely the size and the truncation, are present (Gumede and Stacey, 2006; Nezomba, 2012). Due to the biases, accuracy on the joint

length measurements is questionable. Correction of these biases is done using the standard sampling theory, i.e. a negative exponential distribution. This correction has been determined from the evaluation of extensive data (Priest and Hudson, 1981). Gumede (2006) summarizes that the given correction is done using a standard length L_s, instead of the actual sampling length L, therefore reducing all data to that which would have been sampled:

$$N''_{\delta j \vartheta j} = N'_{\delta j \vartheta j} L_s / L \qquad [4]$$

Where:

$N'_{\delta j \vartheta j}$ = Number of joints that would have been mapped

L_s = Standard length

L = Actual sampling length

$N''_{\delta j \vartheta j}$ Is the number of joints in a given class interval that would have been sampled had the stope been long enough to measure the standard length of the joint L_s.

The trace length is also referred to as persistence, Figure 2.9. The relationship between trace length and persistence is summarized in Table 2.5.

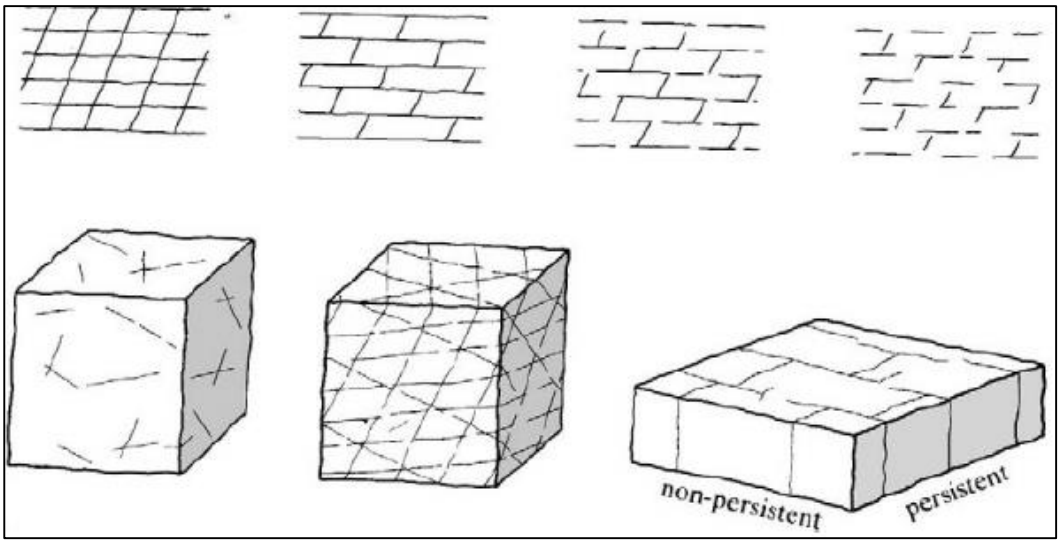


Figure 2.9: The illustration of the definition of persistence of discontinuity (Brady and Brown, 1993).

Table 2.5: The discontinuity persistence classification (Brady and Brown, 1993, ISRM 1978).

Description	Modal trace length (m)
Very low persistence	<1
Low persistence	1-3
Medium persistence	3-10
High persistence	10-20
Very high persistence	>20

2.5.4 Shear strength

Shear strength is an important property in discontinuities as it will either promote stability or sliding of blocks along the planes of each discontinuity. It is not only the geometry of the discontinuities, but also the shear strength, that plays a role in rock mass stability. Shear strength is described as the resistance to the sliding of blocks. In shallow environments, where the

stresses are low, the behaviour of the rock masses is largely controlled by sliding on the discontinuities. It is therefore important to understand the components that control sliding (Hoek, 2007). Several papers are written within the industry to determine shear strength. The two main factors that influence discontinuity strength are infilling material (in the discontinuities) and the roughness of the discontinuity plane. Authors such as Coulomb, 1776; Roberds and Eistein, 1978; Barton 1973, 1976 and Barton *et al*. 1984 developed methodologies to estimate the shear strength along joint surfaces. These models are summarized in Hoek, 2007 and Nezomba, 2012.

Coulomb (1776) developed a relationship between the peak shear strength τ_p and the normal stress σ_n and represented as the Mohr-Coulomb criteria as:

$$\tau_p = \mathrm{C} + \sigma_\mathrm{n}\tan\phi \qquad [5]$$

Where C is the cohesive strength of the cemented surface and ϕ is the friction angle. Coulomb (1776) highlights the shortcoming of this theory to be that it assumes a linear relation of the shear strength and the normal stress whereby at higher normal stresses, the shear strength will be overestimated, eliminating that reality of a non-linear shear-strength normal-stress relationship. Patton (1966) showed a bilinear relationship when 'saw tooth' specimens were used to perform tests and the results were used to establish an empirical formula represented as:

$$\tau = \mathrm{C} + \tan(\phi_{\mathrm{b}} + \mathrm{i}) \qquad [6]$$

Where $\phi_b$the basic friction is angle of the surface and i is the angle of the saw-tooth face.

The Patton (1966) criterion illustrates natural discontinuities which are known to have asperities and undulations which influences the shear behaviour. The saw teeth tend to be damaged at higher normal stresses where strength of the intact rock is surpassed therefore resulting in a shear strength behaviour similar to the one of the intact material strength. A similar trend is observed on the smooth plane in that both are non-linear at higher normal stresses (Jager and Ryder, 2002). The frictional characteristics of surfaces is illustrated in Figure 2.10 (Patton, 1966). The Patton theory is valid for low normal stresses.

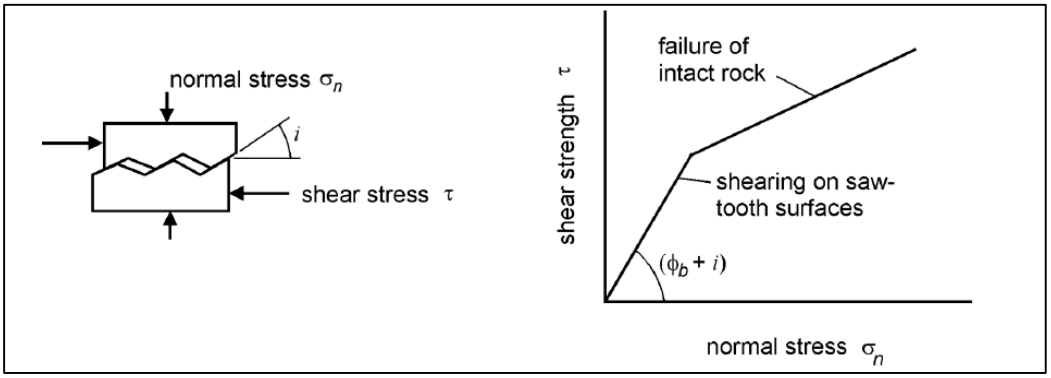


Figure 2.10: The illustration of Patton's experiment on shear strength of saw-tooth specimens (after Patton, 1966).

Barton (1973; 1976) proposed an empirical approach that replicates reality, in that it allows for a non-linear normal stress with shear strength relationship. The relationship is shown by:

$$\tau = \sigma_n \tan\left(\phi_b \mathrm{JRC} \log_{10}\left(\frac{\mathrm{JCS}}{\sigma_n}\right)\right) \quad [7]$$

Where JRC is the joint roughness coefficient and JCS is the joint wall compressive strength. The equation above was subsequently modified by Barton and Choubey (1977), where the basic friction angle was substituted by the residual friction angle following a number of direct shear tests. This empirical formula has shortcoming as the joint behaviour is well represented at peak shear strength but does not cater for post- and pre-yield behaviour (Nezomba, 2012).

An approach to determine the friction angle was provided by Barton (2002) as a representation of sheared discontinuities, outlined as:

$$\phi = \tan^{-1}\left(\frac{\mathrm{Jr}}{\mathrm{Ja}}\right) \quad [8]$$

Where Jr is the joint roughness condition and Ja is the joint alteration number. This approach assumes that discontinuities have no cohesion which is the reality for sheared discontinuities.

CHAPTER 3

3. METHODOLOGY

The previous Chapter detailed the different support design methods used in a shallow mining environment along with the shortcomings of each method. A probabilistic approach with benefits outlined in Chapter 2 was found to be the appropriate design method to apply in this Mine to determine support requirements. The probabilistic analysis in this report, was done using the version of the JBlock program that was modified by Joughin *et al.* (2012a, 2012b). The input parameters for JBlock modelling, as well as the method used for joint data collection were described in the previous Chapter. This Chapter will describe the underground collection and analysis of the data and show the resultant inputs that were used in the JBlock software program. The results of the analysis will be provided in Chapter 4.

The JBlock program generates keyblocks and provides failure probabilities, using data that was collected underground. The data was accumulated from geotechnical mapping of discontinuities as described in Chapter 2. The data collection was done on both reef- strike and dip directions to ensure accuracy of the data collection (Joughin *et al.,* 2012a, 2012b).

The following discontinuity parameters are needed for the JBlock evaluation:

- The orientation (dip and dip direction);

- Persistence/length;
- Spacing and
- Shear strength (roughness and infill characteristics).

Each input parameter is described in Chapter 2. The discontinuity dip and dip direction were measured using a compass. The persistence was measured using a distance measuring device. Distances between the discontinuities along a line traverse were converted to calculate the true spacings (perpendicular to each discontinuity strike). The shear strength was estimated using a method described by Barton (1973; 1976); Barton and Choubey (1977); Barton and Bandis, (1990) and Barton (2002) as described in Chapter 2. The mean and standard deviation of each component was required for the analysis.

3.1 Underground Joint Mapping

Scanline mapping was done in all active panels/stopes on the Mine. Seven mining levels were included in the mapping, on both the eastern and western sides of the Mine. These levels range in depths between 386.0 m and 527.0 m. The mapping was carried out along scanline tapes parallel and perpendicular to the face (Figure 3.1), as well as in the vertical direction, i.e. down the face. A minimum joint length cut off limit of 0.5 m was used in the exercise (Nezomba, 2012). The dip and dip directions of the panels in two different mining directions are 9° and 005°, and 0° and 095°, respectively.

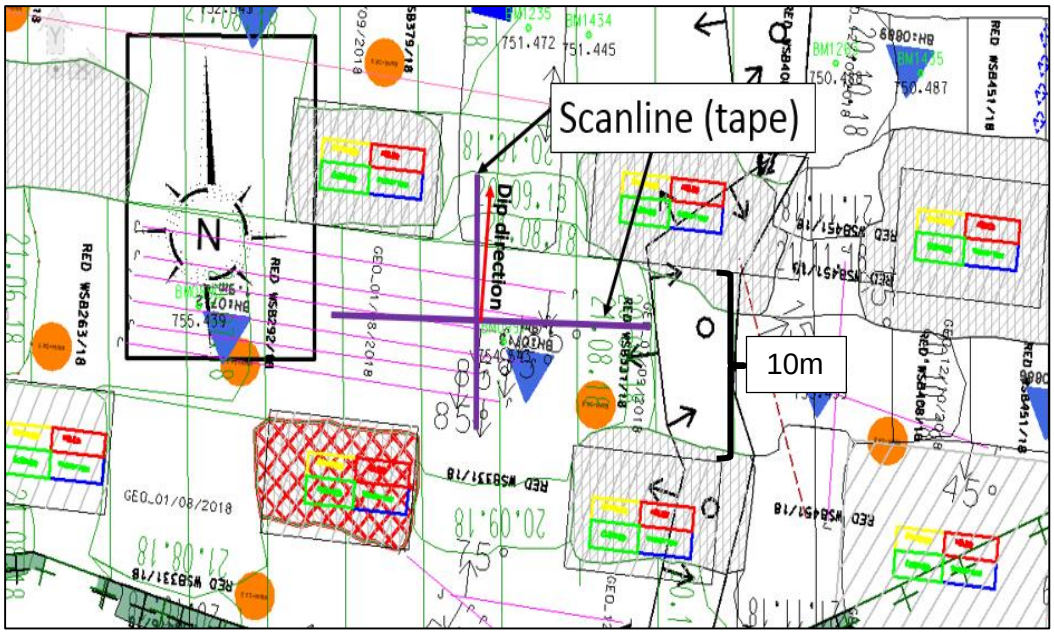


Figure 3.1: The Mine plan indicating mapped panel and the direction of the scanline tape.

A total of 1113 joints were mapped for the purpose of this project. This number greatly exceeds the 150-350 observations, suggested by Priest (1993) for a reasonable assessment. The scanline lengths ranged between 10.0 m to 12.0 m. The orientations of the joints were measured using a Brunton TRUARCH 15 compass (Figure 3.2). Readings were done cautiously away from magnetic objects such as tendons and dykes. The readings taken on dykes were confirmed on the mining plans using the software program micro-station, which allows for relative dip direction measurements to be corrected.



Figure 3.2: The Brunton TRUARC 15 compass (Brunton, 2018).

Recordings of the joint distances were done where the joints intersected the tape. The persistence/length was measured along the length of exposure, as the extent along strike where the joint intersected the hangingwall. Visual analysis of the joint planes was done when assessing the joint wall and infill properties. Section 2.5.4 describes the Barton (2002) method that was used to determine the joint shear strength properties. The orientation of the scanline was recorded to ensure that the spacing correction error was properly done. Table 3.1 shows the log sheet that was used for the mapping. All the collected information is provided in Appendix C.

Table 3.1: The scanline mapping log sheet (OHMS, 2019).

JBLOCK LOG SHEET

Workplace: Excavation height: Excavation width:
Scanline: Date:
Dip: Recorded by:
Dip direction:

Location	Lithology	Joint set	Joint number	Distance from start	Persist	Ends	JRC	M	H	J_a	S	T	HL	S/Wall or H/Wall	Notes and Comments	Dip	Dip Direction

3.2 Joint Data Analysis

From the range of collected joint data, the joints were grouped into sets using the Dips program (Rocscience, 2001). A magnetic declination of 17.8° was used to correct orientations, and the true orientation was entered into the Dips program. This program enables the determination of mean and the standard deviation for joint orientations. The mean and standard deviation was checked manually using excel during the data processing stage.

The Dips program allows the clustering of the joints to be done manually, which allows visual grouping of the joints into sets. Once the joints have been grouped, the analysis of the data is simplified. Figure 3.3 and 3.4 shows the joint set analysis, as provided by the Dips program. Note that these Figures do not show all 1113 joints, as some of the joints plotted on top of each other (Rocscience, 2001). However, the contour plot shown in Figure 3.4 included the influence of all the joints.

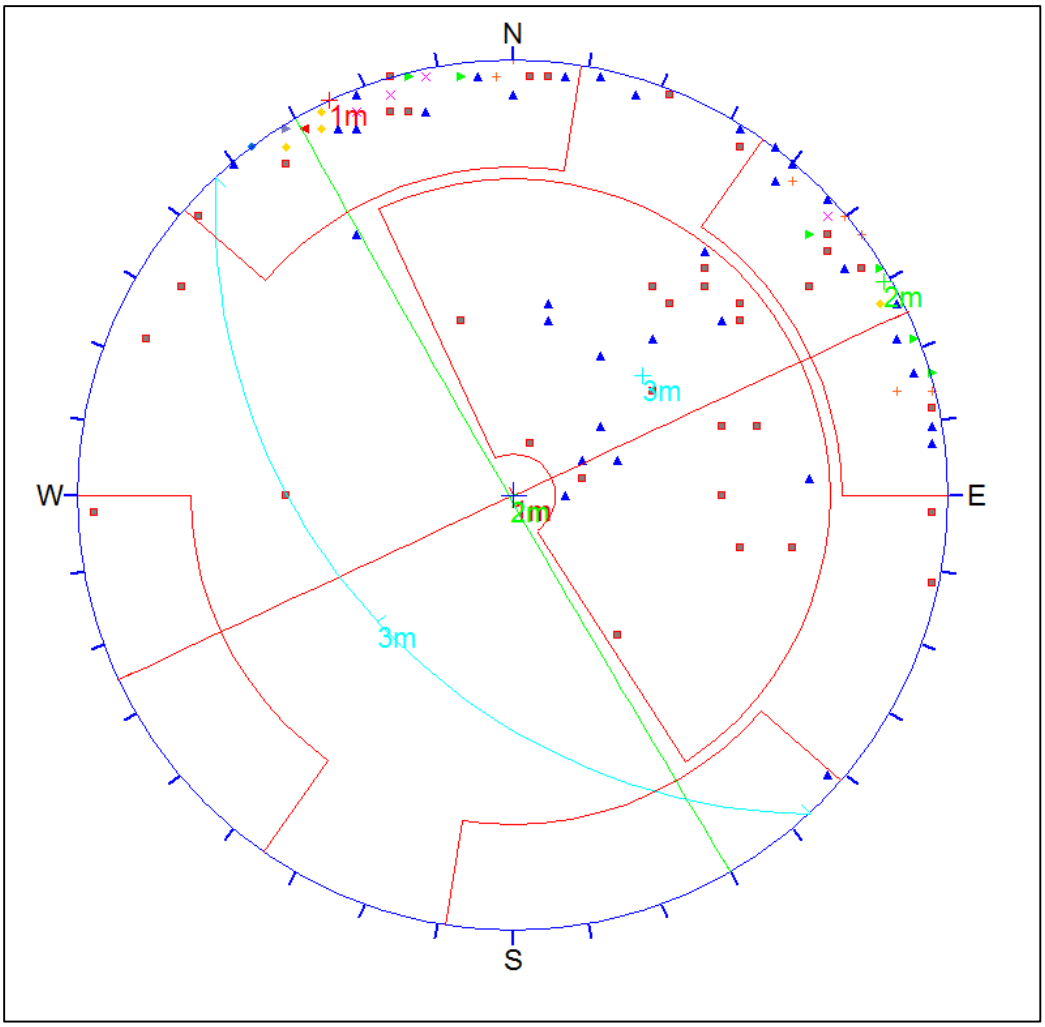


Figure 3.3: Lower hemisphere meridional stereonet projections of the mapped joint poles and the great circles of the manually evaluated sets using the Dips program.

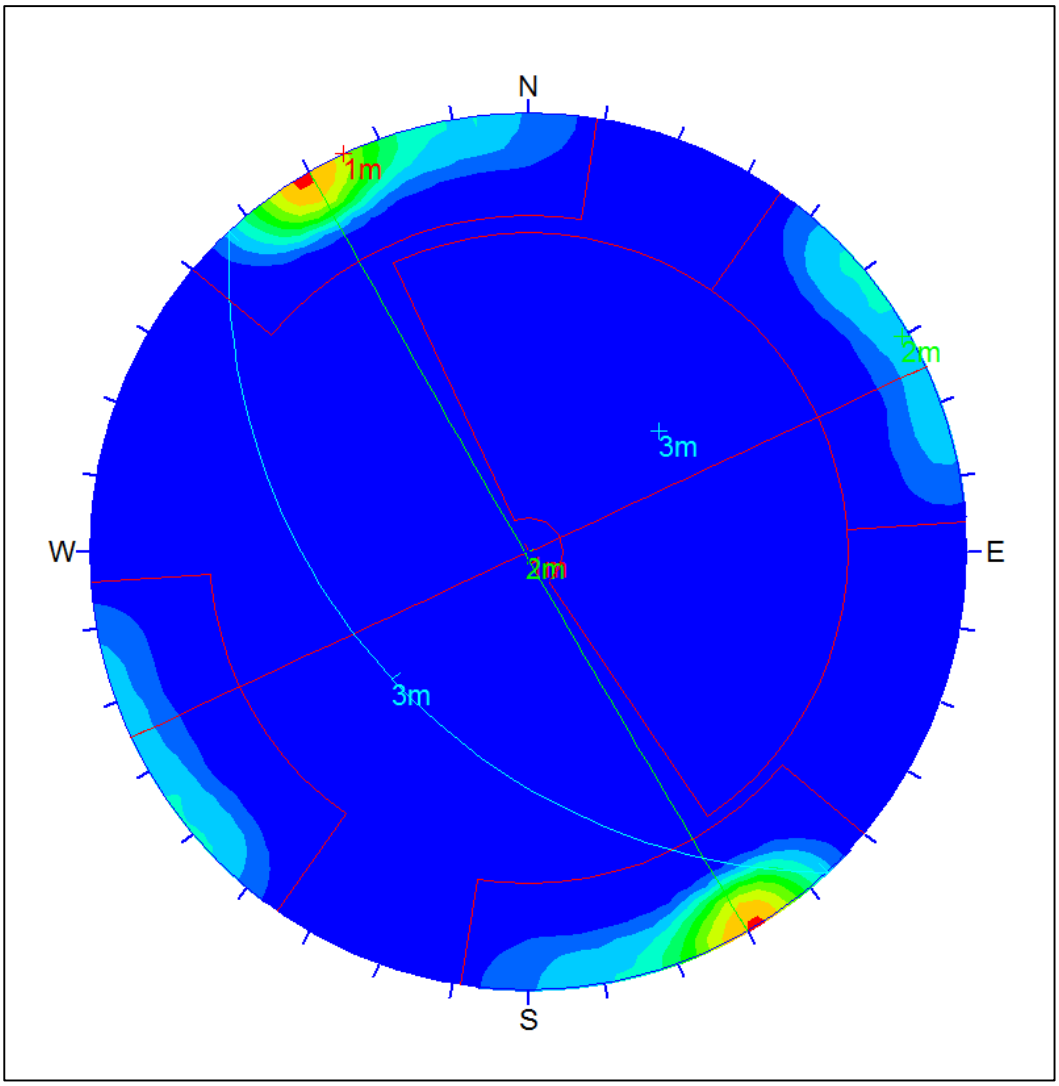


Figure 3.4: Lower hemisphere meridional stereonet projections showing the Dips program contour plot of joint poles and the manually evaluated sets shown by the great circle.

Joint lengths were limited to exposures. The minimum joint lengths are considered to be more accurate than the maximum joint lengths as they were based on observed exposures. A minimum value of 0.5 m and a maximum of 30.0 m was used in this research. Note the dip of the low angled random joint set was averaged to 50.5°±18.6°.

The Barton (2002) model was used to calculate the friction angle as shown in Section 2.5.4, equation number 8. Friction angles were calculated for each joint. Since there were variations in friction angles for each joint, a mean and standard deviation were calculated for each set. The two main infill types were serpentinite and calcite. A slight amount of weathering was also observed along the majority of the joints planes. The vast majority of joints had smooth to rough, planar surfaces.

The apparent spacings of joints was determined using the distance between the consecutive joints along the scanlines. The spacing was corrected to the true joint spacing by applying the correction of orientation bias, described in Section 2.5.2. This correction uses the angle θ between the scanline tape and the joint set. A mean and standard deviation was determined for the orientations of each set. The joint spacings of the two orthogonal joint sets follow a negative exponential curve as shown in Figure 3.5, 3.6 and 3.7. This distribution is similar to data obtained by Priest and Hudson (1981), and again by Gumede (2006). The negative exponential curve was therefore used in the analysis to determine the correction of the discontinuity bias. The results of the calculated joint properties for all joint sets are provided in Table 3.2.

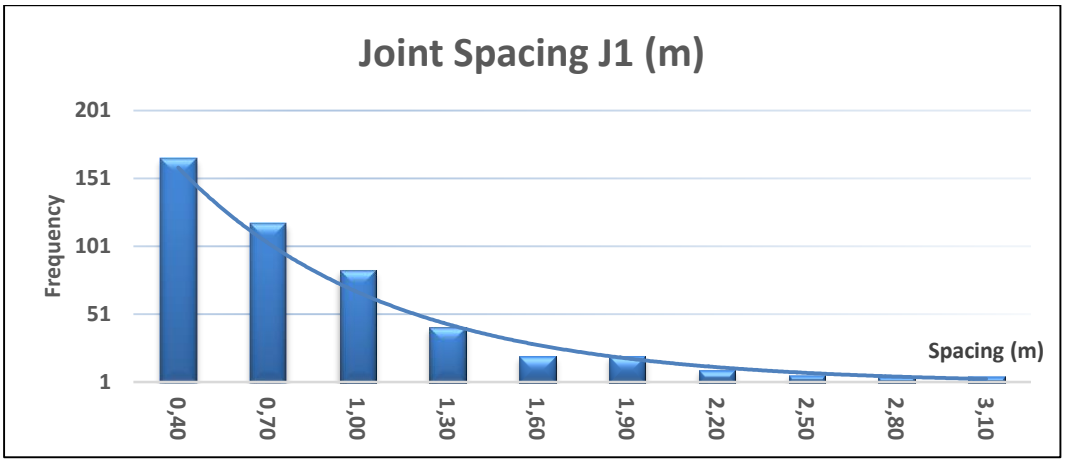


Figure 3.5: Joint spacing data of Joint set 1 indicating a negative exponential distribution.

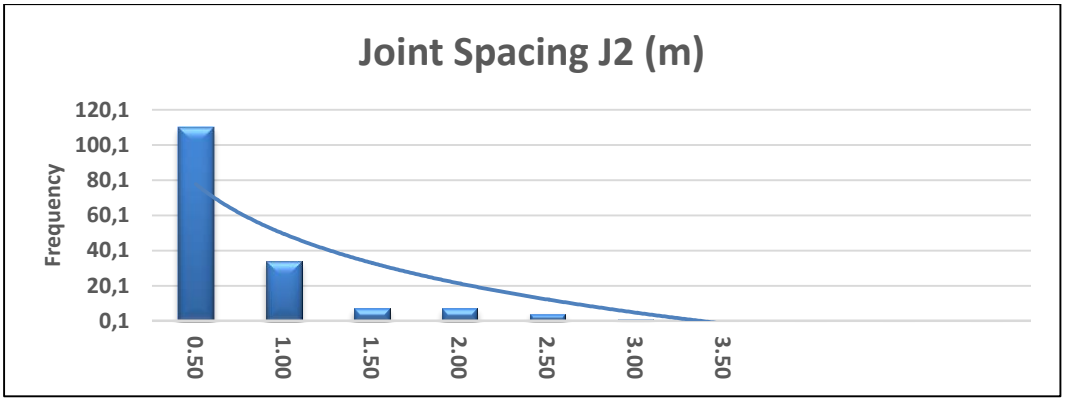


Figure 3.6: Joint spacing data of Joint set 2 indicating a negative exponential distribution.

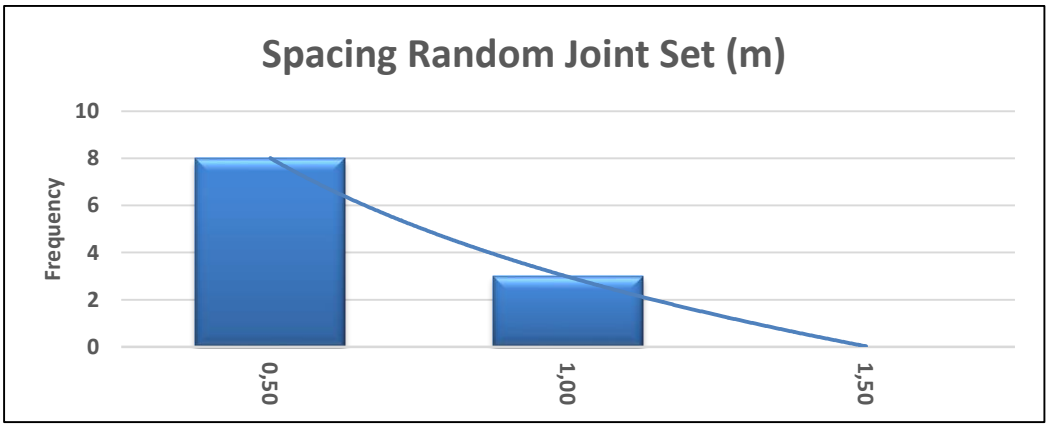


Figure 3.7: Joint spacing data of the random joint set indicating a negative exponential distribution.

Table 3.2: Summary of joint properties.

Factor	Descriptive Statistics	Joint Set 1	Joint Set 2	Random Joint Set 3
Dip	Mean	89.74°	87.30°	50.50°
	St dev	1.66°	9.65°	18.63°
Dip Direction	Mean	156.48°	239.33°	225.15°
	St dev	13.13°	14.71°	42.14°
Persistence	Mean	24.92 m	9.40 m	13.00 m
	St dev	0.31 m	0.40 m	0.52 m
JRC	Mean	1.26	1.18	1.30
	St dev	1.08	1.32	2.06
Wall Hardness	Mean	2.00	2.00	2.00
	St dev	0.00	0.00	0.00
Joint Alteration	Mean	1.00	1.00	1.00
	St dev	0.00	0.00	0.00
Thickness	Mean	2.26 mm	2.26 mm	1.85 mm
	St dev	0.49 mm	0.46 mm	0.48 mm
Healing	Mean	0.00	0.00	0.00
Spacing	Mean	0.88 m	0.78 m	0.65 m
	St dev	0.61 m	0.54 m	0.34 m
Φ (Barton)	Mean	47.96°	45.88°	45.10°
	St dev	9.47°	5.58°	7.77°

3.3 Description of JBlock input parameters

The joint information such as the joint orientation, length/persistence, spacing and the friction angle were used as input parameters in the JBlock file. These parameters were saved as the geotechnical domain file.

3.3.1 Geotechnical domain file

The geotechnical parameters for each joint set was entered into the JBlock file as shown in Figures 3.8 and 3.9. The program was run for two Scenarios:

- Scenario one was done without the random low angled joint set and;
- Scenario two included the random low angled joint set.

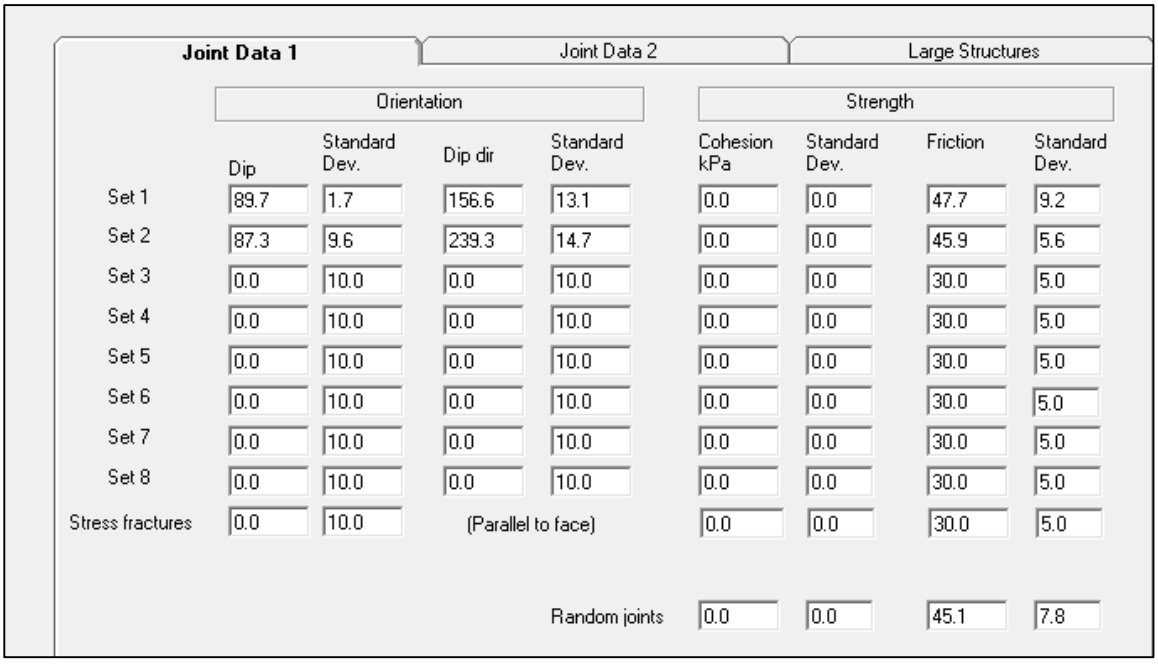


Figure 3.8: JBlock image of the joint data 1 input.

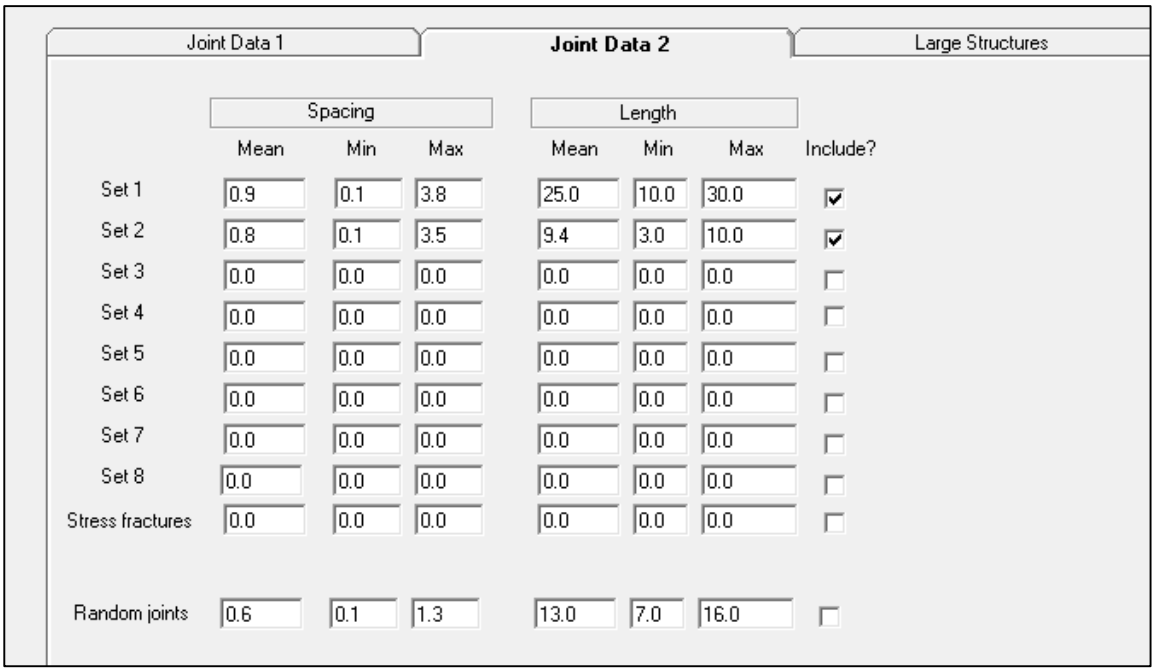


Figure 3.9: JBlock image of the joint data 2 input.

The large structures included in the geotechnical domain file described the Triplets layer, which form part of the parting planes (Figure 3.10). The height of the Triplets parting planes was determined from the geological UG2 to Triplets isopachs, and borehole data, drilled at every intersection on the Mine. The isopachs are shown in Figure 3.11. Triplets heights of 2.5 m, 2.3 m, 2.0 m, 1.8 m, 1.7 m, 1.5 m and 1.3 m were used in separate models. The lowest modelled Triplets height was 1.3 m, considering that the current 1.5 m resin bolt, with critical bond length of 25 mm, would be able to carry the weight of any thickness less than 1.2 m provided no discontinuity weakens the rock mass. Zero tensile strength and zero cohesion was applied to the Triplets and joint planes, respectively. The zero cohesion assumption was applied to all joint sets, therefore, assuming a worst case Scenario for the project purposes.

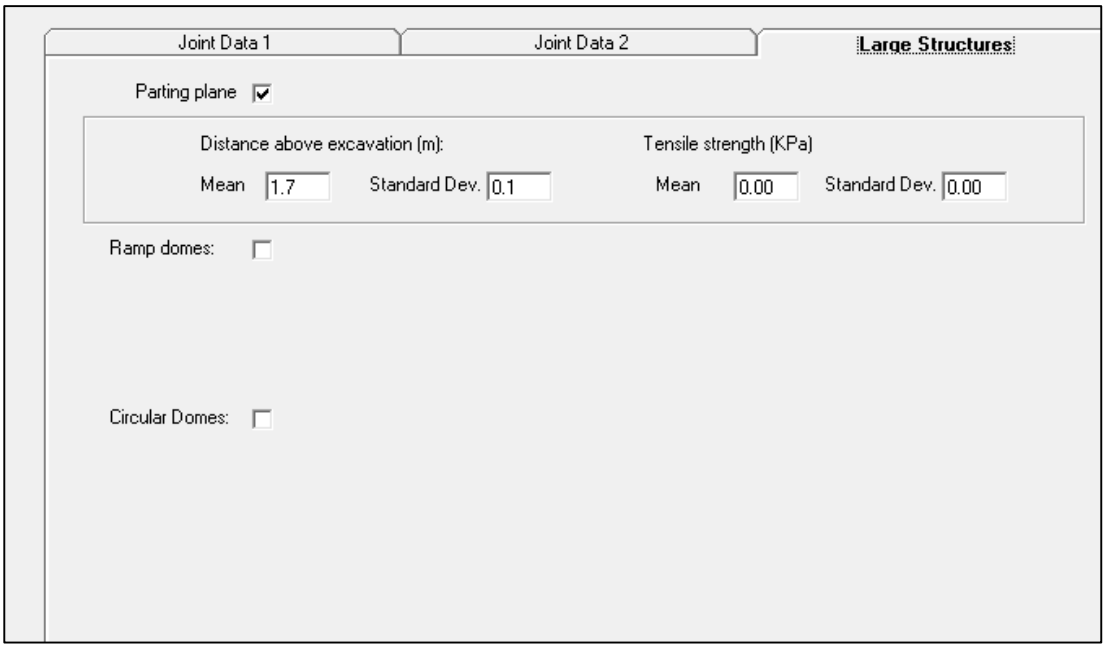


Figure 3.10: JBlock image of the large structures input.

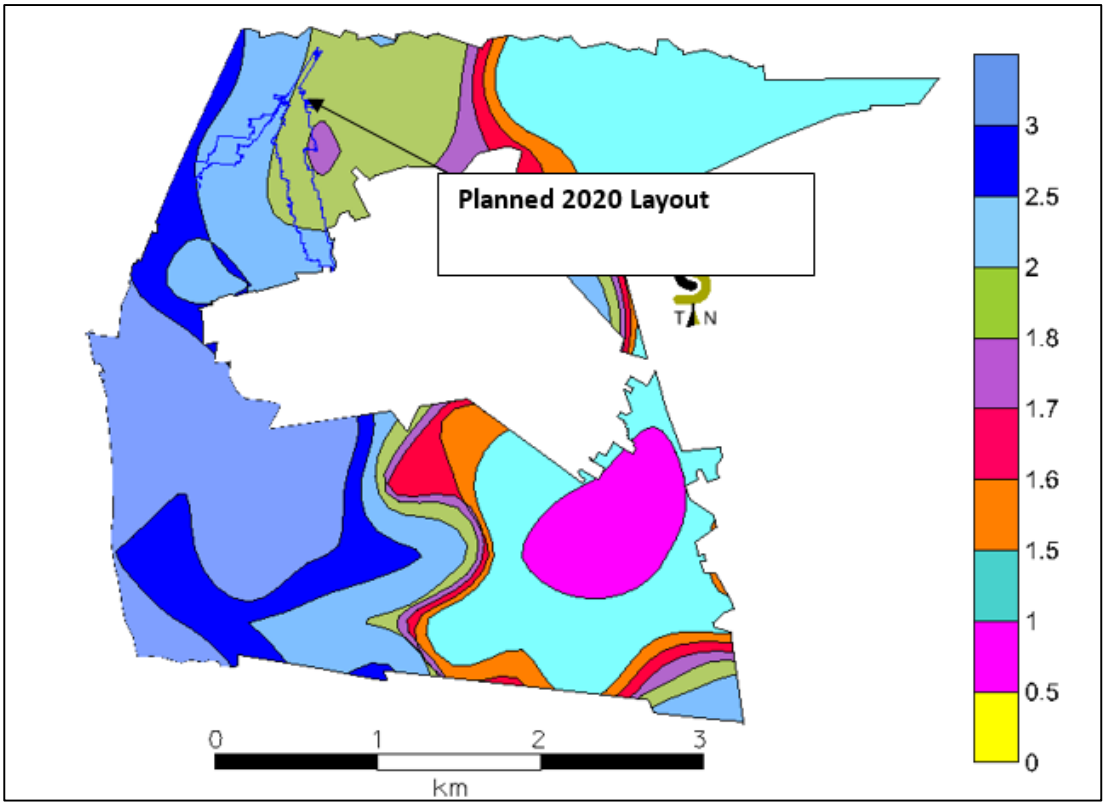


Figure 3.11: UG2 to Triplets layer isopachs (Kekana, 2018).

3.3.2 Excavation file

This file provides for the panel geometries and mining. The excavation outlines shown in Figures 3.12 and 3.13 represent the panels developed along strike and along the dip of the reef. Both excavation directions were used for each model Scenario as described in Section 3.3.1. The two Scenarios were necessary to ensure that both mining directions, currently done at Mine A were accommodated (Figure 3.12 and Figure 3.13). The excavation orientations, face advance per blast (2.1 m) and the direction of the advancing face also formed part of the input parameters.

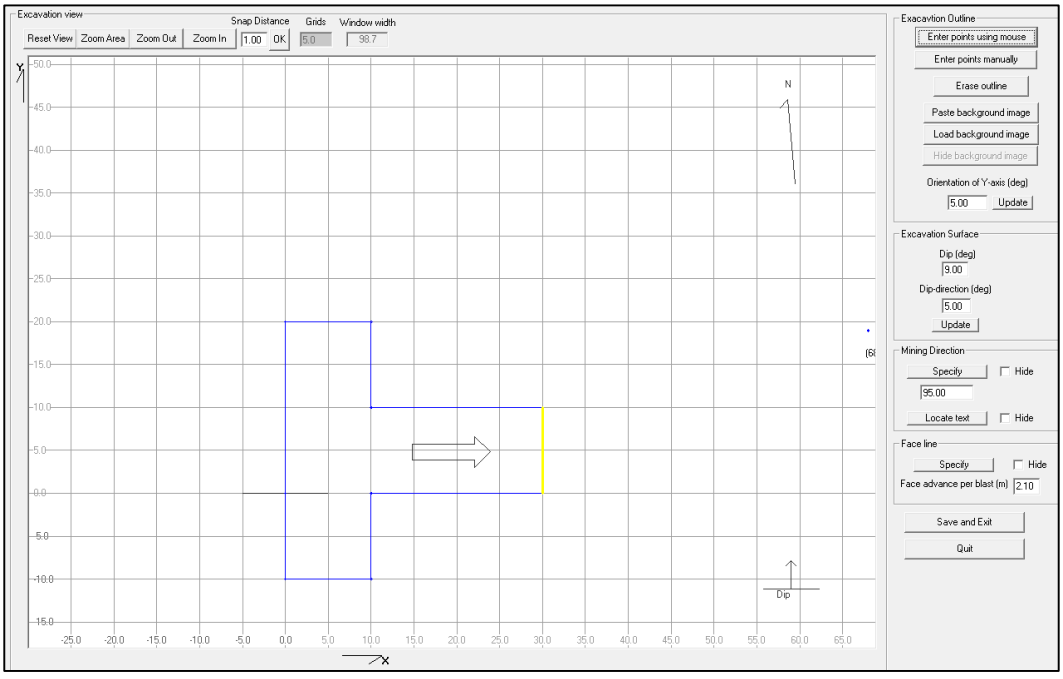


Figure 3.12: JBlock image of the excavation file for a panel along strike.

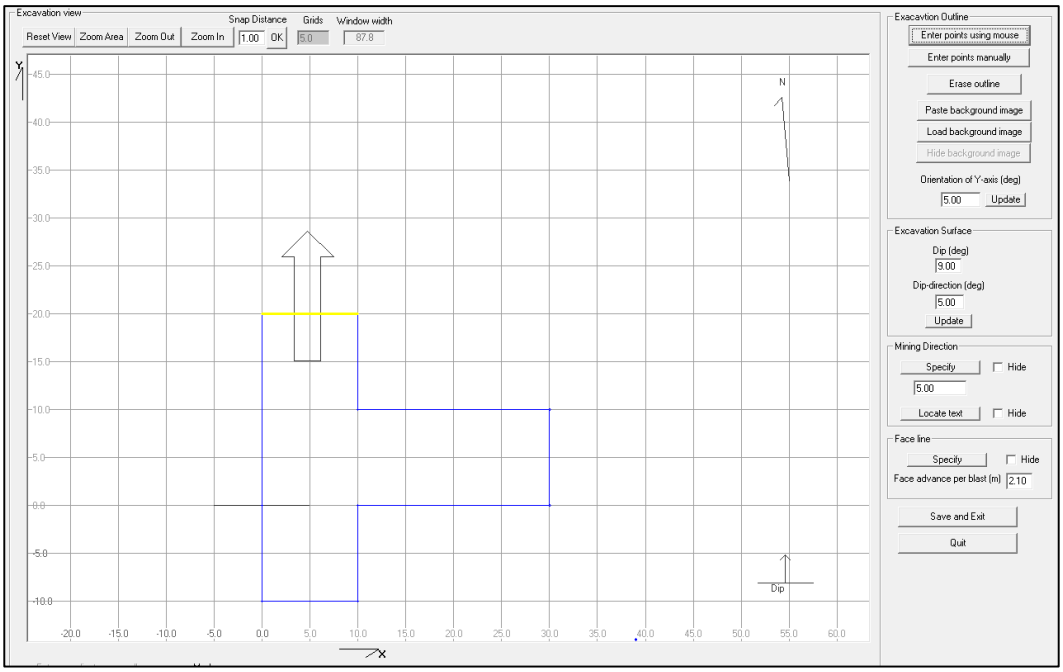


Figure 3.13: JBlock image of the excavation file for a panel along dip.

In the final analysis, the geotechnical domain file is combined with the excavation file so that the distribution and size of possible keyblocks may be calculated.

3.3.3 Support file

As described in Section 1.3, the research focuses on the face area, which was described as the first 3.1 m from the face. This area is defined in the research as the “high risk” area where many activities are executed during mining.

The support elements and spacings currently used on the Mine are shown in Figure 1.6 (Section 1.1), attached again below.

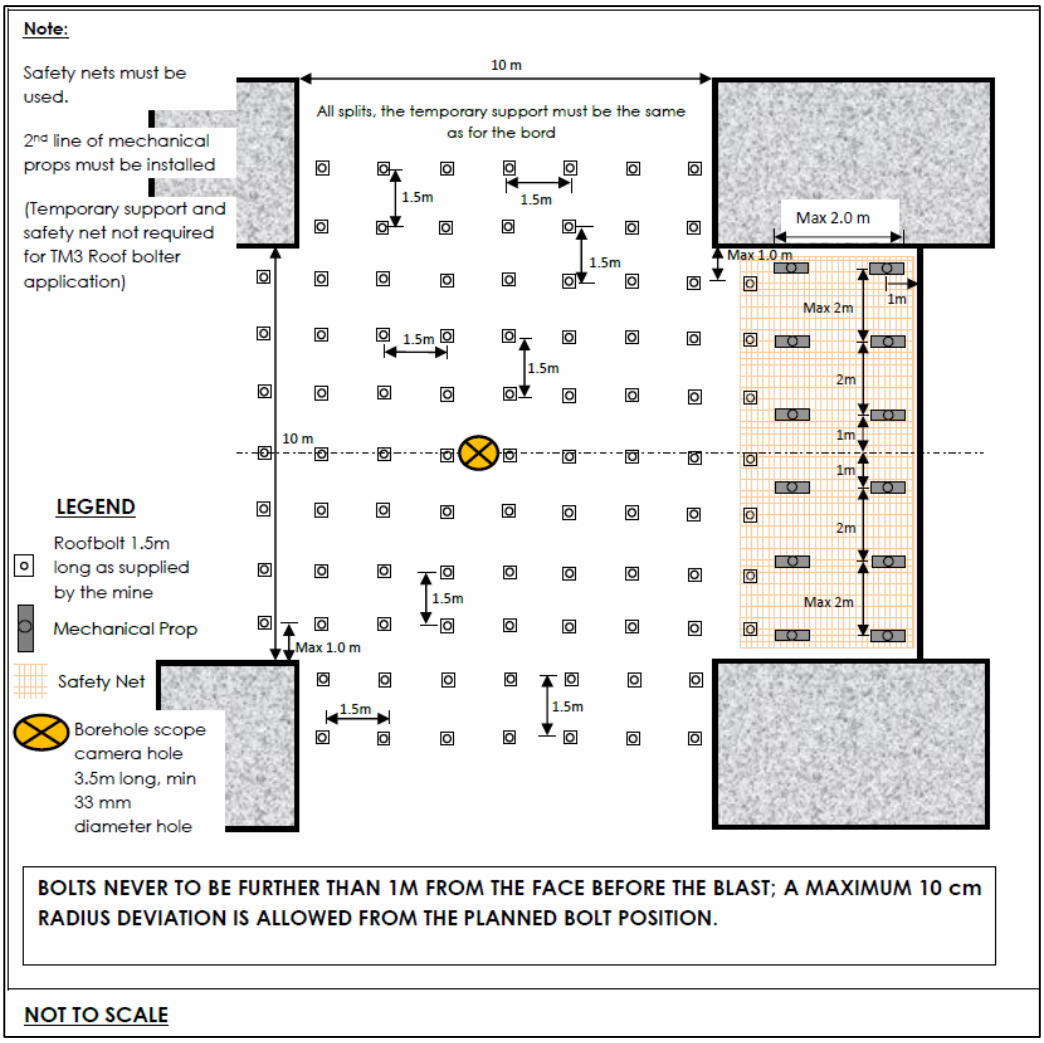


Figure 3.14: The support standard for the UG2 reef, (Sibanda, 2018).

Resin bolts of 1.5 m in length were initially modelled at a spacing of 1.5 m X 1.5 m. These bolts have a peak strength of 117.8 kN ± 13.7 kN (90.0 % confidence as shown in appendix E) and a resin bond strength of 392.0 kN/m ± 39.0 kN (values obtained from short encapsulation tests done at the Mine).

The support units were added into the model, in the same sequence as underground. Therefore, the unsupported span where people are exposed during the drilling of the support holes, was included. This is the time after

the face has been advanced, and requiring the installation of temporary support units. This phase is deemed to be the most dangerous part of the entire cycle.

Sensitivity analyses were done on several bolt lengths, i.e. 1.5 m, 1.8 m and 2.5 m, and support configurations. The 1.5 m long resin bolts were incorporated with a strength of 117.8 kN ± 13.7 kN and a resin bond strength of 392.0 kN/m ± 39.0 kN. The 1.8 m long resin bolts were incorporated with a strength of 200.0 kN ± 5.0 kN and a resin bond strength of 400.0 kN/m. The 2.5 m long coupling resin bolts were incorporated with a peak strength of 213.8 kN ± 38.4 kN and a grout bond strength of 430.0 kN/m ± 43.0 kN (90.0 % confidence as outlined in appendix E). The difference in the strength is because there is a standard diameter for each bolt length on the Mine. The bolts diameters are 18 mm, 20 mm and 22 mm for 1.5 m, 1.8 m and 2.5 m long bolts, respectively.

Safety nets and the Camlok props were incorporated in the model, as the main purpose of the project is to validate the current design used at Mine A. The Camlok props and the nets were installed at a peak strength of 80.0 kN ± 8.0 kN and loading capacity of 20.0 kN/m^2 ± 2.0 kN/m^2, respectively.

Wire-mesh and Osro straps were omitted in the initial models as they are currently not used in the Mine. However, the Wire-mesh and Osro straps were incorporated in later models to determine the influence of Wire-mesh

on stability. Watson and Gerber (2018), suggested that where shallow dipping discontinuities exists in a 6.0 m span (bolt spacing of 1.5 m X 1.5 m), a bolt length of 1.8 m is required at a minimum support resistance of 48.0 kN/m^2 for typical UG2 excavations. The combination of the Wire-mesh and Osro straps used in the analysis had a tensile strength of 45.0 kN/m^2 ± 5.0 kN/m^2 (Watson *et al.*, 2017).

The support file allows the simulations of the hazard zones; two zones were identified for the purposes of this project:

- Face area up to 3.1 m behind the face; and
- Back area, i.e. between 3.1 m and 10.0 m from the face.

Out of a total of 7 people in the panel, 5 are Rock Drill Operators (RDO's) which are mainly in the face area zone. It is in this zone where most activities such as drilling, blasting, supporting and cleaning takes place. Most of the recorded falls of ground in the Mine are observed within this zone. The back area is where the entry examinations begins, i.e. early entry examination focuses on the first 10.0 m back from to the panel face. There is minimal work done in the back area during the shifts, however, temporary storage of material, used in the shift, is sometimes within this zone, and painting of the support grid lines to ensure the support is correctly installed is also done from 10.0 m back.

The presence of exposure was allocated in the models as hazard zones. These zones allow the input of people numbers, expressed as a percentile

of time. 80.0 % of time was allocated for zone 1, which is the face area, and the remaining 20.0 % of time was allocated to zone 2, which is the back area (Figure 3.14). This assumption was made based on the underground observations during the start to the end of shift. It is this information, together with the number of the people present in each zone, which allows JBlock to calculate/estimate the injuries. The analysis is provided in Chapter 4.

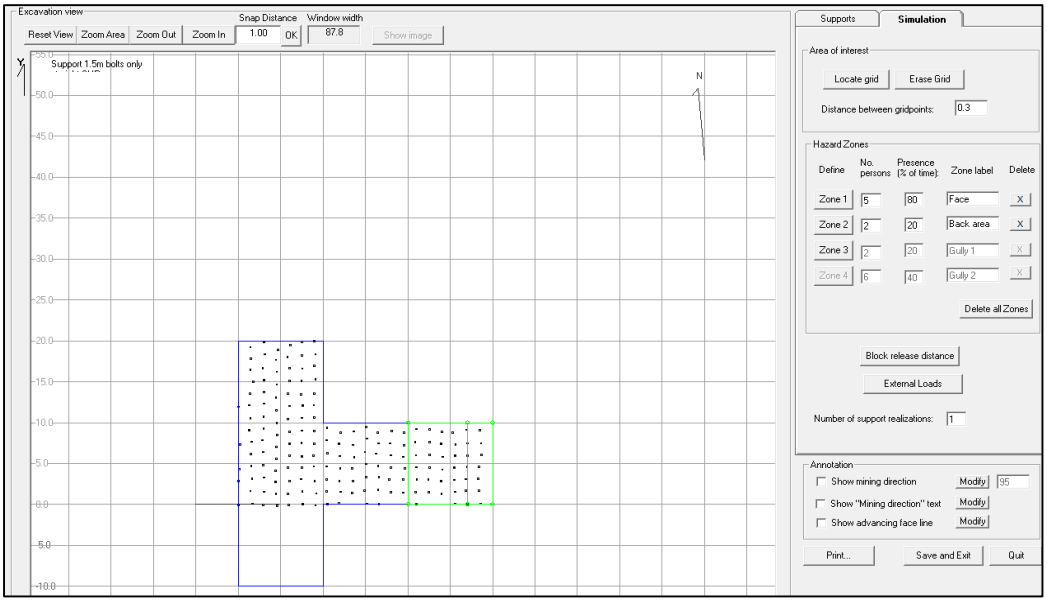


Figure 3.15: JBlock image of the excavation and the delineated hazard zone.

Nezomba (2012) determined that 65.0 % of rock fall occurred with the blast, using both daily observations and historic data. The probability and location of the block fall outs, relative to the face, are shown in Figure 3.15. In this analysis, 69.0 % of the keyblocks were fixed to fall out during the blast in zone 1, as soon as they get totally exposed on the face and 31.0 % were fixed to fall later after the blast within 3.1 m to 10.0 m of the face at a

probability of 90.0 %. These values are based on the historical rock fall data summarized in Table 3.3.

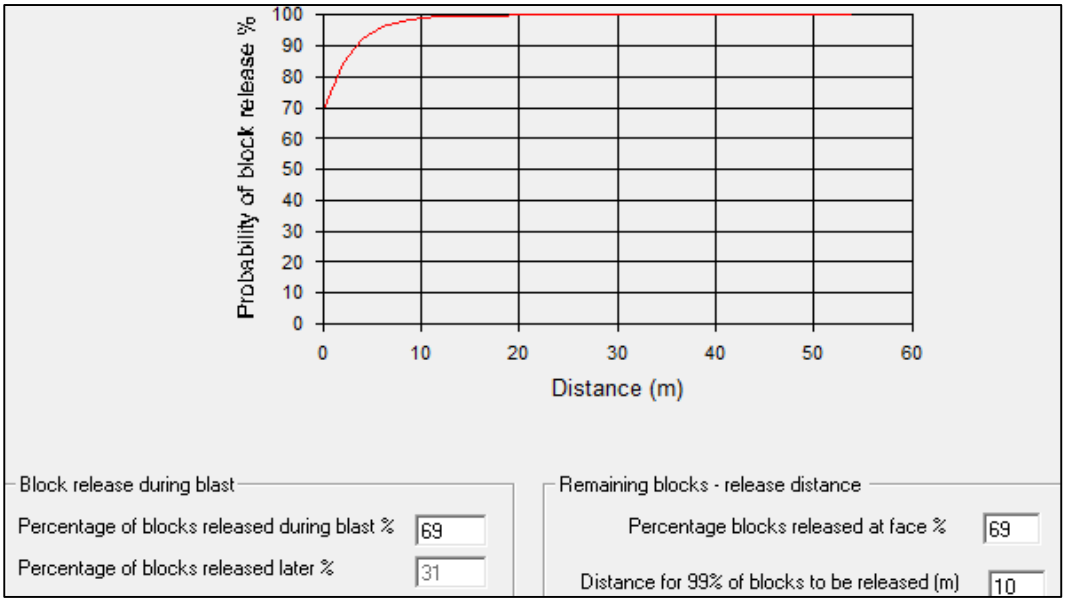


Figure 3.16: JBlock image of the keyblock release distance and probabilities.

Table 3.3: Summary of historical rock fall data at Mine A from 2012-2018.

% of FOG falling with the blast	% of FOG falling after the blast	Total number of FOG
69	31	35

100.0 % of the loose rocks were assumed to fall within 10.0 m from the face. The modelling was done to include both the face area and the back area zones, i.e. the first 10.0 m of the panel.

No signs of seismicity have ever been observed in the Mine and therefore no external loading forces or seismicity were included in the models. The

Mine operates under shallow environment conditions with the expected failure mechanism outlined in Section 2.3.

3.3.4 Summary

The JBlock program relied on the geotechnical data and the excavation outline to get an output of the distribution of the volume of possible keyblocks. From the keyblocks data incorporated with the support Scenarios, the number of falls and possible injuries were determined for each zone. The results are provided in Chapter 4.

CHAPTER 4

4. JBLOCK RESULTS AND ANALYSIS

Chapter 3 detailed the methods of underground collection and analysis of the data and provided the inputs used in the program. This Chapter shows the results of the numerical analyses. The investigation results will be compared to internationally acceptable risk in Chapter 5.

JBlock quantifies the potential rock fall by allowing a set of various size keyblocks to be generated. The formation of keyblocks in the JBlock program is simulated from the recorded discontinuities, which are projected in 3D (Figure 4.1). This is achieved by allowing the hangingwall of the excavation to be simulated with the discontinuity traces (Joughin *et al.*, 2012a). A record of the hangingwall surface that did not form keyblocks is also kept within the program. The total area is the combination of the hangingwall surface area of all blocks (hangingwall surface area exposed during the simulation), referred as the area mined as illustrated in Figure 4.1 (Joughin *et al.*, 2012a). The area mined plays a role in standardizing the data. In this research, the results data was normalized to a total exposed area of 10 000 m^2. For comparative reasons it was necessary to normalize the exposed area, and for ease of calculation, a rounded figure of 10 000 m^2 was used. However, there is no other reason for normalizing to this particular area.

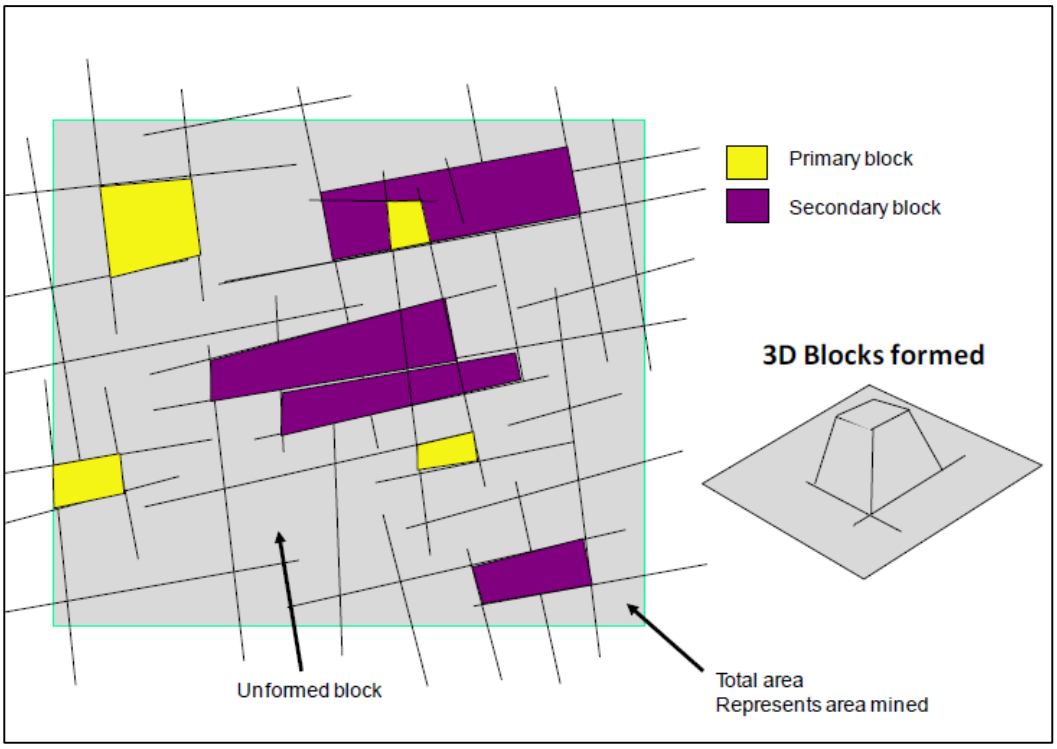


Figure 4.1: A plan view of a mining area indicating the trace of joints in the hangingwall with primary and secondary block formation (after Joughin et al., 2012b).

The stability of each block is tested in JBlock as all blocks will be placed in the stope area one by one. JBlock will test this stability by examining the support in relation to where the blocks were placed, therefore, further checking if the installed support unit/s are sufficient to carry each block. The failed blocks will therefore be defined as rock fall (Joughin *et al.*, 2012a).

The input parameters used in the JBlock program to evaluate the possibility of injuries is based on number of people in each zone and the percentile of time spent in that specific zone (Joughin *et al.*, 2012a). This is achieved by a program RiskEval which is integrated in the JBlock program for the quantification of the injuries (Joughin *et al.*, 2012a). This program uses the

event tree methodology outlined in Figure 4.2 (Joughin *et al.*, 2012a). The event tree will thereof analyze the probability of a specific rock fall resulting in an injury. Each rock fall produced by the keyblock analysis will have its own separate event tree (Joughin *et al.*, 2012a).

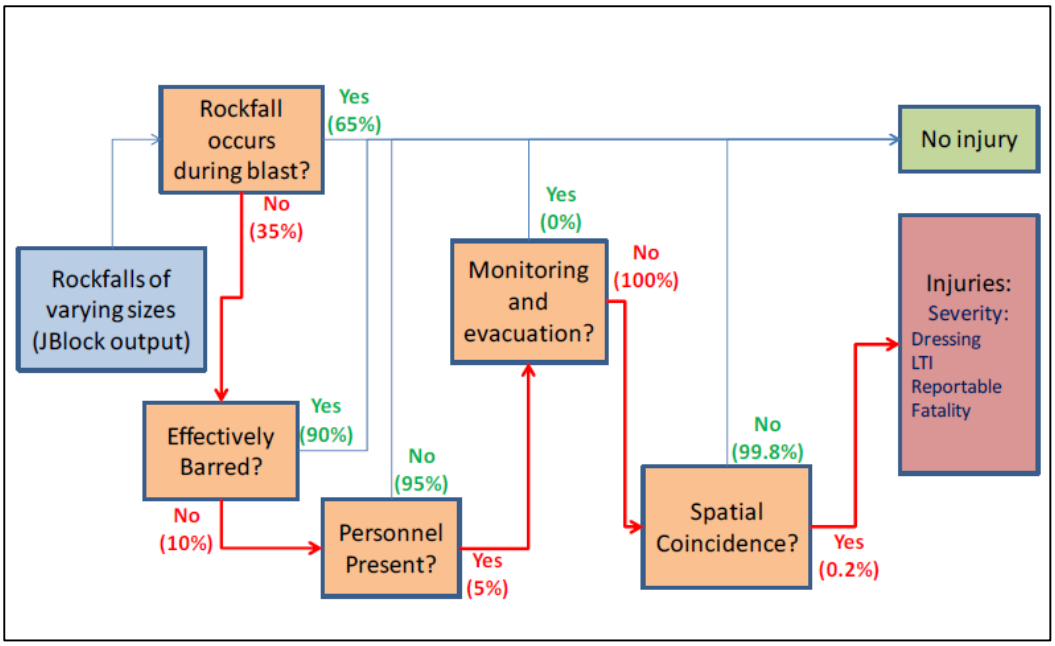


Figure 4.2: Event tree analysis for injuries (after Joughin et al., 2012a).

A step represents a blast or face advance, which is 2.1 m. JBlock allows the excavation to advance 2.1 m, thus keyblocks can now be exposed at the face (unsupported area) that is no longer stable due to the face position. This is the main reason why most falls occur at the face. The support was set for after the blast, during the support drilling phase as outlined in Section 3.3.3.

4.1 Rock fall Distribution

The rock fall described in this Section (4.1) pertain to the area of interest (the first 3.1 m), as described in Section 3.3.3. These falls occur randomly at different locations within the zone of interest.

The results in Section 4.2 include the entire panel i.e. a combination of the face and the back area as described in Section 3.3.3. The back area results may be slightly exaggerated as they considered worst case Scenario, not accounting for the fact that loose rocks had already fallen out before the installation support.

The results outlined in this Chapter are a product of the geotechnical domain file used in conjunction with the excavation file to generate the keyblock distribution file. The combination of the keyblock distribution file and the support file will define the rock fall distributions and the statistics discussed in Sections 4.1 and 4.2.

4.1.1 Support using 1.5 m long bolts spaced at 1.5 m X 1.5 m with the Triplets horizon at 1.7 m above the hangingwall

The support system currently used on the Mine A is 1.5 m long bolts spaced 1.5 m X 1.5 m apart. This configuration was studied first, to determine if the length and support resistance is sufficient. It was also used as a benchmark for comparison to other support Scenarios to optimize the support system.

The maximum number of falls per blast in the analyses are summarized for two jointing Scenarios in Figure 4.3 (with and without the shallow dipping random set. The distribution shows an increase in the maximum number of falls per blast when the random joint set is included (Scenario 2). The strike and dip panel-orientations showed the same number of FOGs when the random joint set was excluded (Scenario 1). However, where the low angled joint sets were present, the panels mining along strike had a comparatively greater number of FOGs.

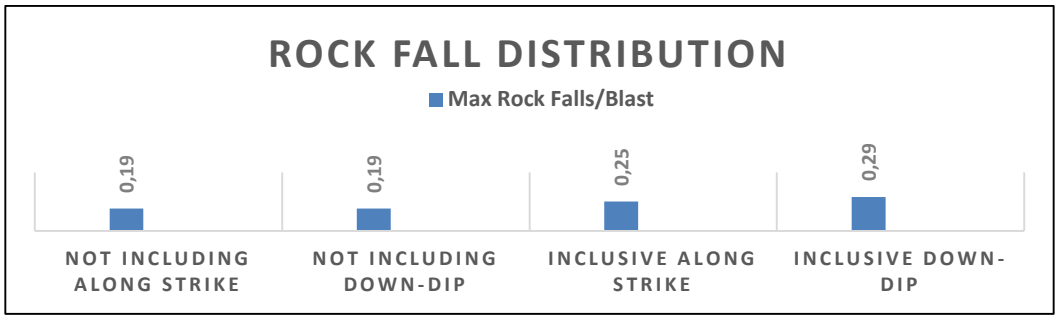


Figure 4.3: Rock fall distributions for both Scenarios.

The bolt analysis was normalized to a mined area of 10 000 m^2 and the results are shown in Figure 4.4. Where the low angled joints were excluded, the failed bolts were similar for both panel Scenarios (along dip and strike). However, significant differences in bolt failures were observed between the dip and strike panels when the shallow dipping discontinuities were included. Failed tendons are the combination of tendons that failed due to the steel break and the grout bond failure. The successful tendons are the ones that were successful in preventing rock fall and hence, were neither too short nor failed.

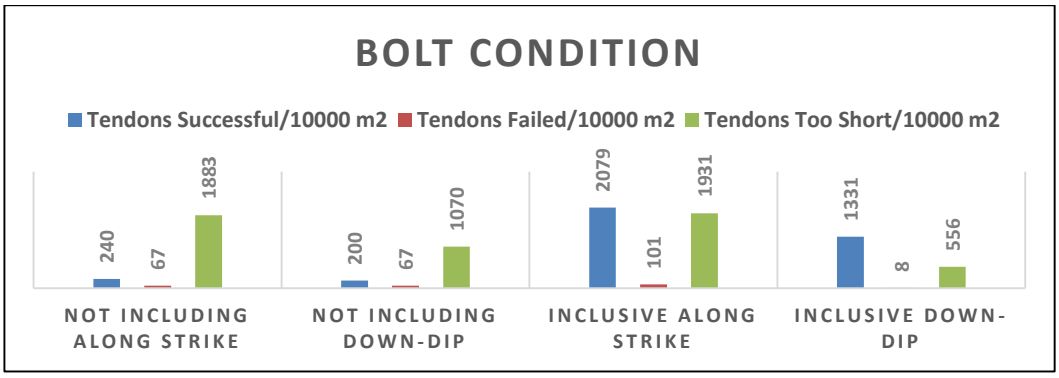


Figure 4.4: Contributing factors to bolt behaviours for both Scenarios.

The successful tendons are observed to be higher in the Scenario that included the low angled random joint set, when compared to the Scenario not including the low angled joint set. This finding could be the result of smaller block sizes being created by the shallow dipping sets. This concept was also shown by Watson and Gerber (2018). The number of tendons shown to be too short are significantly higher on the panel mining along strike than on dip. It is not clear why there is a drop in the number of short bolts when comparing the results of the Scenarios with and without shallow dipping joints, respectively. It is recommended that further work be done to establish the observed phenomenon, but is beyond the scope of this research, and will not be investigated further.

4.1.2 Sensitivity analysis on the Triplets height for 1.5 m long bolts spaced at 1.5 m X 1.5 m

Variable Triplet heights were used to test the current support configuration at Mine A for Scenario 1 (without the random low angled joint set).

The results are shown in Figure 4.5. The highest maximum number of falls per blast is observed when the Triplet height is at 1.7 m. The number of successful and failed bolts normalized to a mined area of 10 000 m^2 are illustrated in Figure 4.6. The number of successful bolts reduced from Triplet height 1.3 m to 1.8 m, and remained fairly constant with any further increase in Triplet height. The successful tendons, tendons too short and failed tendons do not add up to the same number for each Triplet height because models for each height were ran separately resulting in different results for each height.

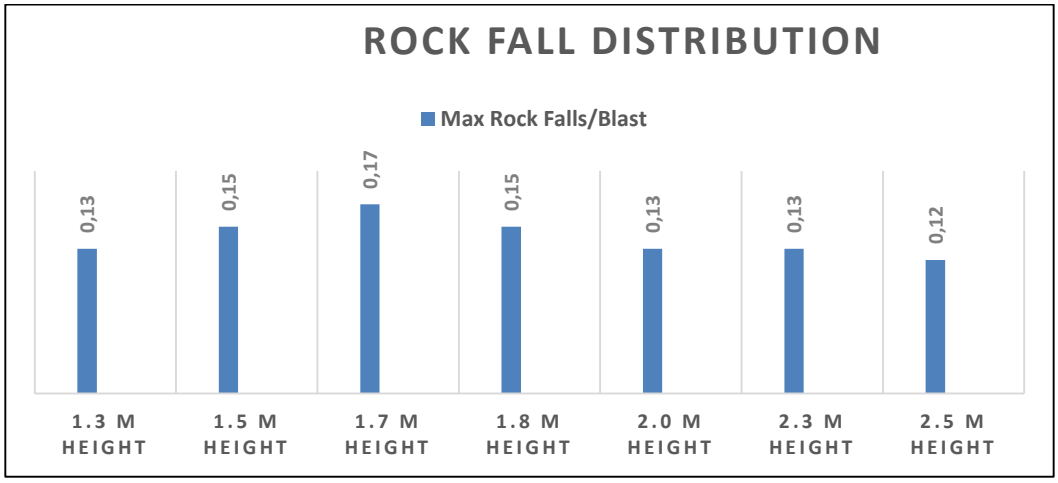


Figure 4.5: Rock fall distributions for the different Triplets heights for Scenario 1.

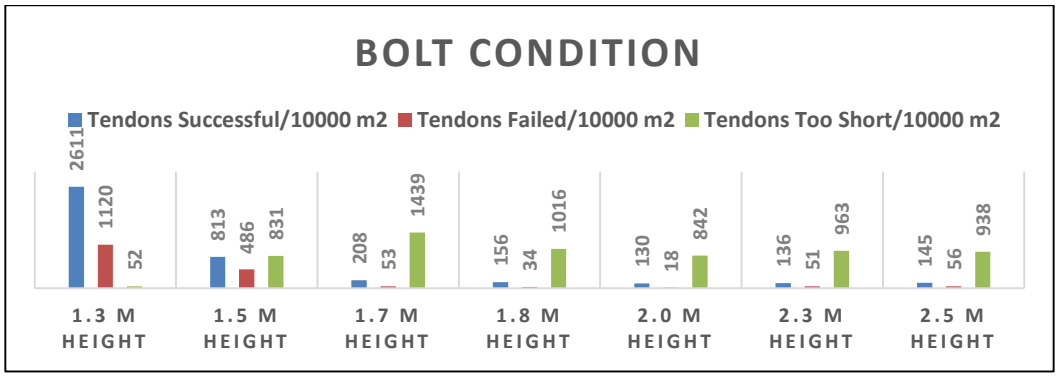


Figure 4.6: Contributing factors to bolt behaviours at various Triplets heights for Scenario 1.

The significant increase in “too short” bolts above a Triplet height of 1.3 m can be explained by the critical bond length of 25 mm and bolt length of 1.5 m. The initial rise and later drop in the number of bolts that were too short, with Triplet height may be the result of a change in support mechanism, i.e.by suspension at lower Triplets heights and beam building at higher Triplet heights, where the Triplets have less influence on the stability. Tendon failure is comparatively higher in the lower Triplet height of 1.3 m, because the 1.5 m bolt length is suspending the weaker rock to a stronger layer above the Triplets. The cantilever formation that occurs when the joints are unfavourably orientated with regards to the bolt position may have also contributed to this tendon failure.

A similar exercise was done for Scenario 2. The maximum number of falls per blast are increased in all Triplet heights when compared to Scenario 1 (Figure 4.7). This number is observed to be higher at Triplet heights of 2.3 m and 2.5 m. The reason for the comparatively higher number of FOGs at

Triplets heights of 2.3 m is not clear from the JBlock results and needs to be investigated further using another modelling technique, e.g. 3DEC.

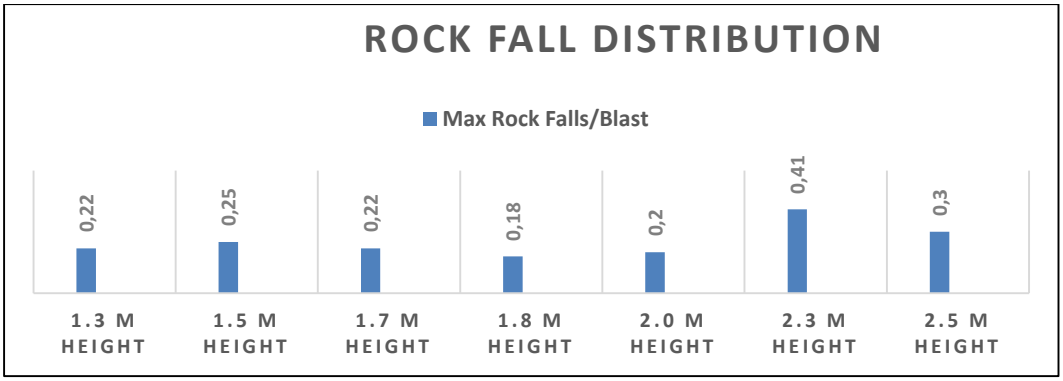


Figure 4.7: Rock fall distributions for the different Triplets heights for Scenario 2.

The bolt behaviour for Scenario 2 is illustrated in Figure 4.8. The bolt results were normalized to a mined area of 10 000 m^2 as in Scenario 1 (Figure 4.6). A significate number of too short tendons are observed at all Triplet heights. Interestingly, the highest number of short bolts occurred when the Triplets were only 1.3 m above the hangingwall. This unexpected result is probably the result of the measured lengths of the shallow dipping discontinuity, and may not be realistic as these discontinuities often truncate on bedding planes.

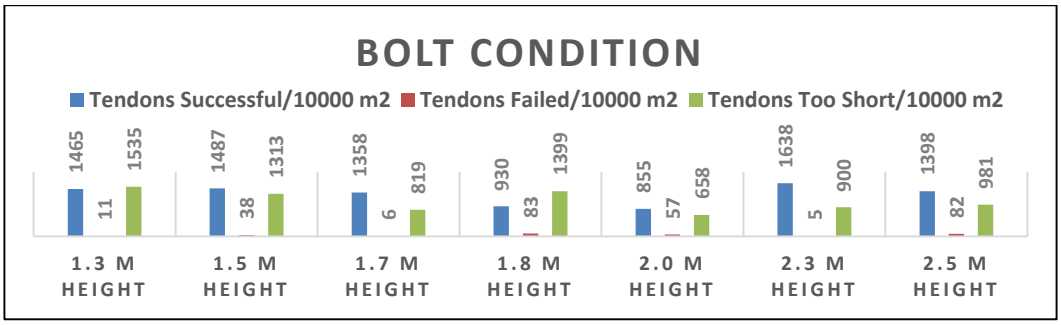


Figure 4.8: Contributing factors to bolt behaviours at various Triplets heights for Scenario 2.

Figures 4.5 to 4.8 suggest that a large contributing factor to the support system was “short tendons”.

Sensitivity analyses were therefore conducted on support length. Subsequently, sensitivity analyses were conducted on support spacing, and improved areal coverage. The risk of FOGs can be mitigated, to some degree, by using barring, but history has shown that this method is not fail-safe. FOG injuries have occurred in the past on Mine A during the barring procedure. A Triplet height of 1.7 m was considered in the sensitivity analysis as it is the lowest Triplet height forming the majority of the planned mined area.

4.1.3 Sensitivity analysis on bolt length (bolt spaced at 1.5 m X 1.5 m and Triplets height of 1.7 m)

Figure 4.9 and 4.10 illustrates the maximum of falls per blast of the different bolts lengths kept at the initial support spacing (of 1.5 m x 1.5 m) for both Scenarios. The results show a significant reduction of the maximum numbers of FOGs per blast in Scenario 1, when the bolt length is increased. However, when the random low angled joint set was included (Scenario 2),

the bolt length increase had little effect on the number of FOGs above 1.8 m.

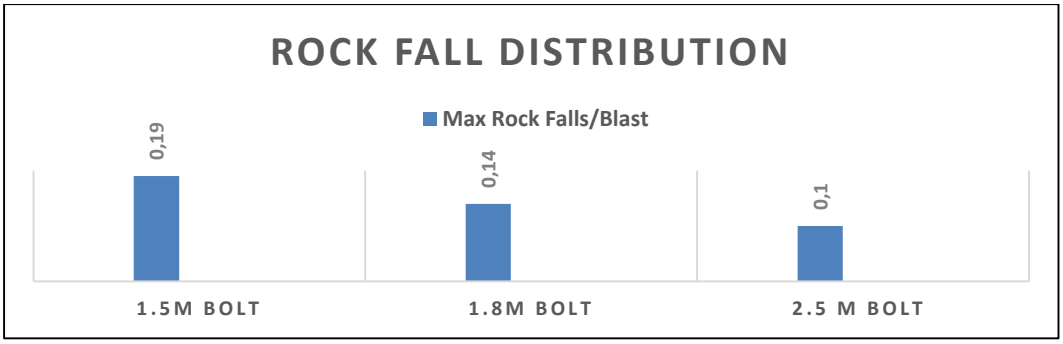


Figure 4.9: Rock fall distributions for various bolt lengths (1.5 m X 1.5 m spacing for Scenario 1, Triplets at 1.7 m).

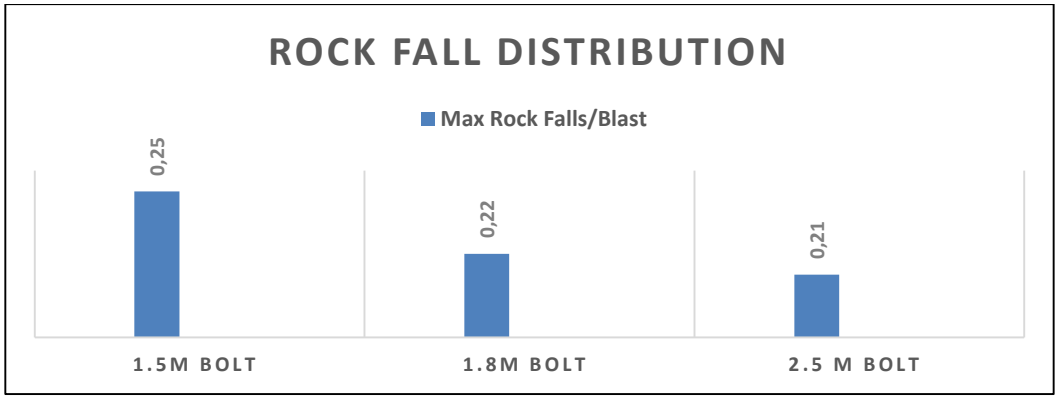


Figure 4.10: Rock fall distributions for the different bolt lengths at 1.5 m X 1.5 m spacing for Scenario 2, 1.7 m Triplet height.

Watson and Gerber (2018), suggested that an increase in support resistance improves stability under certain conditions, even if support elements were not penetrating the Triplets planes.

4.1.4 Sensitivity analysis of Triplets heights for a 1.8 m long bolt (spaced at 1.5 m X 1.5 m for Scenario 1 and 2)

Different Triplet heights were used to test 1.8 m long bolts lengths spaced at 1.5 m X 1.5 m at Mine A in Scenario 1 and 2, and the results are shown in Figure 4.11 and 4.12. A slight reduction of the maximum of falls per blast in Scenario 1 was observed below 1.8 m when the bolt length is increased, however, the value remained constant in Triplet heights greater than the bolt length (comparing Figure 4.5 to Figure 4.11). Note the similar falls per blast in all Triplet heights in Scenario 1 and a clear increase in this number at Triplet height above 2.0 m in Scenario 2. A clear increase in the number of FOGs per blast was noted at Triplet height above 2.0 m in Scenario 2. A bolt length of 2.5 m was therefore investigated.

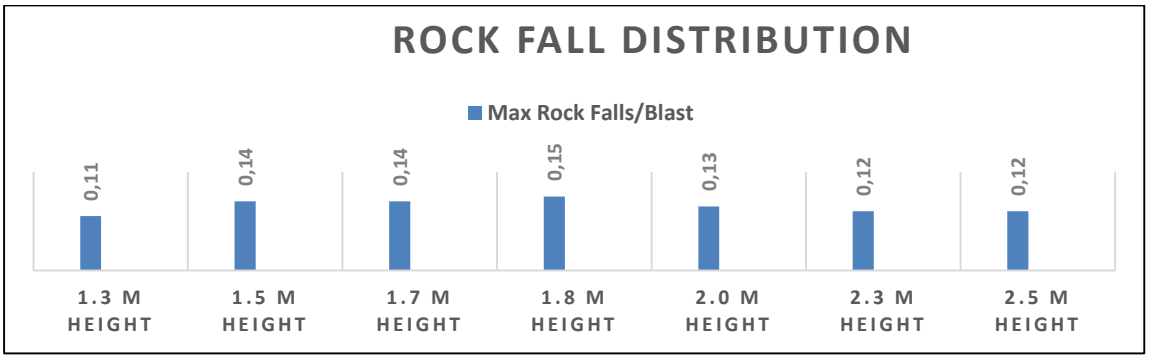


Figure 4.11: Rock fall distributions for the 1.8 m bolt length spaced at 1.5 m X 1.5 m for Scenario 1.

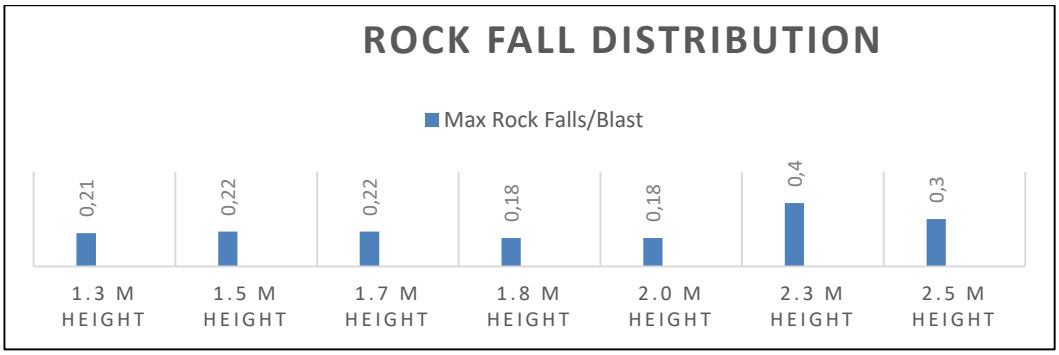


Figure 4.12: Rock fall distributions for the 1.8 m bolt length spaced at 1.5 m X 1.5 m for Scenario 2.

4.1.5 Sensitivity analysis of Triplets heights for a 2.5 m long bolt (spaced at 1.5 m X 1.5 m for Scenarios 1 and 2)

Distributions for all the modelled Triplets heights (1.3 m to 2.5 m) using the 2.5 m long bolts in Scenario 1 are shown in Figure 4.13. Comparing the results of 1.8 m long to 2.5 m long bolts, the following was noted:

- A slight reduction in the FOGs per blast were observed for Scenario 1; and
- No improvements were observed in Scenario 2 (Figure 4.14).

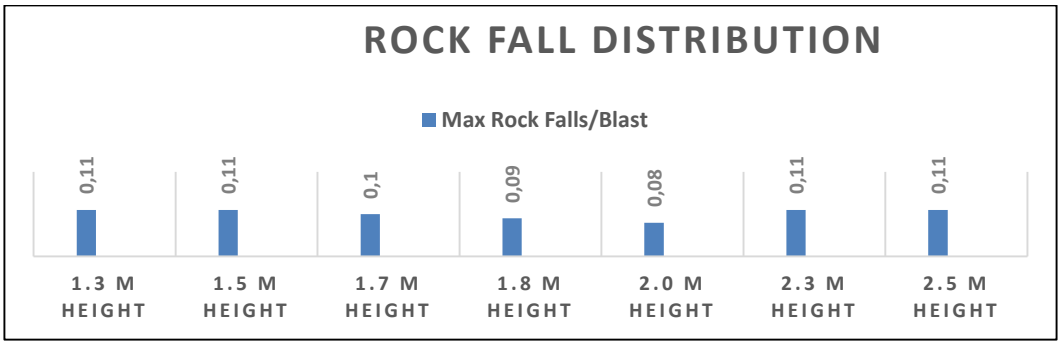


Figure 4.13: Rock fall distributions for the 2.5 m bolt length spaced at 1.5 m X 1.5 m for Scenario 1.

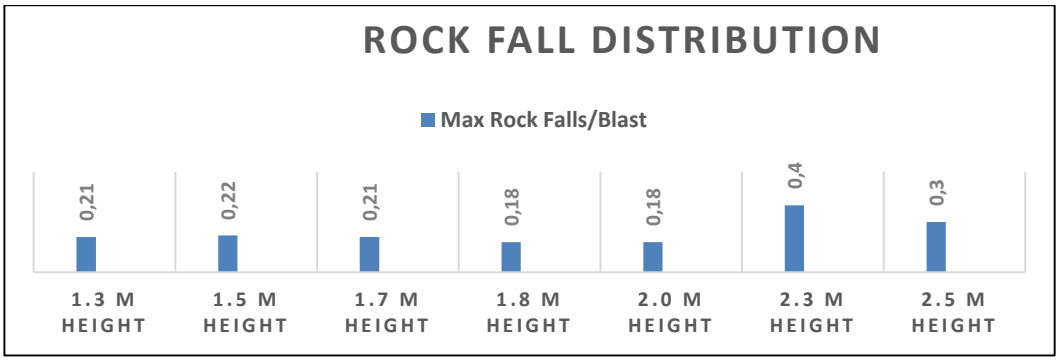


Figure 4.14: Rock fall distributions for the 2.5 m bolt length spaced at 1.5 m X 1.5 m for Scenario 2.

While there appears to be a slight improvement in the number of FOGs when increasing the bolt lengths to suspend the rock below the Triplets planes for Scenario 1, there is little justification for increasing the bolt length beyond 1.5 m for Scenario 2. In particular, the number of FOGs for Scenario 2 was unchanged above a height of 2.0 m, even though the bolt penetrates the Triplets. A sensitivity analysis was therefore done on spacing (support resistance) and the results are described below.

4.1.6 Comparison of bolt spacings at 1.5 m X 1.5 m and 2.0 m X 2.0 m (1.7 m Triplet height for Scenario 1 and 2)

A significant increase in FOGs resulted when the support spacings were increased, i.e. the support resistance was decreased (Figure 4.15 and Figure 4.16). Note that the 2.5 m long bolts also represent a slightly higher support resistance than the 1.8 m long bolts, as described in Section 3.3.3. Even this slight increase in the support resistance shows a consistent reduction in FOGs, suggesting that the current support resistance is too low. An increase in support resistance may be more beneficial than

increasing support length, in the context of the investigated support Scenarios.

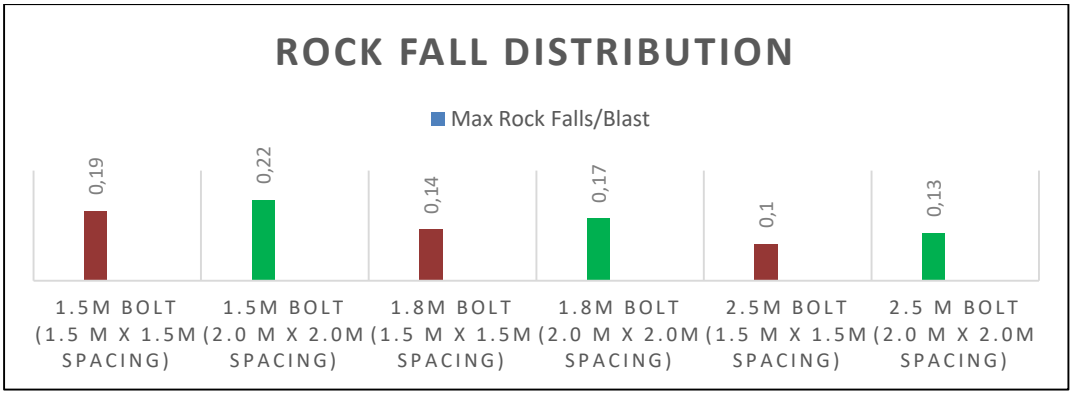


Figure 4.15: Rock fall distributions for three bolt lengths at different spacings for Scenario 1, (1.7 m Triplet height).

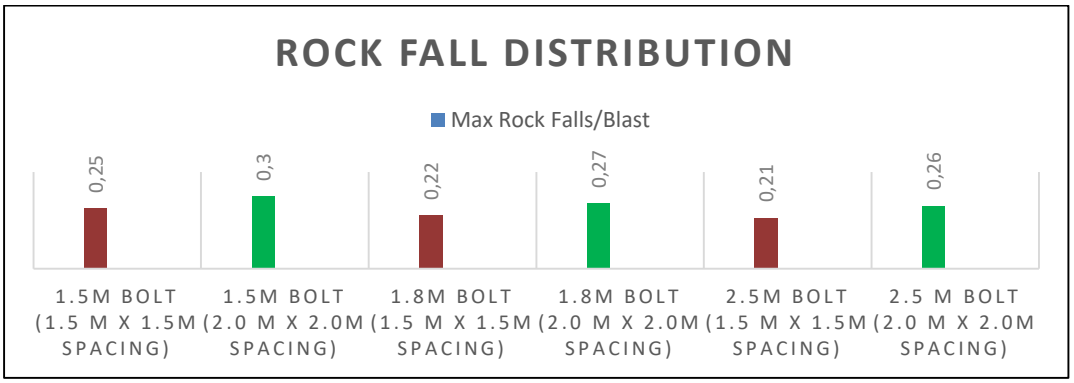


Figure 4.16: Rock fall distributions for three bolt lengths at different spacings for Scenario 2, (1.7 m Triplet height).

4.2 Statistics

This Section outlines the hazards and risks results of the models which were ran. The hazards are represented as the number of rock fall per specified area and the risks are presented in form of injuries per the specific given area. The hazard and risk results in this Section considered both Scenarios, however, the worst case (Scenario 2) is more realistic since the

program does not consider clamping effects that exists on vertically included discontinuities. The Scenario that included the random low angled joint set is thus deemed to be closer to reality. A description of how the hazard and risk results were determined is provided in Section 3 (page 46).

4.2.1 Hazard and risk results for 1.5 m long bolts spaced at 1.5 m X 1.5 m for Scenarios 1 and 2 (Triplet height at 1.7 m)

The bolt length and spacings describe in this Section correspond to the current support system on the Mine. The hazard and risk results for the two jointing Scenarios are provided in Table 4.1. The number of rock fall per mining step in Scenario 1 (not including the random joint set) is less than Scenario 2 (panels that do include the random joint set). Similarly, the same trend is observed on the injuries. The injuries in the panel inclusive of the low angled joint are significantly higher than those that do not including the set. The panel mining along strike has a higher number of injuries than those mining along dip. This trend is probably due to the orientation of the joint sets.

Table 4.1: The hazard and risk results for a support Scenario of 1.5 m long bolts spaced at 1.5 m X 1.5 m for Scenarios 1 and 2 (Triplets height at 1.7 m).

Triplets height	Rock fall/10 000 m²	Injuries/10 000 m²
Scenario 2 along strike	78.0	2.29
Scenario 2 down-dip	73.2	2.28
Scenario 1 along strike	4.1	0.21
Scenario 1 down-dip	3.4	0.17

4.2.2 Hazard and risk results for a support configuration of 1.5 m long bolts spaced at 1.5 m X 1.5 m for various Triplet heights

Table 4.2, suggests that the rock fall and injuries are higher when the Triplets are between heights of 1.3 m and 1.8 m than above 1.8 m, for Scenario 1. However, the differences are small and could be within the margin of error associated with statistical analyses. Importantly, Table 4.3 shows a significant increase in number of rock fall and injuries, over Scenario 1, at all Triplet heights. These numbers appear more pronounced when the Triplets are above a height of 2.0 m. The results suggest that the support resistance may not be sufficient, particularly when the Triplets are above a height of 2.0 m. At Triplets heights below 2.0 m, the significantly larger risk of injury in Scenario 2 is probably because areal coverage of the support elements is insufficient.

Table 4.2: The hazard and risk results for a support Scenario of 1.5 m bolts spaced at 1.5 m X 1.5 m at different Triplet heights for Scenario 1.

Triplets height	Rock fall/10 000 m²	Injuries/10 000 m²
1.3 m	3.3	0.18
1.5 m	3.3	0.14
1.7 m	3.8	0.19
1.8 m	3.4	0.13
2.0 m	2.2	0.12
2.3 m	2.1	0.12

Table 4.3: The hazard and risk results for a support Scenario of 1.5 m bolts spaced at 1.5 m X 1.5 m at different Triplet heights for Scenario 2.

Triplets height	Rockfall/10 000 m²	Injuries/10 000 m²
1.3 m	19.2	0.62
1.5 m	34.7	1.33
1.7 m	12.2	0.40
1.8 m	8.8	0.30
2.0 m	126.2	4.30
2.3 m	72.9	2.14

4.2.3 Hazard and risk results for a 1.8 m long bolt spaced at 1.5 m X 1.5 m for various Triplets heights

Comparisons between Table 4.4 and 4.2, and 4.5 and 4.3 show only a very small advantage of increasing the bolt length.

Table 4.4: The hazard and risk results for a 1.8 m bolt length spaced at 1.5 m X 1.5 m at different Triplet heights for Scenario 1.

Triplets height	Rock fall/10 000 m²	Injuries/10 000 m²
1.3 m	3.2	0.15
1.5 m	3.2	0.14
1.7 m	2.7	0.12
1.8 m	3.3	0.15
2.0 m	3.4	0.00
2.3 m	2.2	0.00
2.5 m	2.1	0.00

Table 4.5: The hazard and risk results for a 1.8 m bolt length spaced at 1.5 m X 1.5 m at different Triplet heights for Scenario 2.

Triplets height	Rock fall/10 000 m²	Injuries/10 000 m²
1.3 m	18.9	0.61
1.5 m	34.1	1.11
1.7 m	34.8	1.08
1.8 m	11.9	0.37
2.0 m	8.8	0.29
2.3 m	124.4	4.30
2.5 m	72.9	2.14

4.2.4 Hazard and risk results for a 2.5 m long bolts spaced at 1.5 m X 1.5 m for various Triplets heights

For Scenario 1, injuries are reduced to zero when the bolt length is increased to 2.5 m (Table 4.6). However, the improvement may be the effect of a higher support resistance provided by 2.5 m long bolts.

For Scenario 2, little change in FOGs were predicted from that of the 1.8 m bolt length (Table 4.7). Similarly, Watson and Gerber (2018), found that 1.8 m long bolts, with a support resistance of 48.0 kN/m^2, was sufficient for a span of 6.0 m and that an increase of support resistance has a positive impact in improving stability if when the bolt does not penetrate the Triplets.

Table 4.6: The hazard and risk results for a 2.5 m bolt length spaced at 1.5 m X 1.5 m at different Triplet heights for Scenario 1.

Triplets height	Rock fall/10 000 m²	Injuries/10 000 m²
1.3 m	3.2	0.00
1.5 m	3.2	0.00
1.7 m	2.7	0.00
1.8 m	3.3	0.00
2.0 m	2.9	0.00
2.3 m	2.0	0.00
2.5 m	2.0	0.00

Table 4.7: The hazard and risk results for a 2.5 m bolt length spaced at 1.5 m X 1.5 m at different Triplet heights for Scenario 2.

Triplets height	Rock fall/ 10 000 m²	Injuries/10 000 m²
1.3 m	18.9	0.61
1.5 m	34.1	1.11
1.7 m	34.2	1.08
1.8 m	11.9	0.37
2.0 m	8.8	0.29
2.3 m	124.4	3.83
2.5 m	72.9	2.14

4.2.5 Hazard and risk results for 1.5 m long bolts spaced at 2.0 m X 2.0 m with Wire-mesh at various Triplets heights

The 1.5 m long resin bolts were incorporated at an increased strength of 140.0 kN ± 14.0 kN and a resin bond strength of 400.0 kN/m ± 40.0 kN. The

support also incorporated Wire-mesh with the strengthening effects of Osro straps (Watson *et al.* (2017) showed a Wire-mesh and Osro strap combined strength of 45 kN). The results are outlined in Tables 4.8 and 4.9. An improvement is observed on both rock fall and injuries numbers when compared to the 1.8 m long bolt installed at a spacing of 1.5 m X 1.5 m. The analysis shows a greater improvement in injury risk by improving area coverage, rather than support resistance or bolt length. A similar observation was observed by Watson and Gerber (2018).

Table 4.8: The hazard and risk results for a 1.5 m bolt length spaced at 2.0 m X 2.0 m installed with Wire-mesh at different Triplet heights for Scenario 1.

Triplets height	**Rock fall/10 000 m²**	**Injuries/10 000 m²**
1.3 m	1.38	0.07
1.5 m	1.01	0.05
1.7 m	1.45	0.07
1.8 m	2.07	0.11
2.0 m	1.98	0.08
2.3 m	1.96	0.08
2.5 m	1.05	0.07

Table 4.9: The hazard and risk results for a 1.5 m bolt length spaced at 2.0 m X 2.0 m installed with Wire-mesh at different Triplet heights for Scenario 2.

Triplets height	Rock fall/10 000 m²	Injuries/10 000 m²
1.3 m	7.93	0.22
1.5 m	18.19	0.39
1.7 m	13.58	0.38
1.8 m	20.42	0.53
2.0 m	18.55	0.47
2.3 m	17.53	0.85
2.5 m	28.42	0.91

4.2.6 Hazard and risk results for 2.5 m long bolts spaced at 2.5 m X 2.5 m with Wire-mesh at various Triplets heights

Tables 4.10 and 4.11 both suggest that the registered FOG fragments in the previous analyses are relatively small, i.e. are occurring between support elements. Although the number of FOGs have increased, due to the opening up of the spacing, the Wire-mesh is able to contain the fragments. Note that the Wire-mesh includes the strengthening effects of Osro straps (Watson *et al.*, 2017).

Table 4.10: The hazard and risk results for a 2.5 m bolt length spaced at 2.5 m X 2.5 m installed with Wire-mesh at different Triplet heights for Scenario 1.

Triplets height	Rock fall/10 000 m²	Injuries/10 000 m²
1.3 m	3.6	0.00
1.5 m	3.4	0.00
1.7 m	2.7	0.00
1.8 m	3.7	0.00
2.0 m	3.3	0.00
2.3 m	2.2	0.00
2.5 m	2.8	0.00

Table 4.11: The hazard and risk results for a 2.5 m bolt length spaced at 2.5 m X 2.5 m installed with Wire-mesh at different Triplet heights for Scenario 2.

Triplets height	Rock fall/10 000 m²	Injuries/10 000 m²
1.3 m	19.0	0.00
1.5 m	33.3	0.00
1.7 m	35.4	0.00
1.8 m	13.0	0.00
2.0 m	8.9	0.00
2.3 m	126.2	0.00
2.5 m	73.3	0.00

4.3 Comparison of JBlock Results with actual Fall of Ground Statistics

The FOG incidents and accidents that occurred in the past 6 years are compared to the JBlock findings for the current Mine support configuration for Scenario 1 and Scenario 2 in Table 4.12. The injuries are broken into two categories; in Figure 4.17, i.e. treat and return (TR) and lost day injuries (LDI). The frequencies in Figure 4.17 represented were calculated per million man hours. An excellent correlation is shown for Scenario 1, providing some confidence in the research described in the report. The injuries are however, not correlating with Scenario 2. There are several possible reasons for the discrepancy:

- The low angled dipping joint set is sparse, randomly found in Mine A
- Most of the fragments are falling out at the time of the blast, when nobody is in the panel and
- The current TARP system employed by the Mine is reducing accidents.

Table 4.12: Mine A yearly FOGs incidents ad accidents Vs JBlock results.

	Stope production per annum (m^2)	Mine A injuries	JBlock Rock fall per annum production of Mine A (Scenario 1)	JBlock injuries per annum production of Mine A (Scenario 1)	JBlock Rock fall per annum production of Mine A (Scenario 2)	JBlock injuries per annum production of Mine A (Scenario 2)
2013	217894	4	89	5	1700	50
2014	179299	5	74	4	1399	41
2015	158614	3	65	3	1237	36
2016	126069	1	52	3	983	29
2017	134782	2	55	3	1051	31
2018	150961	3	62	3	1177	35

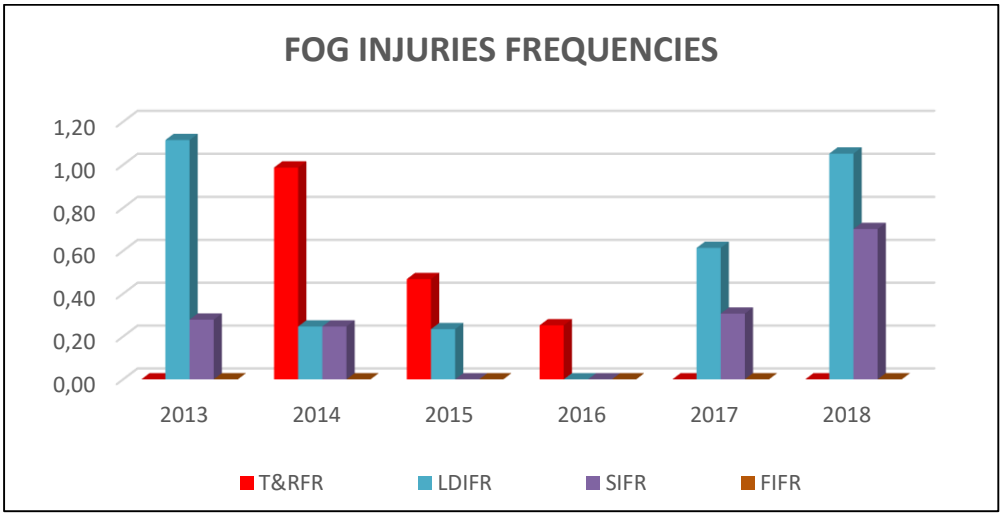


Figure 4.17: Mine A yearly FOGs accident frequencies. T&R (Treat and Return), LDI (Lost Day Injury).

Table 4.12, suggest that JBlock overestimated the number of FOGs. This is clearly observed when comparing columns 3 and 5 of Table 4.12. However, it should be remembered that as many FOGs occur during the time of the blast, and are not recorded by the Mine.

CHAPTER 5

5. DISCUSSIONS

Societal risk in various industries are normally expressed using the F-N graph (Figure 5.1). An F-N graph plots annual probability of failure or occurrence of an event (F) against the number (N) of lost lives (Joughin *et al.*, 2012a). The graph follows the "As Low As Reasonably Possible/Attainable" (ALARP) concept which allows reasonable benchmarking of risk. High risk working environments need to have a low number of people working, or the risk must be mitigated by means of support etc., i.e. the larger the number of people in a working environment, the lower the risk must be in order to comply with internationally acceptable standards. Joughin *et al.* (2012a) states that "Individual risk can be benchmarked and an annual fatal frequency rate of 10^{-4} can be treated as negligible risk", thus this risk represents an acceptable annual probability of a single fatality.

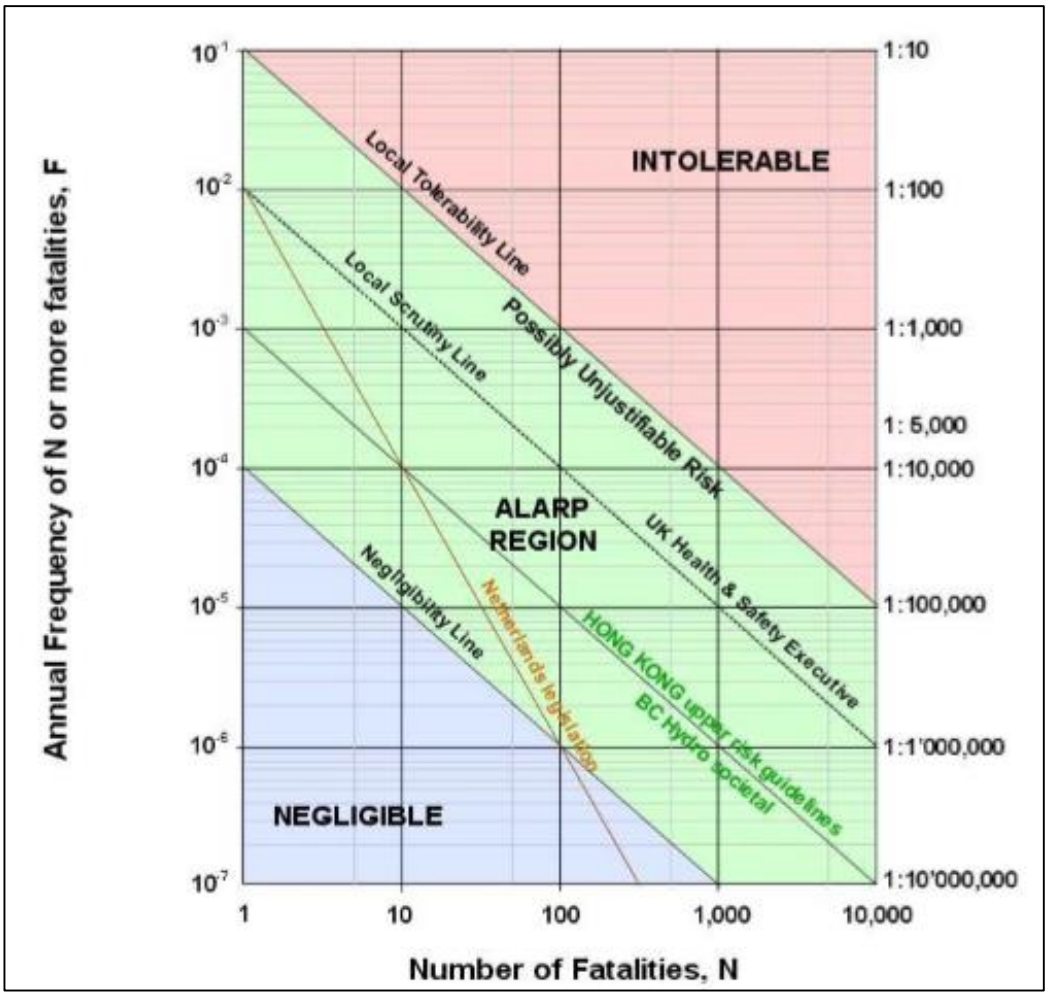


Figure 5.1: F-N graph for bench marking safety impact (Joughin et al., 2012a).

Joughin (2018) maintains that as much as the mining companies have a safety target of “zero harm”, an engineer cannot design for zero injury probability, as this is not possible. According to the author, it is the duty of the management to adhere to guidelines such as shown in Figure 5.1. These guidelines must be accepted by society and mechanisms must be installed to achieve the targets. In mining, acceptable risk levels are not clear. Since zero harm is not achievable, engineers and the industry as a whole cannot achieve their safety target. The need for the Mines to provide labour works against the concept is provided in Figure 5.1.

Joughin (2018) also suggests that a risk based design process is required, which is based on geotechnical uncertainty.

The injuries shown in the above Chapter 4 will be converted using both the F-N graph and the Heinrich's Triangle Theory (Kuder, 2017), shown in Figure 5.2, for the purposes of comparing Mine A to internationally acceptable risk. Heinrich's concept was initially done based on a pyramid ratio of 300:29:1, which is explained as: for every 300 near misses or unsafe behaviours, 29 minor injuries will occur and those number of injuries will likely result in a major injury/fatal (Kuder, 2017).

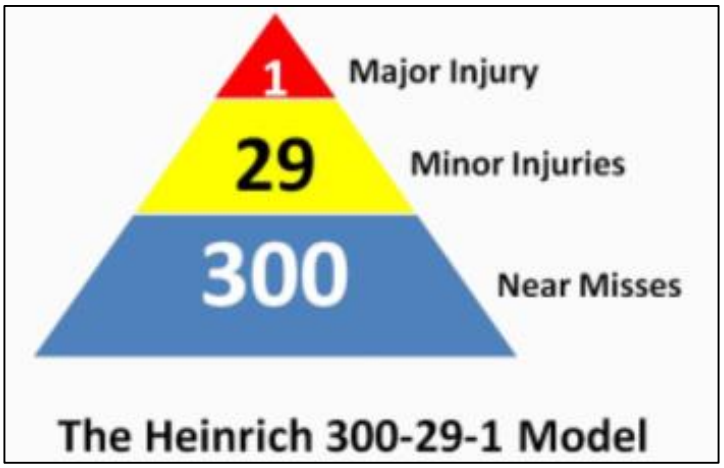


Figure 5.2: Heinrich's accidents triangle (Kuder, 2017).

Table 4.12 compares Mine A's yearly FOGs statistics with the JBlock results for joint Scenario 1 and 2 using the current support design. Heinrich's accidents triangle suggests that significant numbers of injuries/accidents could result yearly for Scenario 2. The yearly injuries suggested by JBlock for Scenario 2 were above the 29 injuries whereas the resulting injuries from Scenario 1 were less than 5.

Injuries were calculated by JBlock for both Scenarios (Table 4.12). The results were converted to probability rates in order to determine the individual fatal accident risk rate per annum, and are represented in Table 5.1 and 5.2 for each Scenario. This is achieved by converting the JBlock results injuries per annum production to injury frequencies per million man hours. The injury of the million man hours are further converted to a thousand frequencies per annum which is used to calculate the individual fatality risk per annum. A similar method was used by Joughin *et al.* (2012a) for calculating/evaluating the individual fatality risk per.

Table 5.1: Mine A's yearly JBlock results converted to accidents rates using Scenario 1.

	(Hours)	**JBlock injuries per annum production of Mine A (Scenario 1)**	**JBlock Total injury frequency rates (per million-man hours)**	**Total accidents frequency rates (per 1000 per annum)**	**Individual fatality risk per annum**
2013	3 588 120	5	1.39	2.79	27.9×10^{-4}
2014	4 052 007	4	0.99	1.97	19.7×10^{-4}
2015	4 271 301	3	0.70	1.40	14.0×10^{-4}
2016	3 966 183	3	0.76	1.51	15.1×10^{-4}
2017	3 259 610	3	0.92	1.84	18.4×10^{-4}
2018	2 851 746	3	1.05	2.10	21.0×10^{-4}

Table 5.2: Mine A's yearly JBlock results converted to accidents rates using Scenario 2.

	(Hours)	JBlock injuries per annum production of Mine A (Scenario 2)	JBlock Total injury frequency rates (per million-man hours)	Total accidents frequency rates (per 1000 per annum)	Individual fatality risk per annum
2013	3 588 120	50	13.93	27.87	2.78×10^{-2}
2014	4 052 007	41	10.12	20.24	2.02×10^{-2}
2015	4 271 301	36	8.43	16.86	1.68×10^{-2}
2016	3 966 183	29	7.31	14.62	1.46×10^{-2}
2017	3 259 610	31	9.51	19.02	1.90×10^{-2}
2018	2 851 746	35	12.27	24.55	2.45×10^{-2}

The results shown in Table 5.1. and 5.2 clearly show that the current support configuration (Table 4.2 and 4.3) is insufficient to meet international standards. The use of 1.5 m long bolts on a 2.0 m X 2.0 m spacing with suitable Wire-mesh and Osro straps (Table 4.8), for Scenario 1, was also tested against international standards and results are shown in Table 5.3. The findings suggest that the injuries, calculated by JBlock, are reduced to one injury per thousand workers, yearly. This support configuration still does not meet the international standards.

Table 5.3: Mine A's yearly JBlock results converted to accidents rates using Scenario 1 for support Scenario results shown in Table 4.8.

	(Hours)	**JBlock injuries per annum production of Mine A (Scenario 1)**	**JBlock Total injury frequency rates (per million-man hours)**	**Total accidents frequency rates (per 1000 per annum)**	**Individual fatality risk per annum**
2013	3 588 120	2	0.56	1.11	11.1×10^{-4}
2014	4 052 007	1	0.25	0.49	4.9×10^{-4}
2015	4 271 301	1	0.23	0.47	4.7×10^{-4}
2016	3 966 183	1	0.25	0.50	5.0×10^{-4}
2017	3 259 610	1	0.31	0.61	6.1×10^{-4}
2018	2 851 746	1	0.35	0.70	7.0×10^{-4}

The individual fatality risk per annum calculated using the results of Scenario where the 2.5m long bolts are used on a spacing of 2.5 m X 2.5 m with suitable Wire-mesh and Osro straps (Tables 4.10 and 4.11) equates to zero. The results of the investigations suggest that this support configuration meet international standards in both joint Scenarios.

CHAPTER 6

6. CONCLUSIONS AND RECOMMEDATIONS

Detailed discontinuity mapping was done across Mine A in order for a probabilistic JBlock evaluation to be performed on stability. The analysis was used to investigate the current support design and find a more suitable configuration to reduce FOG accidents. The JBlock program uses the generation of keyblocks to determine probabilistic evaluations of FOGs and related injuries.

The geotechnical investigation showed that Mine A has two major joint sets plus a random low angled joint set. The randomness of the low angled joint set suggests a number of random low angled joints, which was confirmed by the large standard deviation on the orientation data.

The joint data was incorporated in JBlock and several support Scenarios were investigated for the two different mining directions, currently used for exploitation of the orebody of the Mine. Two joint Scenarios were investigated, i.e. with and without the inclusion of the random joint set, Scenarios 1 and 2, respectively. Various support configurations and Triplets parting plane heights were also investigated. From the JBlock results the following was concluded:

- A good correlation of the injury results was obtained between the JBlock analysis and actual Mine A falls of ground injury statistics, if Scenario 1 was assumed to be predominant across the Mine.
- The Scenario that is inclusive of the low angled joint set resulted in almost twenty times the number of FOGs and ten times the number of injuries compared to the one that does not include the random low angled joint set.
- The down-dip configuration yields slightly less rock fall and injuries compared to the strike configuration in both joint-Scenarios.
- The current support design at Mine A needs to be modified to ensure that injuries are reduced to international levels.
- A significant reduction of rock fall and injuries was realized by increasing the support resistance.
- **Injuries could be reduced to international standards by using 2.5 m long bolts on a 2.5 m X 2.5 m spacing (34 kN/m^2) with Wire-mesh and Osro straps having a combined strength of 45 kN (Watson *et al.*, 2017)**.

This research project concludes that 2.5 m long bolts spaced at 2.5 m X 2.5 m with suitable Wire-mesh and Osro straps, reduce the FOG injury risk to internationally accepted values, irrespective of the height of the Triplets or the orientation of the discontinuities. The support resistance of the bolts used in the analysis was 34 kN/m^2 with Wire-mesh and Osro straps at a combined strength of 45 kN (Watson *et al.*, 2017).

Bolts of a length of 1.5 m installed on a 2.0 m X 2.0 m spacing (30 kN/m^2), with Wire-mesh and suitable straps, will significantly reduce the current risk of FOG injury in Scenario 1 areas. Areas including the low angled joint set must then be treated separately to determine appropriate support for such localized zones. This can be achieved using systems such as:

- Trigger Action Response Plan (TARP), a system used by the production personnel for the identification and reporting of hazards to allow a separate support designed to be recommended.
- Identification of future hazards based on the current observations, in planning meetings and recorded on Mine plans.

Ongoing data collection must be done to further update the current data. This will ensure that the support design is continuously validated during reviewing periods. It should be noted that the results of this investigation were found purely by statistical keyblock analyses. Further investigation using distinct element software is recommended to verify the results.

CHAPTER 7

7. REFERENCE LIST

Barton, N.R. (1973). A review of the shear strength of filled discontinuities in rock. Norwegian Geotechnical Institute. Publ. No. 105. Oslo: Norwegian Geotech. Inst.

Barton, N., Lien, R. and Lunde, J. (1974). Analysis of rock mass quality and support practice in tunnelling, and a guide for estimating support requirements. NGI Internal Report, 19th June.

Barton, N. (1976). The shear strength of rock and rock joints. International Journal of Rock Mechanics and Mining Sciences and Geo-mechanical, Abstracts, 13, pp 1 – 24.

Barton, N.R. and Choubey, V. (1977). The shear strength of rock joints in theory and practice. Rock Mechanics, no. 10(1 – 2), pp 1 – 54.

Barton, N., Bandis, S. and Bakhtar, K. (1984). Strength, deformation and conductivity coupling of rock joints. International Journal of Rock Mechanics and Mining Sciences and Geomechanical Abstracts. 22 (3), pp 121-140.

Barton, N.R. and Bandis, S.C. (1990). Review of predictive capabilities of JRC-JCS model in engineering practice. In Rock joints, proc. int. symp. on

rock joints, Loen, Norway, (eds N. Barton and O. Stephansson), pp 603 – 610. Rotterdam: Balkema.

Barton, N. (1988). Rock mass classification and tunnel reinforcement selection using the Q-system. Rock classification systems for Engineering Purposes, A.S.T.M. 984, (ed. Kirkaldie), American Society for Testing and Materials, pp 59 – 88.

Barton, N. (2002). Some new Q-value correlations to assist in site characterization and tunnel design. International Journal of Rock Mechanics and Mining Sciences, vol. 39, pp 185 – 216.

Baecher, G.B. and Lanney, N.A. (1978). Trace length biases in joint surveys. Proceedings 19th U.S. Symposium on Rock Mechanics, Nevada, pp 56 – 65p.

Baecher, G.B. (1983). Statistical analysis of rock mass fracturing. Journal of Mathematical Geology, 15 (2), pp 329 – 347.

Bieniawski, Z.T. (1976). Rock mass classifications in rock engineering. Proc. Symp. On Exploration for Rock Engineering, Johannesburg, November, pp 97 – 106.

Bieniawski, Z.T. (1989). Engineering rock mass classifications. New York: Wiley.

Bieniawski, Z.T. (1993). Classification of rock masses for engineering: The RMR system and future trends. Comprehensive Rock Engineering, (ed. Hudson), Oxford: Pergamon, 3, pp 553 – 573.

Billings, M.P. (1972). Structural geology. 3rd ed., Prentice Hall, New Delhi, pp 606.

Brady, B. H. G. and Brown, E. T. (1993). Rock mechanics for underground mining, Allen and Unwin, London, pp 571.

Brink, A.V.Z., Roberts, M.K.C. and Spottiswoode, S.M. (2002). Further assessment of seismic hazard/risk in the Bushveld Complex platinum Mines and the implication for regional and local support design. Final Report, Project GAP 821, Safety in Mines Advisory Committee, Johannesburg, South, pp 42.

Brunton (2018). INTERNET. https://www.brunton.com/products/truarc-15?variant=31740473147451. Cited 24 January 2020.

Carmichael, R.S. (1988). Practical handbook of physical properties and Minerals. Abridged ed, CRC-Press, pp 741.

Coulomb, C.A. (1776). Essai sur une application des rëgles de maximis et minimis a quelques problèmes de statique, relatifs a l'architecture,

Mémoires de Marhématique de l'Académie Royale des Sciences, Paris, 7, pp 343 – 382.

Daehnke, A., Van Zyl, M. and Roberts, M.K.C. (2001). Review and application of stope support design criteria. Journal of the South African Institute of Mining and Metallurgy, vol. 101(3), pp 135 – 164.

Daehnke, A., Anderson, L.M., De Beer, D., Esterhuizen, G.S., Glissen, F.J., Grodner, M.W., Hagan, T.O., Jacu, E.P, Kuijpers, J.S., Peak, A.V., Piper, P.S., Quaye, G.B., Reddy, N., Roberts, M.K.C., Schweitzer, J.K., Stewart, R.D. and Wallmach, T. (1998). Stope face support systems, *SIMRAC GAP330 Final Report,* The Safety in Mines Research Advisory Committee (SIMRAC), Braamfontein, South Africa.

Deere, D.U., Hendron, A.J., Patton, F.D. and Cording, E.J. (1967). Design of surface and near surface construction in rock. Failure and breakage in rock, (ed. Fairhurst), New York: AIME, pp 237 – 302.

Dight, P.M., and Baczynski, N.R.C. (2009). Rock bridges and their influence on slope stability. International Symposium on Rock Slope Stability in Open Pit and Civil Engineering, Santiago, Chile.

Dunn, M.J., Earl, P. and Watson, J. (2008). Support design using probabilistic keyblock methods, in Proceedings 6th International Symposium on Ground Support in mining and civil engineering

applications, T.R. Stacey and D.F. Malan (eds), 30 March–3 April 2008, Cape Town, South Africa, The Southern African Institute of Mining and Metallurgy, Johannesburg, pp 623 – 636.

Esterhuizen, G.S. (1996). JBlock user's manual and technical reference, Pretoria.

Esterhuizen, G.S. (2003). JBlock user's manual, Pretoria.

Esterhuizen, G.S. and Streuders, S.B. (1998). Rock fall hazard evaluation using probabilistic keyblock analysis. Journal of the Southern African Institute of Mining and Metallurgy, vol. 98, no. 2, pp 59 – 63.

Esterhuizen, G.S. (2014). Extending empirical evidence through numerical modelling in Rock Engineering Design. The Southern African Institute of Mining and Metallurgy 6th South African Rock Engineering Symposium, pp 251 – 267.

Feng, C. (1996). Correction of discontinuity spacing bias caused by finite length scanline survey. Transactions of Nonferrous Metals Society of China, vol. 6, no. 3.

Grimstad, E., and Barton, N. (1993). Updating the Q-system for NMT. Proc. Int. Symp. On Sprayed Concrete, Fagernes, (eds. Kompen, Opsahl and Berg), Oslo: Norwegian Concrete Association.

Grimstad, E., Barton, N. and Løset, F. (1993). NMT Tunnel support design. World Tunnelling, September, pp 270.

Gumede, H. (2006). Development of data sets on joint characteristics and consideration of associated instability for a typical South African gold Mine. MSc.Eng Dissertation, University of the Witwatersrand.

Gumede, H. and Stacey, T.R. (2006). Measurement of typical joint characteristics in South African gold Mines and the use of these characteristics in the prediction of rock fall. Journal of the South African Institute of Mining and Metallurgy, no. 107 (5), pp 335 – 344.

Hoek, E. (2007). Practical Rock Engineering. Balkema, Rotterdam.

Hoek, E., Kaiser, P. K. and Bawden, W. F. (1995). Support of underground excavations in hard rock. Balkema, Rotterdam.

Hutchinson, D.J. and Diederichs, M.S. (1996). Cable bolting in underground Mines. BiTech publishers LTD, Richmond, Canada, pp 401.

International Society for Rock Mechanics. (1978). Suggested methods for the quantitative description of discontinuities in rock masses. International Journal of Rock Mechanics and Mining Sciences and Geomechanical, Abstracts, 15(6), pp 319 – 368.

Jager, A.J. and Ryder, J.A. (1999). A handbook on Rock Engineering practice for tabular hardrock Mines. Johannesburg, Department of Mineral and Energy Affairs.

Jager, A.J. and Ryder, J.A. (2002). A textbook on Rock Engineering practice for tabular hardrock Mines. Johannesburg, Safety in Mines Research Advisory Committee (SIMRAC).

Joughin, W. C., (2018). Dealing with uncertainty and risk in the Rock Engineering design. First International Society for Rock Mechanics and Rock Engineering. Hammamet, Tunisa, pp 23 – 36.

Joughin, W.C., Nezomba, E., Rwodzi, L. and Jager, A.J. (2012a). A risk evaluation model for support design In Bushveld Complex underground Mines: Part I—description of the model. Journal of the Southern African Institute of Mining and Metallurgy, vol. 112, no. 2, pp 83 – 94.

Joughin, W.C., Nezomba, E., Rwodzi, L. and Jager, A.J. (2012b). A risk evaluation model for support design In Bushveld Complex underground Mines: Part II—model validation and case studies. Journal of the Southern African Institute of Mining and Metallurgy, vol. 112, no. 2, pp 95 – 104.

Kekana, L. (2018). SS-ZA-PGM's-MCOP-MTS-GEO-1001 – Business plan document (unpublished internal report).

Kemeny, J. and Post, R. (2003). Estimating three-dimensional rock discontinuity orientation from digital images of fracture traces. Computers and Geosciences, no. 29, pp 65 – 77.

Kuder, J. (2017). AvatarMS News. INTERNET. https://avatarms.com/whats-300291-really-mean/. Cited 24 January 2020.

Laubscher, D.H. (1993). Planning mass mining operations. Comprehensive Rock Engineering: Principles, Practice and Projects, (ed. Hudson), Oxford: Pergamon Press, no. 2, pp 547 – 583.

Laubscher, D.H. and Taylor, H.W. (1976). The importance of geomechanics classification of jointed rock masses in mining operations. Exploration for rock engineering, Cape Town: A.A. Balkema, (ed. Bieniawski), no. 1, pp 119 – 128.

Mathews, K.E., Hoek, E., Wyllie, D.C. and Stewart, S.B.V. (1981). Prediction of stable excavations for mining at depth below 1000 metres in hard rock. CANMET Report DSS Serial No. OSQ80-00081, DSS File No. 17SQ.23440-0-9020, Ottawa: Dept. Energy, Mines and Resources, pp 39.

MOSH Learning Hub (2019). Welkom falls of ground COPA safety presentation. Mineral Council of South Africa.

Mponya, E. (2016). Determination of rock material properties to design robust support at Unki Mine. MSc.Eng Dissertation, University of the Witwatersrand.

Nezomba, H. (2012). Use of joint trace data to evaluate stability of mining excavations, and validation against underground observations. MSc.Eng Dissertation, University of the Witwatersrand.

Open House Management Solutions (2019). JBlock Course Notes.

Patton, F.D. (1966). Multiple modes of shear failure in rock. In Proceedings 1st International Congress. International Society of Rock Mechanics. Colouste Gulbenkian Foundation, Lisbon, pp 509 – 513.

Potvin, Y. (1988). Empirical open stope design in Canada. Ph.D. Thesis, Dept. Mining and Mineral Processing, University of British Columbia, pp 343.

Priest SD. (1993). Discontinuity analysis for Rock Engineering. London: Chapman & Hall.

Priest, S. D. and Hudson, J. A. (1981). Estimation of discontinuity spacing and trace length using scanline surveys. International Journal of Rock Mechanics and Mining Sciences and Geomechanics, Abstracts, vol.18, pp 183 – 197.

Priest, S.D and Hudson, J.A (1976). Discontinuity spacings in rock. International Journal of Rock Mechanics and Mining Sciences and Geomechanics, Abstracts, 13(5), pp 135 – 148.

Priest, S.D. and Samaniego, J.A. (1983). A model for the analysis of discontinuity characteristics in two dimensions. In Proceedings. 5th International Society for Rock Mechanics Congress, Melbourne.

Rocscience (2001). Dips User's Guide.

Rocscience (2007). Unwedge User's Guide.

Rocscience (2011). JBlock User's Guide.

Schouwstra, R.P. and Kinloch, E.D. (2000). A short geological review of the Bushveld Complex. Platinum Metals, vol. 44, no. 1, pp 33 – 39.

Sibanda, S.M. (2018). SS-ZA-PGM's-MCOP-MTS-RE-1001 – Mandatory code of practice to combat rockfall and rock burst accidents (unpublished internal report).

Singhal, B.S. and Gupta, R.P. (2010). Applied hydrogeology of fractured rocks (2nd ED). Springer Science and Business Media, pp 408.

Stacey, T.R. and Swart, A.H. (2001). Booklet: Practical Rock Engineering practice for shallow and opencast Mines. The Safety in Mines Research Advisory Committee (SIMRAC), pp 66.

Swart, A.H. and Handley, M.F. (2005). The design of stable stope spans for shallow mining operations. Journal of the Southern African Institute of Mining and Metallurgy, vol. 105, no. 2, pp 275 – 286.

Terzaghi, R. D. (1965). Sources of error in joint surveys. Geo-technique, vol. 15, no. 3, pp 287 – 304.

Van Der Merwe, J.N. and Madden, B.J. (2002). Rock Engineering for coal mining. Safety in Mines Research Advisory Committee (SIMRAC). SAIMM Special Publications Series 7.

Van Der Merwe, J. N. (2014). Design of support systems for underground Mine workings (MINN 7018) lecture notes. University of the Witwatersrand.

Walls, J. (2018). GEOTECHNICAL REPORT: Support design benchmark assessment for the Sibanye Stillwater Rustenburg operations (unpublished internal report).

Watson, B.P. (2004). A rock mass rating system for evaluating stope stability on the Bushveld Platinum Mines. Journal of the Southern African Institute of Mining and Metallurgy, vol. 04, no. 4, pp 229 – 238.

Watson, B.P., Van Niekerk, D. and Page, M. (2017). An improved method of testing tendon straps and weld Wire-mesh. Journal of the Southern African Institute of Mining and Metallurgy, vol. 117, pp 01 – 06.

Watson, B.P. and Gerber. (2018). Determination of stable spans in UG2 excavation. Journal of the Southern African Institute of Mining and Metallurgy, vol. 118, pp 493 – 504.

APPENDIX A. Mine A's FOGs Accidents

Kroondal Section - Bambanani Shaft
ACCIDENTS

No	Date	Time	Area	Acc. Class	Description	Nature of Injury	Design	Name of Injured	Source	Thickness [m]	Basic Cause	Work Place	Position (Peg to@)	Mining Cycle
6	2013-08-26	19:43	Bam	SERIOUS	Whilst installing the resin capsules into the drilled hole, a rock dislodge from the face and struck Mr. Monaiwa on his right foot. The size of the rock was 0.68 m x 0.24 m x 0.36 m	Laceration right foot with fractured 3rd, 4th and 5th toes	RDO	Mr. Monaiwa	Face	0,36	Poor Barring and poor entry examination	Strike 18 Mid East Scalping Line	D5882 + 12,0m South	Supporting
7	2013-08-26	19:43	Bam	LDI	Whilst installing the resin capsules into the drilled hole, a rock dislodge from the face and struck Mr. Monaiwa on his right foot. The size of the rock was 0.68 m x 0.24 m x 0.36 m	Contused neck	RDO	Mr. B. Maqekoane	Face	0,36	Poor Barring and poor entry examination	Strike 18 Mid East Scalping Line	D5882 + 12,0m South	Supporting
8	2013-11-21	01:30	Bam	LDI	A FOG took place from a channel formation between two parallel joints. The danger was identified, Oslo straps installed but... Not over both joints, causing toppling to take place. Size of rock 2.6m x 0.9m x 0.35m thick	Laceration forehead	RDO	Mr. Nhantumbo	Hangingwall	0,35	Poor support installation	Strike 9 Mid East Road Way	Q2372 + 38,1m	Supporting
9	2013-11-21	01:30	Bam	LDI	A FOG took place from a channel formation between two parallel joints. The danger was identified, Oslo straps installed but... Not over both joints, causing toppling to take place. Size of rock 2.6m x 0.9m x 0.35m thick	Contused neck	RDO	Mr.Gumasholo	Hangingwall	0,35	Poor support installation	Strike 9 Mid East Road Way	Q2372 + 38,1m	Supporting
10	2014-01-15	09:55	Bam	T&Return	Whilest installing the pig tail eyebolts into drilled holes in the hangingwall a piece of rock dislodge from the hangingwall. The rock size is 0.16 m x 0.125 m x 0.055 m	Swollen Lip	PTV	Mr. Ramosito	Hangingwall	0,055	Poor barring	Strike 18 West Bunker	Q1073 + 0,2m	Construction
11	2014-04-02	09:00	Bam	T&Return	Whilst preparing the footwall to install a camlock jack, a piece of rock dislodge from a hanging wall and struck Mr Nzinya on his back	Contused lower back	RDO	Mr. D. Z. Nzinya	Hangingwall	0,1	Poor barring	Ackermans East West 105 West	Q7560 + 7,0m	Supporting
12	2014-04-21	23:50	Bam	SERIOUS	Whilst barring the hangingwall a rock dislodged from the sidewall and struck Mr Sikhipha on his left lower leg and foot	Fracture left lower leg and laceration between the fifth and fourth toes	Act Team Leader	Mr. Sikhipha	Sidewall	0,21	Poor barring	Strike 17 Mid East Road Way Up Dip	W6974 + 25,5m South	Cleaning
13	2014-10-03	17:00	Bam	T&Return	Whilst marking the face a rock dislodged from the face and it fell on the footwall and some rock fell onto the bridge of the now injured's left foot.	Swollen bridge of the left foot.	Act S/Boss	M Maoka	Face area	0,32	Poor Barring and poor entry examination	Strike 16 Mid East Panel 1 Up Dip 2	A3532 + 20,1m South	Blasting
14	2014-10-17	00:50	Bam	T&Return	Whilst connecting up his drilling machine, a rock dislodged from the face and struck the now injured on his thigh	Abrasion and laceration right thigh	RDO	MA Cossa	Face area	0,1	Poor Barring	Strike 16 Mid East Panel 1	A3532 + 35,7m	Blasting
15	2015-01-14	08:10	Bam	LDI	Whilst installing safety net, a rock dislodged from roofbolt washer and struck injured in face	Laceration & Abrasion forehead, Abrasion on top of nose & laceration upper lip	RDO	S Nyambasi	Hangingwall	0,06	Poor Barring	Far East Strike 9 West Panel 70	A1547 + 25,1 m	Blasting
16	2015-01-14	17:20	Bam	T&Return	Whilst Mr Mokoetje was cleaning the panel with an LHD, a rock dislodged from the hanging wall and fell on top of the LHD canopy. A piece of rock broke off and struck him on the lower thigh.	Contused left lower thigh	LHD Operator	MT Mokoetje	Hangingwall	0,48	Poor Entry examination	Far East Strike 9 East Panel 53 West	CE 1004 - 11,0 m	Cleaning
17	2015-09-09	10:15	Bam	T&Return	Whilst barring (making safe) a piece of rock dislodged from the hanging wall, struck the now injured on the forehead and deflected on the side of his left foot.	Abrasion on the forehead and laceration on the side of left foot	RDO	HN Mangatya	Hangingwall	0,025	Poor Barring	Far East Strike 8 East Panel 47 Tip	A14312 – 11.6m	Supporting
18	2016-03-29	18H00	Bam	SERIOUS	Whilst barring a rock dislodged from a hanging wall and struck the now injured's finger	Left Thumb	Miner	D Redelinghuys	Hangingwall	0,02	Poor Barring	Strike_10_Mid_East_Belt_Line	5.0 m west from survey peg X4281	Supporting
19	2017-05-20	1H30	Bam	LDI	Whilst exchanging jumper after drilling support hole using a bolter a rock dislodges from the hangingwall and struck the injured on the hard hat. In the process of trying to have balance he injured his index and middle fingers.	Left index and middle fingers	Spotter	Jacquin Novunga	Hangingwall	0,09	Poor Barring	Ackerman Strike 18 West Panel 147	C12604 + 19.1 m	Supporting
20	2017-09-13	10H29	Bam	SERIOUS	The now injured was in the process of exhanging the jumpers, his ring and middle fingers were caught between the falling rock and drilling machine	Left index and middle fingers	RDO	Sthembiso Candlovo	Hangingwall	0,03	Poor Barring	Ackerman Strike 20 West Panel 165 West	M0075 + 11 m	Supporting
21	03-Feb-18	11H11	Bam	LDI	Whilst busy barring 20 East Tip excavation a loose rock was barred from the hanging wall. The barred rock was not identified by the now injured as a key block and as a result the rock that was held in place by the key block dislodged from the hanging wall and struck the now injured.	Soft tissue injury top of left knee and cut/laceration to the top of right knee	RDO	Franco Mhlotshana	Hangingwall	0,09	Poor Barring	Ackerman Strike 20 East Tip	BM0631 + 3,2 m West	Supporting
22	2018-06-11	20:06	Bam	SERIOUS	Failure to identify and bar loose rocks on the face after blasting. The rock dislodged from the face and struck the now injured on the finger.	Amputation of left tip of index finger	RDO	Joseph Ponde	Face area	0,25	Poor Barring	Ackerman Strike 22 West 25G u-dip	BM0760 + 14,9 m South	Supporting
23	2018-09-08	15:21	Bam	SERIOUS	Whilst busy barring 20 East PNL006B the now injured failed to identify the loose rock above him that dislodged from the hangingwall and struck him.	Laceration head, sprained lumbar spine and calcaneal fracture left foot.	Spotter	Mr. Uate	Hangingwall	0,03	Poor Barring	Ackerman Strike 20 East PNL006B	BM1306 + 8.9 m east	Supporting

APPENDIX B. Mine A's FOGs Incidents

Kroondal Section - Bambanani FOG Incidents

No	Date	Time	Shaft	Description	Basic Cause	Working Place	Source	Panel Span	Tonnes	Volume m3	Thickness [m]	Position (Peg position)	Support
1	2012-05-23	09h30	Bambanani	Whilst drilling a blast hole into the hangingwall for additional support a wedge structure dislodged from the hangingwall.	Poor early entry examination and poor barring.	Mid East 11	Hangingwall	7.3m	2,998	0,94	0,72	Back Area	GV bolts
2	2012-05-25	09h30	Bambanani	Whilst busy preparing a drilling machine to drill a support hole into the hangingwall for additional support, rocks dislodged from the hangingwall.	Poor early entry examination and poor barring.	Strike 9E panel 10E	Hangingwall	10	3,37	1,05	0,78	Back Area	GV bolts
3	2012-07-22	17h00	Bambanani	A FOG occurred when rock dislodge from the hangingwall between a fault zone and dyke.	Near vertical serpentinized joints. Near vertical fault zone, dyke, water	Strike 17 East, bord 86 East	Haningwall	6.0 m	1497,6	468,00	7,5	Face Area	2.5 m Coupling Bolts
4	2012-12-11	During Night Shift blast	Bambanani	A FOG occurred when rock dislodge from the hangingwall between a fault zone and dyke.	Mining parallel with fault/dyke/shear zone	Strike 17 East, Panel 2 Up Dip 1	Haningwall	10.0 m	854,4	267,00	5,9	Face Area	2.5 m Coupling Bolts
5	2013-05-23	11:00	Bambanani	A FOG occurred when rocks dislodged from the hangingwall along a shear zone	Up-dip blasted incorrect length and position	12 Mid East Belt Line	Haningwall	10 .0 m	370,2	115,69	3,7	Back Area	2.5 m Coupling Bolts
6	2014-06-03	Unknown	Bambanani	A FOG with dimension 4.7 m3 occurred when rocks dislodged from the hangingwall.	Poor installation of permanent systematic support. Only bottom portion of 2.5 m resin bolts are installed	Strike 7 Mid East Scalping Line	Hangingwall	5.0 m	15,14	4,73	2,2	Back Area	2.5 m Coupling Bolts
7	2016-05-20	17h50	Bambanani	A gravity induced fall - of- ground occurred with intersection of low angle fault and near vertical joints	Poor mining practice (area was not on the mine planning and no start up RA was done.)	Far East Strike 10 East panel 62 Reverse	Hanging wall	9,0 m	885	276,56	4,1	Back Area	2.5 m Coupling Bolts
8	2016-10-19	2h20	Bambanani	Whilst joining electrical cable, a piece of rock dislodged from the hanging wall and struck Mr Thage on his shoulder.	Poor barring.	Ackerman Strike 20 West Panel 165	Hangingwall	5,8	0,005	0,002	0,005	Back Area	2.5 m Coupling Bolts
9	2017-08-09	13:00	Bambanani	Cantilever wedge failure due to insufficient protrusion length. 15° joint were not identified during the safe declaration of the panel.	Insufficient support due to a un reported Tarp 3 panel	Ackermans Strike 22 East Panel 177 East Up-dip (11E)	Hangingwall	10	77,35	24,172	0,85	C12554 + 27.8 m East + 5.8 m South.	1.5 m long resin bolts
10	2017-11-28	21:15	Bambanani	A blast induced fall of ground occurred when the hangingwall was blasted to try and remove a concerning portion of the hnagingwall as identified by the line supervision.	Insufficient support due to a un reported Tarp 3 panel	Ackermans strike 22 West PNL002	Hangingwall	10	904	282,600	1,95	BM0323 + 13.7 m	1.5 m long resin bolts
11	2018-01-12	12:00	Bambanani	Sub-standard installation of the primary support in terms of the incorrect length being installed and the poor mixing of the resin along with the sub-standard application of the recommended thickness of the fibrecrete resulted in unravelling of the hanging wall, hence, the fall of ground.	Sub-standard installation of the primary support in terms of the incorrect length being installed and the poor mixing of the resin along with the sub-standard application of the recommended thickness of the fibrecrete	Ackermans Strike 19 East PNL005R 9D	Hangingwall	8	630,9	197,100	2,2	BM0460 + 5.4 m North	2.5 m Coupling Bolts
12	2018-08-22	14:30	Bambanani	A gravitational fall resulted from wedge failure that occurred along a domal feature which was truncated by a vertical feldspar vein on the weaker side. The vein was only exposed after the fall.	Failure to temporally stop the panel after the TARP trigger has been identified. A report for the TARP 3 trigger intersected in the area of concern was brought to the Rock Engineering Department on the 22nd of August 2018. The panel was however blasted on the same day.	Ackermans Strike 22 East PNL003 17CN	Hangingwall	9.9 m	15,14	4,730	1,3	BM0685 + 19.9 m east + 6.4 m north	1.5 m long resin bolts

APPENDIX C. Joint Mapping Data

Processed Data (from Dips)																
Panel Name	Distance	Rock	Dip	Azimuth	P	E	Jr	M	H	Ja	S	T	HL	Joint Set	Tape Azimuth	Tape Plunge
Sinking	6	PYX	90	170	3	0	1	1	2	1	0	2	0	1	5	0
Sinking	2,4	PEG VEIN	90	166	3	0	1	1	2	1	0	4	0	1	5	0
Sinking	3,5	PEG VEIN	90	166	3	0	1	1	2	1	0	4	0	1	5	0
Sinking	4,5	PYX	90	164	3	0	1	1	2	1	0	2	0	1	5	0
Sinking	0,1	PYX	90	150	3	0	1	1	2	1	0	2	0	1	5	0
Sinking	1,1	PYX	90	160	3	0	1	1	2	1	0	2	0	1	5	0
Sinking	2,2	PYX	90	158	3	0	1	1	2	1	0	2	0	1	5	0
Sinking	2,8	PYX	90	164	3	0	1	1	2	1	0	2	0	1	5	0
19LE PNL 3	0	PYX	90	166	4	1	1	1	2	1	0	3	0	1	5	0
19LE PNL 3	0,5	PYX	90	166	4	1	1	1	2	1	0	3	0	1	5	0
19LE PNL 3	1,4	PYX	90	166	4	1	1	1	2	1	0	3	0	1	5	0
19LE PNL 3	2,2	PYX	90	166	4	1	1	1	2	1	0	3	0	1	5	0
19LE PNL 3	2,5	PYX	90	166	4	1	1	1	2	1	0	3	0	1	5	0
19LE PNL 3	3,4	PYX	90	166	4	1	1	1	2	1	0	3	0	1	5	0
19LE PNL 3	3,6	PYX	90	166	4	1	1	1	2	1	0	3	0	1	5	0
19LE PNL 3	4,3	PYX	90	166	4	1	1	1	2	1	0	3	0	1	5	0
19LE PNL 3	5	PYX	90	166	4	1	1	1	2	1	0	3	0	1	5	0
19LE PNL 3	5,8	PYX	90	166	4	1	1	1	2	1	0	3	0	1	5	0
19LE PNL 3	6,2	PYX	90	166	4	1	1	1	2	1	0	3	0	1	5	0
19LE PNL 3	6,9	PYX	90	166	4	1	1	1	2	1	0	3	0	1	5	0
19E-5 up-dip	1,1	DYKE	85	186	4	1	1	1	2	1	0	2	0	1	5	0
19E-5 up-dip	1,5	DYKE	85	186	4	1	1	1	2	1	0	2	0	1	5	0
19E-5 up-dip	3,8	DYKE	85	140	4	1	1	1	2	1	0	2	0	1	5	0
19E-5 up-dip	4,9	DYKE	85	132	4	1	1	1	2	1	0	2	0	1	5	0
19LE PNL5	0	PYX	90	168	4	0	1	1	2	1	0	2	0	1	5	0
19LE PNL5	0,5	PYX	90	164	3	0	1	1	2	1	0	2	0	1	5	0
19LE PNL5	1,3	PYX	90	166	3	0	1	1	2	1	0	2	0	1	5	0
19LE PNL5	3,6	PYX	90	160	1	0	1	1	2	1	0	2	0	1	5	0
19LE PNL5	6,5	PYX	70	166	4	0	1	1	2	1	2	2	0	1	5	0
23LW PNL 9	0	PEG VEIN	90	180	3	0	2,5	1	2	1	0	3	0	1	5	0
23LW PNL 10	0,8	PEG VEIN	90	180	3	0	2,5	1	2	1	0	3	0	1	5	0
23LW PNL 08	0	PEG VEIN	90	178	4	0	2,5	1	2	1	0	3	0	1	5	0
23LW PNL 08	0,2	PEG VEIN	90	178	4	0	2,5	1	2	1	0	3	0	1	5	0
23LW PNL 08	0,5	PEG VEIN	90	174	4	0	2,5	1	2	1	0	3	0	1	5	0
23LW PNL 08	1,8	PYX	90	174	4	0	1	1	2	1	0	3	0	1	5	0
23LW PNL 08	3,2	PEG VEIN	90	180	4	0	2,5	1	2	1	0	4	0	1	5	0
23LW PNL 08	3,9	PEG VEIN	90	180	4	0	2,5	1	2	1	0	3	0	1	5	0
21LE PNL 1	0	PYX	90	160	4	1	1	1	2	1	0	2	0	1	5	0
21LE PNL 1	0,7	PEG VEIN	90	160	4	1	1	1	2	1	0	3	0	1	5	0
21LE PNL 1	1,6	PYX	90	160	4	1	1	1	2	1	0	2	0	1	5	0
21LE PNL 1	2,8	PYX	90	160	4	1	1	1	2	1	0	2	0	1	5	0
21LE PNL 1	6,6	PYX	90	160	4	1	1	1	2	1	0	2	0	1	5	0
21LE PNL 1	7,7	PYX	90	160	4	1	1	1	2	1	0	2	0	1	5	0
21LE PNL 2	0	PYX	90	172	3	1	1	1	2	1	0	2	0	1	5	0
21LE PNL 2	1,5	PEG VEIN	90	168	4	1	1	1	2	1	0	2	0	1	5	0
21LE PNL 2	2,4	PYX	90	164	4	1	1	1	2	1	0	2	0	1	5	0
21LE PNL 2	6	PYX	90	164	4	0	1	1	2	1	0	2	0	1	5	0
21LE PNL 2	6,4	PYX	90	164	2	0	1	1	2	1	0	2	0	1	5	0
21LE PNL 3	0,2	PYX	90	164	3	0	1	1	2	1	0	2	0	1	5	0

Processed Data (from Dips)																
Panel Name	Distance	Rock	Dip	Azimuth	P	E	Jr	M	H	Ja	S	T	HL	Joint Set	Tape Azimuth	Tape Plunge
21LE PNL 3	0,5	PYX	90	164	3	0	1	1	2	1	0	2	0	1	5	0
21LE PNL 3	3,2	PYX	90	160	3	0	1	1	2	1	0	3	0	1	5	0
21LE PNL 3	4,1	PEG VEIN	90	160	4	0	1	1	2	1	0	3	0	1	5	0
21LE PNL 3	6	PYX	90	160	4	0	1	1	2	1	0	2	0	1	5	0
21LE PNL 3	7,9	PYX	90	160	3	0	1	1	2	1	0	2	0	1	5	0
21LE PNL 3	9	PYX	90	160	3	0	1	1	2	1	0	2	0	1	5	0
21LE PNL 4	0	PYX	90	160	3	0	1	1	2	1	0	2	0	1	5	0
21LE PNL 4	1,2	PYX	90	160	3	0	1	1	2	1	0	2	0	1	5	0
21LE PNL 4	2,4	PYX	90	160	4	0	1	1	2	1	0	2	0	1	5	0
21LE PNL 4	3,2	PYX	90	160	4	0	1	1	2	1	0	2	0	1	5	0
21LE PNL 4	4,9	PYX	90	160	4	0	1	1	2	1	0	2	0	1	5	0
21LE PNL 4	6,5	PYX	90	160	4	0	1	1	2	1	0	2	0	1	5	0
21LE PNL 4	7,8	PYX	90	160	4	0	1	1	2	1	0	2	0	1	5	0
21LE PNL 4	0	PYX	90	244	3	0	1	1	2	1	0	2	0	1	95	0
21LE PNL 4	2,4	PYX	90	244	3	0	1	1	2	1	0	2	0	1	95	0
21LE PNL 6	0	PYX	90	160	4	0	1	1	2	1	0	3	0	1	5	0
21LE PNL 6	1	PYX	90	160	4	0	1	1	2	1	0	2	0	1	5	0
21LE PNL 6	1,6	PYX	90	160	4	0	1	1	2	1	0	2	0	1	5	0
21LE PNL 6	1,8	PYX	90	160	4	0	1	1	2	1	0	2	0	1	5	0
21LE PNL 6	2,8	PYX	90	160	4	0	1	1	2	1	0	2	0	1	5	0
21LE PNL 6	3	PYX	90	160	4	0	1	1	2	1	0	2	0	1	5	0
21LE PNL 6	4,4	PYX	90	160	4	0	1	1	2	1	0	2	0	1	5	0
21LE PNL 6	5,8	PEG VEIN	90	160	4	0	1	1	2	1	0	3	0	1	5	0
21LE PNL 6	6,3	PYX	90	160	4	0	1	1	2	1	0	2	0	1	5	0
21LE PNL 6	7	PYX	90	160	4	0	1	1	2	1	0	2	0	1	5	0
23LE PNL 1	0	PYX	90	160	4	0	1	1	2	1	0	2	0	1	5	0
23LE PNL 1	2,1	PYX	90	160	4	0	1	1	2	1	0	2	0	1	5	0
23LE PNL 1	2,4	PYX	90	160	4	0	1	1	2	1	0	2	0	1	5	0
23LE PNL 1	4,7	PYX	90	160	4	0	1	1	2	1	0	2	0	1	5	0
23LE PNL 1	6,1	PEG VEIN	90	160	4	0	1	1	2	1	0	3	0	1	5	0
19LE PNL 3	0,1	PYX	90	160	4	0	0,5	1	2	1	0	3	0	1	5	0
19LE PNL 3	0,3	PYX	90	160	4	0	0,5	1	2	1	0	3	0	1	5	0
19LE PNL 3	2,4	PYX	90	160	4	0	1	1	2	1	0	2	0	1	5	0
19LE PNL 3	3,5	PYX	90	160	4	0	1	1	2	1	0	2	0	1	5	0
18LE PNL 7	0	PYX	90	160	4	0	1	1	2	1	0	2	0	1	5	0
18LE PNL 7	1,3	PYX	90	160	4	0	1	1	2	1	0	2	0	1	5	0
18LE PNL 7	2,5	PYX	90	160	4	0	1	1	2	1	0	2	0	1	5	0
18LE PNL 7	2,9	PYX	90	160	4	0	1	1	2	1	0	2	0	1	5	0
18LE PNL 7	3,5	PYX	90	160	4	0	1	1	2	1	0	2	0	1	5	0
18LE PNL 7	4,1	PYX	90	160	4	0	1	1	2	1	0	2	0	1	5	0
18LE PNL 7	4,6	PYX	90	160	4	0	1	1	2	1	0	2	0	1	5	0
21LW PNL 2	0	PYX	90	160	3	0	1	1	2	1	0	2	0	1	5	0
21LW PNL 2	0,2	PEG VEIN	90	160	4	0	1	1	2	1	0	3	0	1	5	0
21LW PNL 2	0,4	PYX	90	160	4	0	1	1	2	1	0	2	0	1	5	0
21LW PNL 2	0,7	PYX	90	160	4	0	1	1	2	1	0	2	0	1	5	0
21LW PNL 2	5,9	PEG VEIN	90	160	4	0	2,5	1	2	1	0	3	0	1	5	0
21LW PNL 2	6,2	PYX	90	160	4	0	1	1	2	1	0	2	0	1	5	0
21LW PNL 2	11	PEG VEIN	90	160	4	0	2,5	1	2	1	0	3	0	1	5	0
21LW PNL 3	1,2	PYX	90	164	3	0	1	1	2	1	0	2	0	1	5	0

Processed Data (from Dips)																
Panel Name	Distance	Rock	Dip	Azimuth	P	E	Jr	M	H	Ja	S	T	HL	Joint Set	Tape Azimuth	Tape Plunge
21LW PNL 3	1,7	PYX	90	164	3	0	1	1	2	1	0	2	0	1	5	0
21LW PNL 3	3	PYX	90	174	4	0	1	1	2	1	0	2	0	1	5	0
21LW PNL 3	4,8	PYX	90	160	4	0	1	1	2	1	0	2	0	1	5	0
21LW PNL 3	5,9	PYX	90	164	3	0	1	1	2	1	0	2	0	1	5	0
21LW PNL 3	7,9	PEG VEIN	90	160	4	0	2,5	1	2	1	0	3	0	1	5	0
21LW PNL 3	9	PYX	90	160	3	0	1	1	2	1	0	2	0	1	5	0
21LW PNL 4	0	PEG VEIN	90	180	3	0	2,5	1	2	1	0	3	0	1	5	0
21LW PNL 4	1,3	PYX	90	184	3	0	1	1	2	1	0	2	0	1	5	0
21LW PNL 4 back	0,1	PYX	90	194	3	0	1	1	2	1	0	2	0	1	5	0
21LW PNL 4 back	2,2	PEG VEIN	90	194	4	0	2,5	1	2	1	0	3	0	1	5	0
21LW PNL 4 back	8,3	PYX	90	190	4	0	1	1	2	1	0	2	0	1	5	0
21LW PNL 4 back	9,9	PYX	90	190	4	0	1	1	2	1	0	2	0	1	5	0
21LW PNL 4 back	10,2	PEG VEIN	90	190	4	0	2,5	1	2	1	0	3	0	1	5	0
21LW PNL 4 back	0	PYX	90	190	4	0	1	1	2	1	0	2	0	1	5	0
21LW PNL 5	1	PEG VEIN	90	170	4	0	2,5	1	2	1	0	3	0	1	5	0
21LW PNL 5	2,3	PEG VEIN	90	170	4	0	2,5	1	2	1	0	3	0	1	5	0
21LW PNL 5	3,5	PEG VEIN	90	170	4	0	2,5	1	2	1	0	3	0	1	5	0
21LW PNL 5	4,5	PEG VEIN	90	170	4	0	2,5	1	2	1	0	3	0	1	5	0
21LW PNL 5	7	PEG VEIN	90	170	4	0	2,5	1	2	1	0	3	0	1	5	0
21LW PNL 6	0,1	PYX	90	160	4	0	1	1	2	1	0	2	0	1	5	0
21LW PNL 6	0,6	PYX	90	160	4	0	1	1	2	1	0	2	0	1	5	0
21LW PNL 6	4,3	PYX	90	160	4	0	1	1	2	1	0	3	0	1	5	0
20LE PNL 2	0	PYX	90	160	4	0	1	1	2	1	0	2	0	1	5	0
20LE PNL 2	0,1	PYX	90	160	4	0	1	1	2	1	0	2	0	1	5	0
20LE PNL 2	0,2	PYX	90	160	4	0	1	1	2	1	0	2	0	1	5	0
20LE PNL 2	0,3	PYX	90	160	4	0	1	1	2	1	0	2	0	1	5	0
20LE PNL 2	2	PYX	90	160	4	0	1	1	2	1	0	2	0	1	5	0
20LE PNL 2	2,5	PYX	90	160	4	0	1	1	2	1	0	2	0	1	5	0
20LE PNL 2	2,8	PYX	90	160	4	0	1	1	2	1	0	2	0	1	5	0
20LE PNL 2	3	PYX	90	160	4	0	1	1	2	1	0	2	0	1	5	0
20LE PNL 2	3,2	PYX	90	160	4	0	1	1	2	1	0	2	0	1	5	0
20LE PNL 2	3,4	PYX	90	160	4	0	1	1	2	1	0	2	0	1	5	0
20LE PNL 2	4	PYX	90	160	4	0	1	1	2	1	0	3	0	1	5	0
20LE PNL 2	6,5	PYX	90	160	4	0	1	1	2	1	0	2	0	1	5	0
20LE PNL 2	6,8	PYX	90	160	4	0	1	1	2	1	0	2	0	1	5	0
20LE PNL 2	7	PYX	90	160	4	0	1	1	2	1	0	2	0	1	5	0
20LE PNL 2	8,2	PYX	90	160	4	0	1	1	2	1	0	2	0	1	5	0
20LE PNL 3	0	PYX	90	164	4	0	1	1	2	1	0	2	0	1	5	0
20LE PNL 3	0,5	PYX	90	164	4	0	1	1	2	1	0	2	0	1	5	0
20LE PNL 3	0,8	PYX	90	164	4	0	1	1	2	1	0	2	0	1	5	0
20LE PNL 3	1,2	PYX	90	164	4	0	1	1	2	1	0	2	0	1	5	0
20LE PNL 3	1,3	PYX	90	164	4	0	1	1	2	1	0	2	0	1	5	0
20LE PNL 3	1,4	PYX	90	164	4	0	1	1	2	1	0	2	0	1	5	0
20LE PNL 3	1,7	PYX	90	164	4	0	1	1	2	1	0	2	0	1	5	0
20LE PNL 3	2,5	PYX	90	160	4	0	1	1	2	1	0	2	0	1	5	0
20LE PNL 3	4,2	PYX	90	158	4	0	1	1	2	1	0	2	0	1	5	0
20LE PNL 3	4,9	PYX	90	162	4	0	1	1	2	1	0	2	0	1	5	0
20LE PNL 3	6,1	PYX	90	164	4	0	1	1	2	1	0	2	0	1	5	0
20LE PNL 3	9,2	PYX	90	164	4	0	1	1	2	1	0	2	0	1	5	0

Processed Data (from Dips)																
Panel Name	Distance	Rock	Dip	Azimuth	P	E	Jr	M	H	Ja	S	T	HL	Joint Set	Tape Azimuth	Tape Plunge
20LE PNL 3	10	PYX	90	164	4	0	1	1	2	1	0	2	0	1	5	0
20LE PNL 4	0	PYX	90	162	3	0	1	1	2	1	0	2	0	1	5	0
20LE PNL 4	2,1	PYX	90	162	3	0	1	1	2	1	0	2	0	1	5	0
20LE PNL 4	3,5	PYX	90	162	3	0	1	1	2	1	0	2	0	1	5	0
20LE PNL 4	5,6	PYX	90	162	3	0	1	1	2	1	0	2	0	1	5	0
20LE PNL 4	6,7	PYX	90	162	3	0	1	1	2	1	0	2	0	1	5	0
20LE PNL 5	0	PYX	90	180	4	0	1	1	2	1	0	2	0	1	5	0
20LE PNL 5	0,7	PEG VEIN	90	180	4	0	2,5	1	2	1	0	3	0	1	5	0
20LE PNL 5	3,2	PYX	90	180	4	0	1	1	2	1	0	3	0	1	5	0
20LE PNL 5	3,7	PYX	90	180	4	0	1	1	2	1	0	2	0	1	5	0
20LE PNL 5	4,3	PYX	90	180	4	0	1	1	2	1	0	2	0	1	5	0
20LE PNL 5	4,7	PYX	90	180	4	0	1	1	2	1	0	2	0	1	5	0
20LE PNL 5	5,5	PYX	90	180	4	0	1	1	2	1	0	2	0	1	5	0
20LE PNL 6	0	PYX	90	160	4	0	1	1	2	1	0	2	0	1	5	0
20LE PNL 6	3,2	PYX	90	160	4	0	1	1	2	1	0	2	0	1	5	0
20LE PNL 6	6,2	PYX	90	160	4	0	1	1	2	1	0	2	0	1	5	0
CHL Decline	0	PYX	90	168	3	1	1	1	2	1	0	1	0	1	5	0
CHL Decline	0,3	PYX	90	168	3	1	1	1	2	1	0	1	0	1	5	0
CHL Decline	0,9	PEG VEIN	90	172	4	0	2,5	1	2	1	0	3	0	1	5	0
CHL Decline	3,3	PYX	90	168	4	0	1	1	2	1	0	2	0	1	5	0
CHL Decline	4,5	PYX	90	168	4	0	1	1	2	1	0	2	0	1	5	0
CHL Decline	7,2	PYX	90	168	4	0	1	1	2	1	0	2	0	1	5	0
CHL Decline	10,1	PYX	90	166	4	0	1	1	2	1	0	3	0	1	5	0
CHL Lateral west	0	PYX	90	162	4	0	1	1	2	1	0	2	0	1	5	0
CHL Lateral west	0,4	PYX	90	162	4	0	1	1	2	1	0	2	0	1	5	0
CHL Lateral west	0,7	PYX	90	162	4	0	1	1	2	1	0	2	0	1	5	0
CHL Lateral west	1,1	PYX	90	162	4	0	1	1	2	1	0	2	0	1	5	0
CHL Lateral west	1,7	PYX	90	162	4	0	1	1	2	1	0	3	0	1	5	0
CHL Lateral west	3,2	PYX	90	162	4	0	1	1	2	1	0	2	0	1	5	0
CHL Lateral west	4,3	PYX	90	162	4	0	1	1	2	1	0	2	0	1	5	0
CHL Lateral west	5,2	PYX	90	162	4	0	1	1	2	1	0	2	0	1	5	0
CHL Lateral west	6	PYX	90	162	4	0	1	1	2	1	0	2	0	1	5	0
MM DECLINE	0	PYX	90	162	4	0	1	1	2	1	0	2	0	1	5	0
MM DECLINE	2,3	PYX	90	170	4	0	1	1	2	1	0	2	0	1	5	0
MM DECLINE	6,2	PYX	90	170	4	0	1	1	2	1	0	2	0	1	5	0
MM DECLINE	8,2	PYX	90	170	4	0	1	1	2	1	0	2	0	1	5	0
MM DECLINE	9	PYX	90	170	4	0	1	1	2	1	0	2	0	1	5	0
MM DECLINE	10	PYX	90	170	4	0	1	1	2	1	0	2	0	1	5	0
MM DECLINE	11	PYX	90	170	4	0	1	1	2	1	0	2	0	1	5	0
22 LE PNL 6 UP DIP	0	PYX	90	186	4	0	1	1	2	1	0	2	0	1	5	0
22 LE PNL 6 UP DIP	1,1	PEG VEIN	90	186	4	0	2,5	1	2	1	0	3	0	1	5	0
22 LE PNL 6 UP DIP	1,8	PYX	90	186	4	0	1	1	2	1	0	2	0	1	5	0
22 LE PNL 6 UP DIP	3	PYX	90	186	4	0	1	1	2	1	0	2	0	1	5	0
22 LE PNL 6 UP DIP	0	PEG VEIN	90	186	4	0	2,5	1	2	1	0	3	0	1	5	0
22 LE PNL 6 UP DIP	1,5	PYX	90	186	4	0	1	1	2	1	0	2	0	1	5	0
22 LE PNL 6 UP DIP	3,1	PYX	90	186	4	0	1	1	2	1	0	2	0	1	5	0
23 LE PNL 6 UP DIP	3,5	PYX	90	186	4	0	1	1	2	1	0	2	0	1	5	0
22 LE PNL 6 UP DIP	3,8	PYX	90	186	4	0	1	1	2	1	0	2	0	1	5	0
22 LE PNL 6 UP DIP	4,3	PEG VEIN	90	186	4	0	2,5	1	2	1	0	3	0	1	5	0

Processed Data (from Dips)																
Panel Name	Distance	Rock	Dip	Azimuth	P	E	Jr	M	H	Ja	S	T	HL	Joint Set	Tape Azimuth	Tape Plunge
22 LE PNL 6 UP DIP	4,7	PYX	90	186	4	0	1	1	2	1	0	2	0	1	5	0
22 LE PNL 6 UP DIP	5,2	PYX	90	186	4	0	1	1	2	1	0	2	0	1	5	0
22 LE PNL 6 UP DIP	6,7	PYX	90	186	4	0	1	1	2	1	0	2	0	1	5	0
22 LE PNL 6 UP DIP	7,3	PYX	90	186	4	0	1	1	2	1	0	2	0	1	5	0
22 LE PNL 6 UP DIP	8,5	PYX	90	186	4	0	1	1	2	1	0	2	0	1	5	0
22 LE PNL 6 UP DIP	9,6	PYX	90	186	4	0	1	1	2	1	0	2	0	1	5	0
22 LE PNL 6 UP DIP	10,7	PYX	90	186	4	0	1	1	2	1	0	2	0	1	5	0
22 LE PNL 7	0	PYX	90	172	4	0	1	1	2	1	0	2	0	1	5	0
22 LE PNL 7	2,5	PYX	90	172	4	0	1	1	2	1	0	2	0	1	5	0
22 LE PNL 7	3,5	PYX	90	172	4	0	1	1	2	1	0	2	0	1	5	0
22 LE PNL 7	5,4	PYX	90	172	4	0	1	1	2	1	0	2	0	1	5	0
22 LE PNL 7	6	PYX	90	172	4	0	1	1	2	1	0	2	0	1	5	0
22 LE PNL 7	6,6	PYX	90	172	4	0	1	1	2	1	0	2	0	1	5	0
22 LE PNL 7	7,7	PYX	90	172	4	0	1	1	2	1	0	2	0	1	5	0
22 LE PNL 7	8,7	PYX	90	172	4	0	1	1	2	1	0	2	0	1	5	0
22 LE PNL 7	9,3	PYX	90	172	4	0	1	1	2	1	0	2	0	1	5	0
22 LE PNL 8	0	PYX	90	164	4	0	1	1	2	1	0	2	0	1	5	0
22 LE PNL 8	0,5	PYX	90	164	4	0	1	1	2	1	0	2	0	1	5	0
22 LE PNL 8	1,4	PYX	90	164	4	0	1	1	2	1	0	2	0	1	5	0
22 LE PNL 8	2,9	PYX	90	164	4	0	1	1	2	1	0	2	0	1	5	0
22 LE PNL 8	4,5	PEG VEIN	90	164	4	0	2,5	1	2	1	0	3	0	1	5	0
22 LE PNL 8	5,5	PYX	90	164	4	0	1	1	2	1	0	2	0	1	5	0
22 LE PNL 8	6,3	PYX	90	164	4	0	1	1	2	1	0	2	0	1	5	0
22 LE PNL 8	7	PYX	90	164	4	0	1	1	2	1	0	2	0	1	5	0
22 LE PNL 8	7,8	PYX	90	164	4	0	1	1	2	1	0	2	0	1	5	0
22 LE PNL 8	8,5	PYX	90	164	4	0	1	1	2	1	0	2	0	1	5	0
22 LE PNL 8	9	PYX	90	164	4	0	1	1	2	1	0	2	0	1	5	0
22 LE PNL 8	9,6	PYX	90	164	4	0	1	1	2	1	0	2	0	1	5	0
22 LE PNL 9	0	PEG VEIN	90	166	4	0	2,5	1	2	1	0	3	0	1	5	0
22 LE PNL 9	1	PYX	90	166	4	0	1	1	2	1	0	2	0	1	5	0
22 LE PNL 9	2	PYX	90	166	4	0	1	1	2	1	0	2	0	1	5	0
22 LE PNL 9	2,3	PYX	90	166	4	0	1	1	2	1	0	2	0	1	5	0
22 LE PNL 9	3,5	PYX	90	166	4	0	1	1	2	1	0	2	0	1	5	0
22 LE PNL 9	4,1	PYX	90	166	4	0	1	1	2	1	0	2	0	1	5	0
22 LE PNL 9	4,6	PYX	90	166	4	0	1	1	2	1	0	2	0	1	5	0
22 LE PNL 9	5,5	PYX	90	166	4	0	1	1	2	1	0	2	0	1	5	0
22 LE PNL 9	6,4	PYX	90	166	4	0	1	1	2	1	0	2	0	1	5	0
22 LE PNL 9	8,5	PYX	90	186	4	0	1	1	2	1	0	2	0	1	5	0
22 LE PNL 9	8,8	PYX	90	166	4	0	1	1	2	1	0	2	0	1	5	0
22 LE PNL 10	0	PYX	90	166	4	0	1	1	2	1	0	2	0	1	5	0
22 LE PNL 10	2	PYX	90	166	4	0	1	1	2	1	0	2	0	1	5	0
22 LE PNL 10	3,3	PYX	90	166	4	0	1	1	2	1	0	2	0	1	5	0
22 LE PNL 10	3,8	PEG VEIN	90	166	4	0	2,5	1	2	1	0	3	0	1	5	0
22 LE PNL 10	4,6	PYX	90	166	4	0	1	1	2	1	0	2	0	1	5	0
22 LE PNL 10	5,1	PYX	90	166	4	0	1	1	2	1	0	2	0	1	5	0
22 LE PNL 10	6,7	PEG VEIN	90	166	4	0	2,5	1	2	1	0	3	0	1	5	0
22 LE PNL 10	7,5	PYX	90	166	4	0	1	1	2	1	0	2	0	1	5	0
22 LE PNL 10	8,3	PYX	90	166	4	0	1	1	2	1	0	2	0	1	5	0
22 LE PNL 10	9	PYX	90	166	4	0	1	1	2	1	0	2	0	1	5	0

Processed Data (from Dips)																
Panel Name	Distance	Rock	Dip	Azimuth	P	E	Jr	M	H	Ja	S	T	HL	Joint Set	Tape Azimuth	Tape Plunge
22 LE PNL 10	9,3	PYX	90	166	4	0	1	1	2	1	0	2	0	1	5	0
22 LE PNL 10	9,5	PYX	90	166	4	0	1	1	2	1	0	2	0	1	5	0
23 LE PNL 1	0	PEG VEIN	90	180	4	0	2,5	1	2	1	0	3	0	1	5	0
23 LE PNL 1	3,2	PYX	90	180	4	0	1	1	2	1	0	2	0	1	5	0
23 LE PNL 1	3,6	PYX	90	180	4	0	1	1	2	1	0	2	0	1	5	0
23 LE PNL 1	4,9	PEG VEIN	90	180	4	0	2,5	1	2	1	0	3	0	1	5	0
23 LE PNL 1	10	PEG VEIN	90	180	4	0	2,5	1	2	1	0	3	0	1	5	0
21 LW PNL 3	0	PYX	90	172	3	1	1	1	2	1	0	2	0	1	5	0
21 LW PNL 3	0,9	PEG VEIN	90	180	4	0	2,5	1	2	1	0	3	0	1	5	0
21 LW PNL 3	1,5	PYX	90	180	3	1	1	1	2	1	0	2	0	1	5	0
21 LW PNL 3	3,1	PYX	90	180	2	1	1	1	2	1	0	2	0	1	5	0
21 LW PNL 3	6	PYX	90	180	4	0	1	1	2	1	0	2	0	1	5	0
21 LW PNL 3	8	PYX	90	180	4	0	1	1	2	1	0	2	0	1	5	0
21 LW PNL 3 DOWN	0	PYX	90	166	4	0	1	1	2	1	0	2	0	1	5	0
21 LW PNL 3 DOWN	0,2	PYX	90	166	4	0	1	1	2	1	0	2	0	1	5	0
21 LW PNL 3 DOWN	2,2	PYX	90	166	4	0	1	1	2	1	0	3	0	1	5	0
21 LW PNL 3 DOWN	3,5	PEG VEIN	90	170	4	0	2,5	1	2	1	0	3	0	1	5	0
21 LW PNL 3 DOWN	4,4	PYX	90	170	4	0	1	1	2	1	0	2	0	1	5	0
21 LW PNL 3 DOWN	5,4	PYX	90	170	4	0	1	1	2	1	0	2	0	1	5	0
21 LW PNL 3 DOWN	7,8	PEG VEIN	90	170	4	0	2,5	1	2	1	0	3	0	1	5	0
21 LW PNL 3 DOWN	9,5	PYX	90	162	4	0	1	1	2	1	0	2	0	1	5	0
21 LW PNL 6	0	PYX	90	170	4	0	1	1	2	1	0	2	0	1	5	0
21 LW PNL 6	0,9	PYX	90	170	4	0	1	1	2	1	0	2	0	1	5	0
21 LW PNL 6	2,1	PYX	90	170	4	0	1	1	2	1	0	2	0	1	5	0
21 LW PNL 6	3,6	PYX	90	170	4	0	1	1	2	1	0	2	0	1	5	0
21 LW PNL 6	5,2	PEG VEIN	90	170	4	0	2,5	1	2	1	0	3	0	1	5	0
21 LW PNL 6	7,1	PYX	90	170	4	0	1	1	2	1	0	2	0	1	5	0
21 LW PNL 6	8,2	PEG VEIN	90	170	4	0	2,5	1	2	1	0	3	0	1	5	0
21 LW PNL 6	10,1	PYX	90	170	4	0	1	1	2	1	0	2	0	1	5	0
21 LW PNL 6 Down	0	PYX	90	168	4	0	1	1	2	1	0	2	0	1	5	0
21 LW PNL 6 Down	0,9	PYX	90	168	4	0	1	1	2	1	0	2	0	1	5	0
21 LW PNL 6 Down	3,3	PYX	90	168	4	0	1	1	2	1	0	2	0	1	5	0
21 LW PNL 6 Down	3,8	PEG VEIN	90	168	4	0	2,5	1	2	1	0	3	0	1	5	0
21 LW PNL 6 Down	8,3	PEG VEIN	90	168	4	0	2,5	1	2	1	0	3	0	1	5	0
22E PNL 6	0	VIEN	90	216	4	0	2,5	1	2	1	0	3	0	1	5	0
22E PNL 6	1,3	PYX	90	195	4	0	1	1	2	1	0	2	0	1	5	0
22E PNL 6	1,9	PYX	90	195	4	0	1	1	2	1	0	2	0	1	5	0
22E PNL 6	2	PYX	90	195	4	0	1	1	2	1	0	2	0	1	5	0
22E PNL 6	3,2	PEG VEIN	90	205	4	0	2,5	1	2	1	0	3	0	1	5	0
22E PNL 6	5,2	PEG VEIN	90	205	4	0	2,5	1	2	1	0	3	0	1	5	0
22E PNL 6	6,3	PYX	90	195	4	0	1	1	2	1	0	2	0	1	5	0
22E PNL 6	7,6	PYX	90	195	4	0	1	1	2	1	0	2	0	1	5	0
22E PNL 6	8,8	PYX	90	195	4	0	1	1	2	1	0	2	0	1	5	0
22E PNL 7	0	PEG VEIN	90	216	4	0	2,5	1	2	1	0	3	0	1	5	0
22E PNL 7	1	PYX	90	198	4	0	1	1	2	1	0	2	0	1	5	0
22E PNL 7	1,6	PYX	90	198	4	0	1	1	2	1	0	2	0	1	5	0
22E PNL 7	1,8	PYX	90	198	4	0	1	1	2	1	0	2	0	1	5	0
22E PNL 7	2,1	PYX	90	198	4	0	1	1	2	1	0	2	0	1	5	0
22E PNL 7	2,6	PYX	90	198	4	0	1	1	2	1	0	2	0	1	5	0

Processed Data (from Dips)																
Panel Name	Distance	Rock	Dip	Azimuth	P	E	Jr	M	H	Ja	S	T	HL	Joint Set	Tape Azimuth	Tape Plunge
22E PNL 7	3,5	PYX	90	198	4	0	1	1	2	1	0	2	0	1	5	0
22E PNL 7	4,3	PYX	90	198	4	0	1	1	2	1	0	2	0	1	5	0
22E PNL 7	4,6	PYX	90	198	4	0	1	1	2	1	0	2	0	1	5	0
22E PNL 7	5,4	PYX	90	198	4	0	1	1	2	1	0	2	0	1	5	0
22E PNL 7	6,2	PYX	90	198	4	0	1	1	2	1	0	2	0	1	5	0
22E PNL 7	6,7	PYX	90	198	4	0	1	1	2	1	0	2	0	1	5	0
22E PNL 7	7,7	PYX	90	198	4	0	1	1	2	1	0	2	0	1	5	0
22E PNL 7	8,7	PYX	90	198	4	0	1	1	2	1	0	2	0	1	5	0
22E PNL 7	9,5	PYX	90	198	4	0	1	1	2	1	0	2	0	1	5	0
22E PNL 7	9,9	PEG VEIN	90	216	4	0	2,5	1	2	1	0	3	0	1	5	0
22E PNL 8	0	PYX	90	196	4	0	1	1	2	1	0	2	0	1	5	0
22E PNL 8	0,6	PYX	90	196	4	0	1	1	2	1	0	2	0	1	5	0
22E PNL 8	0,8	PYX	90	196	4	0	1	1	2	1	0	2	0	1	5	0
22E PNL 8	1,2	PYX	90	196	4	0	1	1	2	1	0	2	0	1	5	0
22E PNL 8	1,8	PYX	90	196	4	0	1	1	2	1	0	2	0	1	5	0
22E PNL 8	2,7	PYX	90	196	4	0	1	1	2	1	0	2	0	1	5	0
22E PNL 8	3,1	PYX	90	196	4	0	1	1	2	1	0	2	0	1	5	0
22E PNL 8	3,6	PYX	90	196	4	0	1	1	2	1	0	2	0	1	5	0
22E PNL 8	4,3	PYX	90	196	4	0	1	1	2	1	0	2	0	1	5	0
22E PNL 8	4,9	PYX	90	196	4	0	1	1	2	1	0	2	0	1	5	0
22E PNL 8	5,8	PYX	90	196	4	0	1	1	2	1	0	2	0	1	5	0
22E PNL 8	7,3	PYX	90	196	4	0	1	1	2	1	0	2	0	1	5	0
22E PNL 8	7,9	PYX	90	196	4	0	1	1	2	1	0	2	0	1	5	0
22E PNL 8	9,2	PYX	90	196	4	0	1	1	2	1	0	2	0	1	5	0
22E PNL 9	0	PYX	90	194	4	0	1	1	2	1	0	2	0	1	5	0
22E PNL 9	0,9	PYX	90	194	4	0	1	1	2	1	0	2	0	1	5	0
22E PNL 9	1,9	PYX	90	194	4	0	1	1	2	1	0	2	0	1	5	0
22E PNL 9	3,5	PYX	90	194	4	0	1	1	2	1	0	2	0	1	5	0
22E PNL 9	4,9	PYX	90	194	4	0	1	1	2	1	0	2	0	1	5	0
22E PNL 9	6	PYX	90	194	4	0	1	1	2	1	0	2	0	1	5	0
22E PNL 9	6,6	PYX	90	194	4	0	1	1	2	1	0	2	0	1	5	0
22E PNL 9	7,6	PEG VEIN	90	194	4	0	2,5	1	2	1	0	3	0	1	5	0
22E PNL 9	11,9	PYX	90	194	4	0	1	1	2	1	0	2	0	1	5	0
22E PNL 10	0	PEG VEIN	90	220	4	0	2,5	1	2	1	0	3	0	1	5	0
22E PNL 10	0,8	PYX	90	198	4	0	1	1	2	1	0	2	0	1	5	0
22E PNL 10	1,5	PYX	90	198	4	0	1	1	2	1	0	2	0	1	5	0
22E PNL 10	2,3	PEG VEIN	90	210	4	0	2,5	1	2	1	0	3	0	1	5	0
22E PNL 10	3,1	PYX	90	198	4	0	1	1	2	1	0	2	0	1	5	0
22E PNL 10	3,6	PEG VEIN	90	198	4	0	2,5	1	2	1	0	3	0	1	5	0
22E PNL 10	4,3	PYX	90	198	4	0	1	1	2	1	0	2	0	1	5	0
22E PNL 10	5,6	PYX	90	198	4	0	1	1	2	1	0	2	0	1	5	0
22E PNL 10	6,1	PYX	90	198	4	0	1	1	2	1	0	2	0	1	5	0
22E PNL 10	6,7	PEG VEIN	90	210	4	0	2,5	1	2	1	0	3	0	1	5	0
22E PNL 10	7,6	PEG VEIN	90	210	4	0	2,5	1	2	1	0	3	0	1	5	0
22E PNL 10	9,2	PYX	90	198	4	0	1	1	2	1	0	2	0	1	5	0
22E PNL 10	10,2	PYX	90	198	4	0	1	1	2	1	0	2	0	1	5	0
23LE PNL 1	0	PYX	90	196	4	0	1	1	2	1	0	2	0	1	5	0
23LE PNL 1	1,6	PYX	90	196	4	0	1	1	2	1	0	2	0	1	5	0
23LE PNL 1	3	PYX	90	196	4	0	1	1	2	1	0	2	0	1	5	0

Processed Data (from Dips)																
Panel Name	Distance	Rock	Dip	Azimuth	P	E	Jr	M	H	Ja	S	T	HL	Joint Set	Tape Azimuth	Tape Plunge
23LE PNL 1	4,4	PYX	90	196	4	0	1	1	2	1	0	2	0	1	5	0
23LE PNL 1	5,3	PYX	90	196	4	0	1	1	2	1	0	2	0	1	5	0
23LE PNL 1	6,4	PEG VEIN	90	196	4	0	2,5	1	2	1	0	3	0	1	5	0
23LE PNL 1	8	PYX	90	196	4	0	1	1	2	1	0	2	0	1	5	0
23LE PNL 1	8,7	PEG VEIN	90	196	4	0	2,5	1	2	1	0	3	0	1	5	0
23LE PNL 1	9,4	PYX	90	196	4	0	1	1	2	1	0	2	0	1	5	0
23LE PNL 2	0	PYX	90	198	4	0	1	1	2	1	0	2	0	1	5	0
23LE PNL 2	0,2	PEG VEIN	90	210	4	0	2,5	1	2	1	0	3	0	1	5	0
23LE PNL 2	0,4	PEG VEIN	90	210	4	0	2,5	1	2	1	0	3	0	1	5	0
23LE PNL 2	2,2	PYX	90	198	4	0	1	1	2	1	0	2	0	1	5	0
23LE PNL 2	4,4	PYX	90	198	4	0	1	1	2	1	0	2	0	1	5	0
23LE PNL 2	5,1	PEG VEIN	90	210	4	0	2,5	1	2	1	0	3	0	1	5	0
23LE PNL 2	6,6	PYX	90	198	4	0	1	1	2	1	0	2	0	1	5	0
23LE PNL 2	7,5	PYX	90	198	4	0	1	1	2	1	0	2	0	1	5	0
23LE PNL 2	8,9	PYX	90	198	4	0	1	1	2	1	0	2	0	1	5	0
23LE PNL 2	10	PYX	90	198	4	0	1	1	2	1	0	2	0	1	5	0
22LW PNL 4	7,9	PEG VEIN	90	168	4	0	2,5	1	2	1	0	3	0	1	5	0
22LW PNL 4	8,3	PYX	90	168	4	0	1	1	2	1	0	2	0	1	5	0
22LW PNL 4	9,3	PYX	90	168	4	0	1	1	2	1	0	2	0	1	5	0
22LW PNL 7	0	PYX	90	166	4	0	1	1	2	1	0	2	0	1	5	0
22LW PNL 7	1,6	PYX	90	166	4	0	1	1	2	1	0	2	0	1	5	0
22LW PNL 7	3,9	PEG VEIN	90	166	4	0	2,5	1	2	1	0	3	0	1	5	0
22LW PNL 7	5,2	PYX	90	166	4	0	1	1	2	1	0	2	0	1	5	0
22LW PNL 7	8,2	PYX	90	166	4	0	1	1	2	1	0	2	0	1	5	0
22LW PNL 7	10,3	PYX	90	172	4	0	1	1	2	1	0	2	0	1	5	0
22LW PNL 8	0	PYX	90	168	4	0	1	1	2	1	0	2	0	1	5	0
22LW PNL 8	1,2	PYX	90	168	4	0	1	1	2	1	0	2	0	1	5	0
22LW PNL 8	2,6	PYX	90	168	4	0	1	1	2	1	0	2	0	1	5	0
22LW PNL 8	4,8	PYX	90	168	4	0	1	1	2	1	0	2	0	1	5	0
22LW PNL 8	4,9	PYX	90	168	4	0	1	1	2	1	0	2	0	1	5	0
22LW PNL 8	5,9	PYX	90	168	4	0	1	1	2	1	0	2	0	1	5	0
22LW PNL 8	6,8	PYX	90	168	4	0	1	1	2	1	0	2	0	1	5	0
22LW PNL 8	8,1	PYX	90	168	4	0	1	1	2	1	0	2	0	1	5	0
22LW PNL 9	0	PYX	90	190	4	0	1	1	2	1	0	2	0	1	5	0
22LW PNL 9	0,5	PYX	90	190	4	0	1	1	2	1	0	2	0	1	5	0
22LW PNL 9	2,3	PYX	90	190	4	0	1	1	2	1	0	2	0	1	5	0
22LW PNL 9	3,5	PYX	90	190	4	0	1	1	2	1	0	2	0	1	5	0
22LW PNL 9	5,7	PYX	90	190	4	0	1	1	2	1	0	2	0	1	5	0
22LW PNL 9	6,5	PYX	90	190	4	0	1	1	2	1	0	2	0	1	5	0
22LW PNL 9	7,8	PYX	90	190	4	0	1	1	2	1	0	2	0	1	5	0
22LW PNL 9	9,2	PYX	90	190	4	0	1	1	2	1	0	2	0	1	5	0
22LW PNL 9	10,1	PYX	90	190	4	0	1	1	2	1	0	2	0	1	5	0
19LE PNL 6	0	PYX	90	168	4	0	1	1	2	1	0	2	0	1	5	0
19LE PNL 6	0,6	PYX	90	168	4	0	1	1	2	1	0	3	0	1	5	0
19LE PNL 6	0,8	PYX	90	168	4	0	1	1	2	1	0	2	0	1	5	0
19LE PNL 6	1,3	PYX	90	168	4	0	1	1	2	1	0	2	0	1	5	0
19LE PNL 6	2	PYX	90	168	4	0	1	1	2	1	0	2	0	1	5	0
19LE PNL 6	2,4	PYX	90	168	4	0	1	1	2	1	0	2	0	1	5	0
19LE PNL 6	3	PYX	90	168	4	0	1	1	2	1	0	2	0	1	5	0

Processed Data (from Dips)																
Panel Name	Distance	Rock	Dip	Azimuth	P	E	Jr	M	H	Ja	S	T	HL	Joint Set	Tape Azimuth	Tape Plunge
19LE PNL 6	3,4	PYX	90	168	4	0	1	1	2	1	0	2	0	1	5	0
19LE PNL 6	3,9	PYX	90	168	4	0	1	1	2	1	0	2	0	1	5	0
19LE PNL 6	4,7	PYX	90	168	4	0	1	1	2	1	0	2	0	1	5	0
19LE PNL 6	5,3	PYX	90	168	4	0	1	1	2	1	0	2	0	1	5	0
19LE PNL 6	5,9	PYX	90	168	4	0	1	1	2	1	0	2	0	1	5	0
19LE PNL 6	6,6	PYX	90	168	4	0	1	1	2	1	0	2	0	1	5	0
19LE PNL 6	7,5	PYX	90	168	4	0	1	1	2	1	0	2	0	1	5	0
19LE PNL 6	8,2	PYX	90	168	4	0	1	1	2	1	0	2	0	1	5	0
19LE PNL 6	9,4	PYX	90	168	4	0	1	1	2	1	0	2	0	1	5	0
19LE PNL 6	10,2	PYX	90	168	4	0	1	1	2	1	0	2	0	1	5	0
19LE PNL 5 up-dip	0	PYX	90	172	4	0	1	1	2	1	0	2	0	1	5	0
19LE PNL 5 up-dip	0,3	PYX	90	172	4	0	1	1	2	1	0	2	0	1	5	0
19LE PNL 5 up-dip	1,1	PYX	90	172	4	0	1	1	2	1	0	2	0	1	5	0
19LE PNL 5 up-dip	1,3	PYX	90	172	4	0	1	1	2	1	0	2	0	1	5	0
19LE PNL 5 up-dip	1,5	PYX	90	172	4	0	1	1	2	1	0	2	0	1	5	0
19LE PNL 5 up-dip	2,1	PYX	90	172	4	0	1	1	2	1	0	2	0	1	5	0
19LE PNL 5 up-dip	2,4	PYX	90	172	4	0	1	1	2	1	0	2	0	1	5	0
19LE PNL 5 up-dip	3	PYX	90	172	4	0	1	1	2	1	0	2	0	1	5	0
19LE PNL 5 up-dip	3,4	PYX	90	172	4	0	1	1	2	1	0	2	0	1	5	0
19LE PNL 5 up-dip	3,6	DYKE	90	190	4	0	1	1	2	1	0	2	0	1	5	0
19LE PNL 5 up-dip	4,3	DYKE	90	190	4	0	1	1	2	1	0	2	0	1	5	0
19LE PNL 5 up-dip	6	DYKE	90	190	4	0	1	1	2	1	0	2	0	1	5	0
21LW PNL 3	0	PYX	90	174	4	0	1	1	2	1	0	2	0	1	5	0
21LW PNL 3	0,5	PYX	90	174	4	0	1	1	2	1	0	2	0	1	5	0
21LW PNL 3	0,8	PYX	90	174	4	0	1	1	2	1	0	2	0	1	5	0
21LW PNL 3	1	PYX	90	174	4	0	1	1	2	1	0	2	0	1	5	0
21LW PNL 3	1,1	PYX	90	174	4	0	1	1	2	1	0	2	0	1	5	0
21LW PNL 3	1,5	PYX	90	174	4	0	1	1	2	1	0	2	0	1	5	0
21LW PNL 3	3,7	PYX	90	174	4	0	1	1	2	1	0	2	0	1	5	0
21LW PNL 3	4,7	PEG VEIN	90	174	4	0	2,5	1	2	1	0	3	0	1	5	0
21LW PNL 3	6,6	PYX	90	174	4	0	1	1	2	1	0	2	0	1	5	0
21LW PNL 4	0	PYX	90	168	4	0	1	1	2	1	0	2	0	1	5	0
21LW PNL 4	1,4	PYX	90	168	4	0	1	1	2	1	0	2	0	1	5	0
21LW PNL 4	1,8	PYX	90	168	4	0	1	1	2	1	0	2	0	1	5	0
21LW PNL 4	2	PYX	90	168	4	0	1	1	2	1	0	2	0	1	5	0
21LW PNL 4	2,2	PYX	90	168	4	0	1	1	2	1	0	2	0	1	5	0
21LW PNL 4	2,6	PYX	90	168	4	0	1	1	2	1	0	2	0	1	5	0
21LW PNL 4	3,4	PYX	90	168	4	0	1	1	2	1	0	2	0	1	5	0
21LW PNL 4	3,6	PYX	90	168	4	0	1	1	2	1	0	2	0	1	5	0
21LW PNL 4	4,1	PYX	90	168	4	0	1	1	2	1	0	2	0	1	5	0
21LW PNL 4	5,3	PYX	90	168	4	0	1	1	2	1	0	2	0	1	5	0
21LW PNL 4	5,5	PEG VEIN	90	168	4	0	2,5	1	2	1	0	3	0	1	5	0
21LW PNL 4	6,5	PYX	90	168	4	0	1	1	2	1	0	2	0	1	5	0
21LW PNL 4	7,3	PYX	90	168	4	0	1	1	2	1	0	2	0	1	5	0
21LW PNL 4	8,1	PYX	90	168	4	0	1	1	2	1	0	2	0	1	5	0
21LW PNL 4	8,9	PYX	90	168	4	0	1	1	2	1	0	2	0	1	5	0
21LW PNL 6	0	PEG VEIN	90	186	4	0	2,5	1	2	1	0	3	0	1	5	0
21LW PNL 6	0,3	PYX	90	186	4	0	1	1	2	1	0	2	0	1	5	0
21LW PNL 6	0,7	PYX	90	186	4	0	1	1	2	1	0	2	0	1	5	0
21LW PNL 6	1,1	PYX	90	186	4	0	1	1	2	1	0	2	0	1	5	0
21LW PNL 6	1,6	PYX	90	186	4	0	1	1	2	1	0	2	0	1	5	0
21LW PNL 6	1,9	PEG VEIN	90	186	4	0	2,5	1	2	1	0	3	0	1	5	0
21LW PNL 6	2	FAULT	60	236	3	0	0,5	1	2	1	0	3	0	1	5	0
21LW PNL 6	2,5	PYX	90	186	4	0	1	1	2	1	0	2	0	1	5	0
21LW PNL 6	3	PEG VEIN	90	186	4	0	2,5	1	2	1	0	3	0	1	5	0
21LW PNL 6	3,8	PEG VEIN	90	186	4	0	2,5	1	2	1	0	3	0	1	5	0
21LW PNL 6	4,6	PEG VEIN	90	186	4	0	2,5	1	2	1	0	3	0	1	5	0
21LW PNL 6	5,5	PEG VEIN	90	186	4	0	2,5	1	2	1	0	3	0	1	5	0

Processed Data (from Dips)																
Panel Name	Distance	Rock	Dip	Azimuth	P	E	Jr	M	H	Ja	S	T	HL	Joint Set	Tape Azimuth	Tape Plunge
21LW PNL 6	6	PYX	90	186	4	0	1	1	2	1	0	2	0	1	5	0
21LW PNL 6	7,3	PEG VEIN	90	186	4	0	2,5	1	2	1	0	3	0	1	5	0
21LW PNL 6 up-dip	0	PYX	90	186	4	0	1	1	2	1	0	2	0	1	5	0
21LW PNL 6 up-dip	0,5	PYX	90	186	4	0	1	1	2	1	0	2	0	1	5	0
21LW PNL 6 up-dip	0,7	DYKE	90	186	4	0	1	1	2	1	0	2	0	1	5	0
21LW PNL 6 up-dip	2,3	DYKE	90	186	4	0	1	1	2	1	0	2	0	1	5	0
21LW PNL 6 up-dip	3,1	PYX	90	186	4	0	1	1	2	1	0	2	0	1	5	0
23LW PNL 5	0	PYX	90	166	4	0	2,5	1	2	1	0	2	0	1	95	0
23LW PNL 5	1	PYX	90	166	4	0	1	1	2	1	0	2	0	1	95	0
23LW PNL 5	1,3	PYX	90	166	4	0	1	1	2	1	0	2	0	1	95	0
23LW PNL 5	1,5	PYX	90	166	4	0	1	1	2	1	0	2	0	1	95	0
23LW PNL 5	2,1	PYX	90	166	4	0	1	1	2	1	0	2	0	1	95	0
23LW PNL 5	2,4	PYX	90	166	4	0	1	1	2	1	0	2	0	1	95	0
23LW PNL 5	2,6	PYX	90	166	4	0	1	1	2	1	0	2	0	1	95	0
23LW PNL 5	8,3	PYX	90	166	3	0	1	1	2	1	0	2	0	1	95	0
23LW PNL 5	9,6	PYX	90	166	4	0	1	1	2	1	0	2	0	1	95	0
23LW PNL 5	10,3	PYX	90	166	4	0	1	1	2	1	0	2	0	1	95	0
23LW PNL 5	11,3	PYX	90	166	4	0	1	1	2	1	0	2	0	1	95	0
23LW PNL 6 REVER	0	PEG VEIN	85	198	4	0	2,5	1	2	1	0	3	0	1	5	0
23LW PNL 6 REVER	0,4	PYX	90	170	3	0	1	1	2	1	0	2	0	1	5	0
23LW PNL 6 REVER	1,7	PYX	90	170	3	0	1	1	2	1	0	2	0	1	5	0
23LW PNL 6 REVER	2,9	PYX	90	170	3	0	1	1	2	1	0	2	0	1	5	0
23LW PNL 6 REVER	3,5	PYX	90	170	3	0	1	1	2	1	0	2	0	1	5	0
23LW PNL 6 REVER	3,8	PYX	90	170	3	0	1	1	2	1	0	2	0	1	5	0
23LW PNL 6 REVER	4,1	PYX	90	170	3	0	1	1	2	1	0	2	0	1	5	0
23LW PNL 6 REVER	6,7	PYX	90	170	3	0	1	1	2	1	0	2	0	1	5	0
23LW PNL 6 REVER	7,4	PYX	90	170	3	0	1	1	2	1	0	2	0	1	5	0
23LW PNL 6 REVER	8,8	PYX	90	170	3	0	1	1	2	1	0	2	0	1	5	0
23LW PNL 6 REVER	9,5	PYX	90	170	3	0	1	1	2	1	0	2	0	1	5	0
23LW PNL 7	0	PEG VEIN	90	184	4	0	2,5	1	2	1	0	3	0	1	5	0
23LW PNL 7	0,7	PYX	90	184	4	0	1	1	2	1	0	2	0	1	5	0
23LW PNL 7	1,6	PEG VEIN	90	184	4	0	2,5	1	2	1	0	3	0	1	5	0
23LW PNL 7	2,6	PEG VEIN	90	184	4	0	2,5	1	2	1	0	3	0	1	5	0
23LW PNL 7	4,6	PEG VEIN	90	184	4	0	2,5	1	2	1	0	3	0	1	5	0
23LW PNL 7	6,5	PYX	90	184	4	0	1	1	2	1	0	2	0	1	5	0
23LW PNL 8 DWN-I	0	VEN	90	186	4	0	2,5	1	2	1	0	3	0	1	5	0
23LW PNL 8 DWN-I	1,2	PYX	90	186	4	0	1	1	2	1	0	2	0	1	5	0
23LW PNL 8 DWN-I	1,6	PYX	90	186	4	0	1	1	2	1	0	2	0	1	5	0
23LW PNL 8 DWN-I	2,5	PYX	90	186	4	0	1	1	2	1	0	2	0	1	5	0
23LW PNL 8 DWN-I	3,3	PYX	90	186	4	0	1	1	2	1	0	2	0	1	5	0
23LW PNL 8 DWN-I	6,6	PYX	90	186	4	0	1	1	2	1	0	2	0	1	5	0
23LW PNL 8 DWN-I	9,2	PEG VEIN	90	186	4	0	2,5	1	2	1	0	3	0	1	5	0
23LW PNL 8 DWN-I	9,9	PEG VEIN	90	186	4	0	2,5	1	2	1	0	3	0	1	5	0
21LE PNL 5	0	PEG VEIN	90	182	4	0	2,5	1	2	1	0	3	0	1	5	0
21LE PNL 5	0,7	PYX	85	186	4	0	1	1	2	1	0	2	0	1	5	0
21LE PNL 5	1	PYX	85	172	4	0	1	1	2	1	0	2	0	1	5	0
21LE PNL 5	1,9	PYX	85	172	4	0	1	1	2	1	0	2	0	1	5	0
21LE PNL 5	3	PYX	85	172	4	0	1	1	2	1	0	2	0	1	5	0
21LE PNL 5	4,3	PYX	85	172	4	0	1	1	2	1	0	2	0	1	5	0
21LE PNL 5	4,5	PYX	85	172	4	0	1	1	2	1	0	2	0	1	5	0
21LE PNL 5	5	PYX	85	172	4	0	1	1	2	1	0	2	0	1	5	0
21LE PNL 5	6,2	PYX	85	172	4	0	1	1	2	1	0	2	0	1	5	0
21LE PNL 5	6,9	PYX	85	172	4	0	1	1	2	1	0	2	0	1	5	0
21LE PNL 5	7,6	PYX	85	172	4	0	1	1	2	1	0	2	0	1	5	0
21LE PNL 5	8,1	PYX	85	172	4	0	1	1	2	1	0	2	0	1	5	0
21LE PNL 5	8,7	PYX	85	172	4	0	1	1	2	1	0	2	0	1	5	0
21LE PNL 5	9,9	PEG VEIN	85	182	4	0	2,5	1	2	1	0	3	0	1	5	0
21LE PNL 6	0	PYX	90	164	4	0	1	1	2	1	0	2	0	1	5	0

Processed Data (from Dips)																
Panel Name	Distance	Rock	Dip	Azimuth	P	E	Jr	M	H	Ja	S	T	HL	Joint Set	Tape Azimuth	Tape Plunge
21LW PNL 6	6	PYX	90	186	4	0	1	1	2	1	0	2	0	1	5	0
21LW PNL 6	7,3	PEG VEIN	90	186	4	0	2,5	1	2	1	0	3	0	1	5	0
21LW PNL 6 up-dip	0	PYX	90	186	4	0	1	1	2	1	0	2	0	1	5	0
21LW PNL 6 up-dip	0,5	PYX	90	186	4	0	1	1	2	1	0	2	0	1	5	0
21LW PNL 6 up-dip	0,7	DYKE	90	186	4	0	1	1	2	1	0	2	0	1	5	0
21LW PNL 6 up-dip	2,3	DYKE	90	186	4	0	1	1	2	1	0	2	0	1	5	0
21LW PNL 6 up-dip	3,1	PYX	90	186	4	0	1	1	2	1	0	2	0	1	5	0
23LW PNL 5	0	PYX	90	166	4	0	2,5	1	2	1	0	2	0	1	95	0
23LW PNL 5	1	PYX	90	166	4	0	1	1	2	1	0	2	0	1	95	0
23LW PNL 5	1,3	PYX	90	166	4	0	1	1	2	1	0	2	0	1	95	0
23LW PNL 5	1,5	PYX	90	166	4	0	1	1	2	1	0	2	0	1	95	0
23LW PNL 5	2,1	PYX	90	166	4	0	1	1	2	1	0	2	0	1	95	0
23LW PNL 5	2,4	PYX	90	166	4	0	1	1	2	1	0	2	0	1	95	0
23LW PNL 5	2,6	PYX	90	166	4	0	1	1	2	1	0	2	0	1	95	0
23LW PNL 5	8,3	PYX	90	166	3	0	1	1	2	1	0	2	0	1	95	0
23LW PNL 5	9,6	PYX	90	166	4	0	1	1	2	1	0	2	0	1	95	0
23LW PNL 5	10,3	PYX	90	166	4	0	1	1	2	1	0	2	0	1	95	0
23LW PNL 5	11,3	PYX	90	166	4	0	1	1	2	1	0	2	0	1	95	0
21LE PNL 6	0,2	PYX	90	164	4	0	1	1	2	1	0	2	0	1	5	0
21LE PNL 6	0,8	PYX	90	164	4	0	1	1	2	1	0	2	0	1	5	0
21LE PNL 6	1,7	PYX	90	164	4	0	1	1	2	1	0	2	0	1	5	0
21LE PNL 6	1,9	PYX	90	164	4	0	1	1	2	1	0	2	0	1	5	0
21LE PNL 6	2,4	PYX	90	164	4	0	1	1	2	1	0	2	0	1	5	0
21LE PNL 6	2,7	PYX	90	164	4	0	1	1	2	1	0	2	0	1	5	0
21LE PNL 6	3,2	PEG VEIN	85	174	4	0	2,5	1	2	1	0	3	0	1	5	0
21LE PNL 6	4	PYX	90	172	4	0	1	1	2	1	0	2	0	1	5	0
21LE PNL 6	4,5	PYX	90	172	4	0	1	1	2	1	0	2	0	1	5	0
21LE PNL 6	5,1	PYX	90	172	4	0	1	1	2	1	0	2	0	1	5	0
21LE PNL 6	5,8	PYX	90	172	4	0	1	1	2	1	0	2	0	1	5	0
21LE PNL 6	6,5	PYX	90	172	4	0	1	1	2	1	0	2	0	1	5	0
21LE PNL 6	6,9	PYX	90	172	4	0	1	1	2	1	0	2	0	1	5	0
21LE PNL 6	7,6	PYX	90	172	4	0	1	1	2	1	0	2	0	1	5	0
21LE PNL 6	8,1	PYX	90	172	4	0	1	1	2	1	0	2	0	1	5	0
21LE PNL 6	8,7	PEG VEIN	85	174	4	0	2,5	1	2	1	0	3	0	1	5	0
21LE PNL 6	9	PYX	90	172	4	0	1	1	2	1	0	2	0	1	5	0
21LE PNL 6	9,4	PYX	90	172	4	0	1	1	2	1	0	2	0	1	5	0
21LE PNL 7	0	PYX	90	164	4	0	1	1	2	1	0	2	0	1	5	0
21LE PNL 7	0,6	PYX	90	164	4	0	1	1	2	1	0	2	0	1	5	0
21LE PNL 7	11	PYX	90	164	4	0	1	1	2	1	0	2	0	1	5	0
21LE PNL 7	1,3	PYX	90	164	4	0	1	1	2	1	0	2	0	1	5	0
21LE PNL 7	1,5	PYX	90	164	4	0	1	1	2	1	0	2	0	1	5	0
21LE PNL 7	1,7	PYX	90	164	4	0	1	1	2	1	0	2	0	1	5	0
21LE PNL 7	3	PYX	90	164	4	0	1	1	2	1	0	2	0	1	5	0
21LE PNL 7	3,5	PYX	90	164	4	0	1	1	2	1	0	2	0	1	5	0
21LE PNL 7	3,7	PYX	90	164	4	0	1	1	2	1	0	2	0	1	5	0
21LE PNL 7	4,4	PYX	90	164	4	0	1	1	2	1	0	2	0	1	5	0
21LE PNL 7	5,4	PEG VEIN	90	164	4	0	2,5	1	2	1	0	3	0	1	5	0
21LE PNL 7	5,8	PYX	90	164	4	0	1	1	2	1	0	2	0	1	5	0
21LE PNL 7	6,9	PYX	90	164	4	0	1	1	2	1	0	2	0	1	5	0
21LE PNL 7	8,3	PYX	90	164	4	0	1	1	2	1	0	2	0	1	5	0
21LE PNL 7	9,4	PYX	90	164	4	0	1	1	2	1	0	2	0	1	5	0
23LE PNL 1	0	PYX	90	184	4	0	1	1	2	1	0	2	0	1	5	0
23LE PNL 1	1,2	PYX	90	184	4	0	1	1	2	1	0	2	0	1	5	0
23LE PNL 1	1,8	PYX	90	184	4	0	1	1	2	1	0	2	0	1	5	0
23LE PNL 1	2,1	PYX	90	184	4	0	1	1	2	1	0	2	0	1	5	0
23LE PNL 1	2,9	PYX	90	184	4	0	1	1	2	1	0	2	0	1	5	0
23LE PNL 1	3,5	PYX	90	184	4	0	1	1	2	1	0	2	0	1	5	0
23LE PNL 1	4	PYX	90	184	4	0	1	1	2	1	0	2	0	1	5	0

Panel Name	Distance	Rock	Dip	Azimuth	P	E	Jr	M	H	Ja	S	T	HL	Joint Set	Tape Azimuth	Tape Plunge
23LE PNL 1	4,5	PYX	90	184	4	0	1	1	2	1	0	2	0	1	5	0
23LE PNL 1	6,1	PYX	90	184	4	0	1	1	2	1	0	2	0	1	5	0
23LE PNL 1	6,6	PYX	90	184	4	0	1	1	2	1	0	2	0	1	5	0
23LE PNL 1	7,1	PYX	90	184	4	0	1	1	2	1	0	2	0	1	5	0
23LE PNL 1	7,9	PYX	90	184	4	0	1	1	2	1	0	2	0	1	5	0
23LE PNL 1	8,3	PEG VEIN	90	180	4	0	1	1	2	1	0	2	0	1	5	0
23LE PNL 4	0	PYX	90	174	4	0	2,5	1	2	1	0	3	0	1	5	0
23LE PNL 4	0,8	PYX	90	174	4	0	1	1	2	1	0	2	0	1	5	0
23LE PNL 4	1,3	PYX	90	174	4	0	1	1	2	1	0	2	0	1	5	0
23LE PNL 4	1,9	PYX	90	174	4	0	1	1	2	1	0	2	0	1	5	0
23LE PNL 4	2,5	PYX	90	174	4	0	1	1	2	1	0	2	0	1	5	0
23LE PNL 4	3	P PEG VEIN	90	174	4	0	2,5	1	2	1	0	3	0	1	5	0
23LE PNL 4	4,1	PYX	90	174	4	0	1	1	2	1	0	2	0	1	5	0
23LE PNL 4	5	PYX	90	174	4	0	1	1	2	1	0	2	0	1	5	0
23LE PNL 4	6,4	PYX	90	174	4	0	1	1	2	1	0	2	0	1	5	0
23LE PNL 4	7,5	PEG VEIN	90	174	4	0	2,5	1	2	1	0	3	0	1	5	0
23LE PNL 4	8,2	PYX	90	174	4	0	1	1	2	1	0	2	0	1	5	0
23LE PNL 4	8,8	PYX	90	174	4	0	1	1	2	1	0	2	0	1	5	0
23LE PNL 4	9,7	PYX	90	174	4	0	1	1	2	1	0	2	0	1	5	0
23LE PNL 5	0	PEG VEIN	85	180	4	0	2,5	1	2	1	0	3	0	1	5	0
23LE PNL 5	1,1	PYX	90	180	4	0	1	1	2	1	0	2	0	1	5	0
23LE PNL 5	1,6	PYX	90	180	4	0	1	1	2	1	0	2	0	1	5	0
23LE PNL 5	3	PYX	90	180	4	0	1	1	2	1	0	2	0	1	5	0
23LE PNL 5	4,3	PYX	90	180	4	0	1	1	2	1	0	2	0	1	5	0
23LE PNL 5	5,4	PYX	90	180	4	0	1	1	2	1	0	2	0	1	5	0
23LE PNL 5	6,5	PYX	90	180	4	0	1	1	2	1	0	2	0	1	5	0
23LE PNL 5	7,4	PYX	90	180	4	0	1	1	2	1	0	2	0	1	5	0
23LE PNL 5	7,7	PYX	90	180	4	0	1	1	2	1	0	2	0	1	5	0
23LE PNL 5	8,1	PYX	90	180	4	0	1	1	2	1	0	2	0	1	5	0
23LE PNL 5	10	PYX	90	180	4	0	1	1	2	1	0	2	0	1	5	0
23LE PNL 6	0	PEG VEIN	85	186	4	0	2,5	1	2	1	0	3	0	1	5	0
23LE PNL 6	1,9	PYX	90	180	4	0	1	1	2	1	0	2	0	1	5	0
23LE PNL 6	2,6	PYX	90	180	4	0	1	1	2	1	0	2	0	1	5	0
23LE PNL 6	3,5	PYX	90	180	4	0	1	1	2	1	0	2	0	1	5	0
23LE PNL 6	4	PYX	90	180	4	0	1	1	2	1	0	2	0	1	5	0
23LE PNL 6	4,7	PYX	90	180	4	0	1	1	2	1	0	2	0	1	5	0
23LE PNL 6	5,5	PYX	90	180	4	0	1	1	2	1	0	2	0	1	5	0
23LE PNL 6	6,7	PYX	90	180	4	0	1	1	2	1	0	2	0	1	5	0
23LE PNL 6	7,8	PYX	90	180	4	0	1	1	2	1	0	2	0	1	5	0
23LE PNL 6	8,6	PYX	90	180	4	0	1	1	2	1	0	2	0	1	5	0
23LE PNL 7	0	PEG VEIN	85	186	4	0	2,5	1	2	1	0	3	0	1	5	0
23LE PNL 7	1,3	PYX	90	166	4	0	1	1	2	1	0	2	0	1	5	0
23LE PNL 7	1,9	PYX	90	166	4	0	1	1	2	1	0	2	0	1	5	0
23LE PNL 7	2,6	PYX	90	166	4	0	1	1	2	1	0	2	0	1	5	0
23LE PNL 7	3,6	PYX	90	166	4	0	1	1	2	1	0	2	0	1	5	0
23LE PNL 7	4,7	PEG VEIN	85	186	4	0	2,5	1	2	1	0	3	0	1	5	0
23LE PNL 7	5,4	PEG VEIN	85	186	4	0	2,5	1	2	1	0	3	0	1	5	0
23LE PNL 7	6,6	PYX	90	166	4	0	1	1	2	1	0	2	0	1	5	0
23LE PNL 7	7,9	PYX	90	166	4	0	1	1	2	1	0	2	0	1	5	0
23LE PNL 7	8,8	PYX	90	166	4	0	1	1	2	1	0	2	0	1	5	0

Processed Data (from Dips)																
Panel Name	Distance	Rock	Dip	Azimuth	P	E	Jr	M	H	Ja	S	T	HL	Joint Set	Tape Azimuth	Tape Plunge
23LE PNL 7	9,8	PEG VEIN	90	166	4	0	2,5	1	2	1	0	3	0	1	5	0
19LE 3	0	PYX	90	168	4	0	1	1	2	1	0	3	0	1	5	0
19LE 3	0,8	PYX	90	168	4	0	1	1	2	1	0	3	0	1	5	0
19LE 3	1	PYX	90	168	4	0	1	1	2	1	0	3	0	1	5	0
19LE 3	2,3	PYX	90	168	4	0	1	1	2	1	0	3	0	1	5	0
19LE 3	2,8	PYX	90	168	4	0	1	1	2	1	0	3	0	1	5	0
19LE 3	3,5	PYX	90	168	4	0	1	1	2	1	0	3	0	1	5	0
19LE 3	4,1	PYX	90	168	4	0	1	1	2	1	0	3	0	1	5	0
19LE 3	5,2	PYX	90	168	4	0	1	1	2	1	0	3	0	1	5	0
19LE 3	5,5	PYX	90	168	4	0	1	1	2	1	0	3	0	1	5	0
19LE 3	6,4	PYX	90	168	4	0	1	1	2	1	0	3	0	1	5	0
19LE 3	7,7	PYX	90	168	4	0	1	1	2	1	0	3	0	1	5	0
19LE 3	8,9	PYX	90	168	4	0	1	1	2	1	0	3	0	1	5	0
19LE 3	9,4	PYX	90	168	4	0	1	1	2	1	0	3	0	1	5	0
19LE 3	10,4	PYX	90	168	4	0	1	1	2	1	0	3	0	1	5	0
19LE 4	0	PYX	90	174	4	0	1	1	2	1	0	3	0	1	5	0
19LE 4	0,5	PYX	90	174	4	0	1	1	2	1	0	3	0	1	5	0
19LE 4	1,1	PYX	90	174	4	0	1	1	2	1	0	3	0	1	5	0
19LE 4	1,3	PYX	90	174	4	0	1	1	2	1	0	3	0	1	5	0
19LE 4	1,6	PYX	90	174	4	0	1	1	2	1	0	3	0	1	5	0
19LE 4	2,1	PYX	90	174	4	0	1	1	2	1	0	3	0	1	5	0
19LE 4	2,6	PYX	90	174	4	0	1	1	2	1	0	3	0	1	5	0
19LE 4	3,3	PYX	90	174	4	0	1	1	2	1	0	3	0	1	5	0
19LE 4	3,7	PYX	90	174	4	0	1	1	2	1	0	3	0	1	5	0
19LE 4	4	PYX	90	174	4	0	1	1	2	1	0	3	0	1	5	0
19LE 4	4,7	PYX	90	174	4	0	1	1	2	1	0	3	0	1	5	0
19LE 4	5,4	PYX	90	174	4	0	1	1	2	1	0	3	0	1	5	0
19LE 4	6,1	PYX	90	174	4	0	1	1	2	1	0	3	0	1	5	0
19LE 4	6,6	PYX	90	174	4	0	1	1	2	1	0	3	0	1	5	0
19LE 4	7,2	PYX	90	174	4	0	11	1	2	1	0	3	0	1	5	0
19LE 4	7,8	PYX	90	174	4	0	11	1	2	1	0	3	0	1	5	0
19LE 4	8,3	PYX	90	174	4	0	11	1	2	1	0	3	0	1	5	0
19LE 4	8,8	PYX	90	174	4	0	11	1	2	1	0	3	0	1	5	0
19LE 4	9,6	PYX	90	174	4	0	11	1	2	1	0	3	0	1	5	0
19LE 6	0	PYX	90	166	4	0	0,5	1	2	1	0	3	0	1	5	0
19LE 6	0,5	PYX	90	166	4	0	0,5	1	2	1	0	3	0	1	5	0
19LE 6	0,7	PYX	90	166	4	0	0,5	1	2	1	0	3	0	1	5	0
19LE 6	0,9	PYX	90	166	4	0	0,5	1	2	1	0	3	0	1	5	0
19LE 6	1	PYX	90	166	4	0	0,5	1	2	1	0	3	0	1	5	0
19LE 6	1,1	PYX	90	166	4	0	0,5	1	2	1	0	3	0	1	5	0
19LE 6	1	PYX	90	166	4	0	0,5	1	2	1	0	3	0	1	5	0
19LE 6	2,1	PYX	90	166	4	0	0,5	1	2	1	0	3	0	1	5	0
19LE 6	2,8	PYX	90	166	4	0	0,5	1	2	1	0	3	0	1	5	0
19LE 6	3,3	PYX	90	166	4	0	0,5	1	2	1	0	3	0	1	5	0
19LE 6	3,7	PYX	90	166	4	0	0,5	1	2	1	0	3	0	1	5	0
19LE 6	4,4	PYX	90	166	4	0	0,5	1	2	1	0	3	0	1	5	0
19LE 6	5,2	PYX	90	166	4	0	0,5	1	2	1	0	3	0	1	5	0
19LE 6	6,4	PYX	90	166	4	0	0,5	1	2	1	0	3	0	1	5	0
19LE 6	7,1	PYX	90	166	4	0	0,5	1	2	1	0	3	0	1	5	0
19LE 6	7,8	PYX	90	166	4	0	0,5	1	2	1	0	3	0	1	5	0
19LE 6	8,2	PYX	90	166	4	0	0,5	1	2	1	0	3	0	1	5	0
19LE 6	9,1	PYX	90	166	4	0	0,5	1	2	1	0	3	0	1	5	0
19LE 6	10	PYX	90	166	4	0	0,5	1	2	1	0	3	0	1	5	0
19LE 8	0	PYX	90	170	4	0	1	1	2	1	0	3	0	1	5	0
19LE 8	0,2	PYX	90	170	4	0	1	1	2	1	0	3	0	1	5	0
19LE 8	0,4	PYX	90	170	4	0	1	1	2	1	0	3	0	1	5	0
19LE 8	0,7	PYX	90	170	4	0	1	1	2	1	0	3	0	1	5	0
19LE 8	1,3	PYX	90	170	4	0	1	1	2	1	0	3	0	1	5	0
19LE 8	1,5	PYX	90	170	4	0	1	1	2	1	0	3	0	1	5	0
19LE 8	2,3	PYX	90	170	4	0	1	1	2	1	0	3	0	1	5	0

Processed Data (from Dips)																
Panel Name	Distance	Rock	Dip	Azimuth	P	E	Jr	M	H	Ja	S	T	HL	Joint Set	Tape Azimuth	Tape Plunge
23LE PNL 7	9,8	PEG VEIN	90	166	4	0	2,5	1	2	1	0	3	0	1	5	0
19LE 3	0	PYX	90	168	4	0	1	1	2	1	0	3	0	1	5	0
19LE 3	0,8	PYX	90	168	4	0	1	1	2	1	0	3	0	1	5	0
19LE 3	1	PYX	90	168	4	0	1	1	2	1	0	3	0	1	5	0
19LE 3	2,3	PYX	90	168	4	0	1	1	2	1	0	3	0	1	5	0
19LE 3	2,8	PYX	90	168	4	0	1	1	2	1	0	3	0	1	5	0
19LE 3	3,5	PYX	90	168	4	0	1	1	2	1	0	3	0	1	5	0
19LE 3	4,1	PYX	90	168	4	0	1	1	2	1	0	3	0	1	5	0
19LE 3	5,2	PYX	90	168	4	0	1	1	2	1	0	3	0	1	5	0
19LE 3	5,5	PYX	90	168	4	0	1	1	2	1	0	3	0	1	5	0
19LE 3	6,4	PYX	90	168	4	0	1	1	2	1	0	3	0	1	5	0
19LE 3	7,7	PYX	90	168	4	0	1	1	2	1	0	3	0	1	5	0
19LE 3	8,9	PYX	90	168	4	0	1	1	2	1	0	3	0	1	5	0
19LE 3	9,4	PYX	90	168	4	0	1	1	2	1	0	3	0	1	5	0
19LE 3	10,4	PYX	90	168	4	0	1	1	2	1	0	3	0	1	5	0
19LE 4	0	PYX	90	174	4	0	1	1	2	1	0	3	0	1	5	0
19LE 4	0,5	PYX	90	174	4	0	1	1	2	1	0	3	0	1	5	0
19LE 4	1,1	PYX	90	174	4	0	1	1	2	1	0	3	0	1	5	0
19LE 4	1,3	PYX	90	174	4	0	1	1	2	1	0	3	0	1	5	0
19LE 4	1,6	PYX	90	174	4	0	1	1	2	1	0	3	0	1	5	0
19LE 4	2,1	PYX	90	174	4	0	1	1	2	1	0	3	0	1	5	0
19LE 4	2,6	PYX	90	174	4	0	1	1	2	1	0	3	0	1	5	0
19LE 4	3,3	PYX	90	174	4	0	1	1	2	1	0	3	0	1	5	0
19LE 4	3,7	PYX	90	174	4	0	1	1	2	1	0	3	0	1	5	0
19LE 4	4	PYX	90	174	4	0	1	1	2	1	0	3	0	1	5	0
19LE 8	2,6	PYX	90	170	4	0	1	1	2	1	0	3	0	1	5	0
19LE 8	3	PYX	90	170	4	0	1	1	2	1	0	3	0	1	5	0
19LE 8	3,4	PYX	90	170	4	0	1	1	2	1	0	3	0	1	5	0
19LE 8	3,9	PYX	90	170	4	0	1	1	2	1	0	3	0	1	5	0
19LE 8	4,5	PYX	90	170	4	0	1	1	2	1	0	3	0	1	5	0
19LE 8	5,2	PYX	90	170	4	0	1	1	2	1	0	3	0	1	5	0
19LE 8	5,8	PYX	90	170	4	0	1	1	2	1	0	3	0	1	5	0
19LE 8	6,3	PYX	90	170	4	0	1	1	2	1	0	3	0	1	5	0
19LE 8	7	PYX	90	170	4	0	1	1	2	1	0	3	0	1	5	0
19LE 8	8	PYX	90	170	4	0	1	1	2	1	0	3	0	1	5	0
19LE 8	8,4	PYX	90	170	4	0	1	1	2	1	0	3	0	1	5	0
19LE 8	9,8	PYX	90	170	4	0	1	1	2	1	0	3	0	1	5	0
19LE 8	10,4	PYX	90	170	4	0	1	1	2	1	0	3	0	1	5	0
21 West 001	2	PYX	85	198	4	2	1	1	2	1	0	1	0	1	5	0
21 West 001	2,1	PYX	90	200	4	2	1	1	2	1	0	1	0	1	5	0
21 West 001	2,6	PYX	90	202	4	2	1	1	2	1	0	1	0	1	5	0
21 West 002	3,3	PYX	90	196	4	0	1	1	2	1	0	4	0	1	5	0
21 West 003	0,9	PYX	90	180	4	0	14	1	2	1	0	1	0	1	5	0
21 West 003	4,1	PYX	90	162	4	0	2,5	1	2	1	0	1	0	1	5	0
21 West 003	6,2	PYX	90	162	4	1	1	1	2	1	0	0	0	1	5	0
21 West 003	8,8	PYX	85	164	4	1	1	1	2	1	0	0	0	1	5	0
21 West 003	10	PYX	90	160	4	1	1	1	2	1	0	1	0	1	5	0
22E PNI 4E	4,6	DYKE	90	180	4	0	1	1	2	1	0	2	2	1	95	0
21 E PNL 6 Up-dip	0	PYX	90	172	4	0	1	1	2	1	0	2	0	1	5	0
21 E PNL 6 Up-dip	0,5	PYX	90	172	4	0	1	1	2	1	0	2	0	1	5	0
21 E PNL 6 Up-dip	0,8	PYX	90	172	4	0	1	1	2	1	0	2	0	1	5	0
21 E PNL 6 Up-dip	1,2	PYX	90	172	4	0	1	1	2	1	0	2	0	1	5	0
21 E PNL 6 Up-dip	1,9	PYX	90	172	4	0	1	1	2	1	0	2	0	1	5	0
21 E PNL 6 Up-dip	2,6	PYX	90	172	4	0	1	1	2	1	0	2	0	1	5	0
21 E PNL 6 Up-dip	3,1	PYX	90	172	4	0	1	1	2	1	0	2	0	1	5	0

Processed Data (from Dips)																
Panel Name	Distance	Rock	Dip	Azimuth	P	E	Jr	M	H	Ja	S	T	HL	Joint Set	Tape Azimuth	Tape Plunge
21 E PNL 6 Up-dip	3,9	PYX	90	172	4	0	1	1	2	1	0	2	0	1	5	0
21 E PNL 6 Up-dip	4,7	PYX	90	172	4	0	1	1	2	1	0	2	0	1	5	0
21 E PNL 6 Up-dip	5,2	VEIN	90	172	4	0	2,5	1	2	1	0	3	0	1	5	0
21 E PNL 6 Up-dip	7,1	PYX	90	172	4	0	1	1	2	1	0	2	0	1	5	0
21 E PNL 6 Up-dip	9,1	PYX	90	172	4	0	1	1	2	1	0	2	0	1	5	0
21 E PNL 6	0	PYX	90	172	4	0	1	1	2	1	0	2	0	1	5	0
21 E PNL 6	0,8	PYX	90	172	4	0	1	1	2	1	0	2	0	1	5	0
21 E PNL 6	1,4	PYX	90	172	4	0	1	1	2	1	0	2	0	1	5	0
21 E PNL 6	2,2	PYX	90	172	4	0	1	1	2	1	0	2	0	1	5	0
21 E PNL 6	3,2	PYX	90	172	4	0	1	1	2	1	0	2	0	1	5	0
21 E PNL 6	4,4	PYX	90	172	4	0	1	1	2	1	0	2	0	1	5	0
21 E PNL 6	5,8	PYX	90	172	4	0	1	1	2	1	0	2	0	1	5	0
21 E PNL 6	6,7	PYX	90	172	4	0	1	1	2	1	0	2	0	1	5	0
21 E PNL 6	7,4	PYX	90	172	4	0	1	1	2	1	0	2	0	1	5	0
21 E PNL 6	7,9	PYX	90	172	4	0	1	1	2	1	0	2	0	1	5	0
21 E PNL 6	9,2	PYX	90	172	4	0	1	1	2	1	0	2	0	1	5	0
Sinking	0	PYX	85	254	4	0	1	1	2	1	0	2	0	2	95	0
Sinking	0,8	PYX	85	254	3	0	14	1	2	1	0	2	0	2	95	0
Sinking	1,3	PYX	80	252	3	0	1	1	2	1	0	2	0	2	95	0
Sinking	2,9	PYX	90	256	3	0	1	1	2	1	0	2	0	2	95	0
Sinking	6	PYX	90	256	3	0	1	1	2	1	0	2	0	2	95	0
Sinking	1,6	PYX	85	248	3	0	1	1	2	1	0	2	0	2	95	0
Sinking	4,7	PYX	90	250	3	0	1	1	2	1	0	2	0	2	95	0
Sinking	5,8	PYX	90	260	3	0	1	1	2	1	0	2	0	2	95	0
Sinking	1,7	PYX	90	260	3	0	1	1	2	1	0	2	0	2	95	0
Sinking	3,9	PYX	90	260	3	0	1	1	2	1	0	2	0	2	95	0
Sinking	0,7	PYX	90	244	3	0	1	1	2	1	0	2	0	2	95	0
Sinking	2,2	PYX	90	244	3	0	1	1	2	1	0	2	0	2	95	0
Sinking	3	PYX	90	246	3	1	1	1	2	1	2	2	0	2	95	0
Sinking	5,4	PYX	90	266	3	1	1	1	2	1	0	2	0	2	95	0
Sinking	0	PYX	90	262	3	1	1	1	2	1	0	2	0	2	95	0
Sinking	0,5	PYX	90	260	3	1	1	1	2	1	0	2	0	2	95	0
Sinking	0,8	PYX	90	262	3	1	1	1	2	1	0	2	0	2	95	0
Sinking	2	PYX	90	260	3	1	1	1	2	1	0	2	0	2	95	0
Sinking	3,9	PYX	90	266	3	1	1	1	2	1	0	2	0	2	95	0
19LE PNL 3	0	PYX	90	252	4	1	1	1	2	1	0	3	0	2	95	0
19LE PNL 3	0,7	PYX	90	252	4	1	1	1	2	1	0	3	0	2	95	0
19LE PNL 3	1,4	PYX	90	252	4	1	1	1	2	1	0	3	0	2	95	0
19LE PNL 3	2,3	PYX	90	252	4	1	1	1	2	1	0	3	0	2	95	0
19LE PNL 3	3	PYX	90	252	4	1	1	1	2	1	0	3	0	2	95	0
19LE PNL 3	3,4	PYX	90	252	4	1	1	1	2	1	0	3	0	2	95	0
19LE PNL 3	4,1	PYX	90	252	4	1	1	1	2	1	0	3	0	2	95	0
19LE PNL 3	5	PYX	90	252	4	1	1	1	2	1	0	3	0	2	95	0
19LE PNL 3	6,3	PYX	90	252	4	1	1	1	2	1	0	3	0	2	95	0
19LE PNL 3	0,4	PYX	90	252	4	1	1	1	2	1	0	3	0	2	95	0
19LE PNL 3	9,1	PYX	90	252	4	1	1	1	2	1	0	3	0	2	95	0
19LE PNL 3	10	PYX	90	252	4	1	1	1	2	1	0	3	0	2	95	0
19LE PNL 3 up-dip	0	PYX	90	246	4	1	1	1	2	1	0	3	0	2	95	0
19LE PNL 3 up-dip	0,5	PYX	90	246	4	1	1	1	2	1	0	3	0	2	95	0
19LE PNL 3 up-dip	1,1	PYX	90	246	4	1	1	1	2	1	0	3	0	2	95	0
19LE PNL 3 up-dip	1,5	PYX	90	246	4	1	1	1	2	1	0	3	0	2	95	0
19LE PNL 3 up-dip	2,1	PYX	90	246	4	1	1	1	2	1	0	3	0	2	95	0
19LE PNL 3 up-dip	2,5	PYX	90	246	4	1	1	1	2	1	0	3	0	2	95	0
19LE PNL 3 up-dip	3,2	PYX	90	246	4	1	1	1	2	1	0	3	0	2	95	0
19LE PNL 3 up-dip	4,1	PYX	90	246	4	1	1	1	2	1	0	3	0	2	95	0
19LE PNL 3 up-dip	4,8	PYX	90	246	4	1	1	1	2	1	0	3	0	2	95	0
19LE PNL 3 up-dip	5,7	PYX	90	246	4	1	1	1	2	1	0	3	0	2	95	0
19LE PNL 3 up-dip	6,4	PYX	90	246	4	1	1	1	2	1	0	3	0	2	95	0
19LE PNL 3 up-dip	7,7	PYX	90	246	4	1	1	1	2	1	0	3	0	2	95	0
19LE PNL 3 up-dip	8	PYX	90	246	4	1	1	1	2	1	0	3	0	2	95	0
19LE PNL 3 up-dip	8,5	PYX	90	246	4	1	1	1	2	1	0	3	0	2	95	0
19LE PNL 3 up-dip	9,6	PYX	90	246	4	1	1	1	2	1	0	3	0	2	95	0
21LE DOWN-DIP PI	3,5	PYX	90	240	3	0	1	1	2	1	0	1	0	2	95	0
21LE DOWN-DIP PI	4,9	PYX	90	240	3	0	1	1	2	1	0	1	0	2	95	0
21LE DOWN-DIP PI	6,6	PYX	90	240	3	0	1	1	2	1	0	2	0	2	95	0
21LE PNL 2	1,7	PYX	90	232	3	0	1	1	2	1	0	2	0	2	95	0
21LE PNL 2	1,9	PYX	90	240	3	0	1	1	2	1	0	2	0	2	95	0
21LE PNL 2	5,5	PYX	90	240	3	0	1	1	2	1	0	2	0	2	95	0
21LE PNL 3	0	PYX	90	260	2	0	1	1	2	1	0	2	0	2	95	0
21LE PNL 3	0,2	PYX	90	260	3	0	1	1	2	1	0	2	0	2	95	0

Processed Data (from Dips)																
Panel Name	Distance	Rock	Dip	Azimuth	P	E	Jr	M	H	Ja	S	T	HL	Joint Set	Tape Azimuth	Tape Plunge
21LE PNL 3	4,6	PYX	90	260	4	0	1	1	2	1	0	2	0	2	95	0
21LE PNL 3	5,3	PYX	90	260	4	0	1	1	2	1	0	2	0	2	95	0
19LE PNL 3	2,5	PYX	90	260	4	0	2,5	1	2	1	0	2	0	2	95	0
19LE PNL 3	4,5	PYX	90	266	4	0	2,5	1	2	1	0	2	0	2	95	0
19LE PNL 3	6,5	PYX	90	270	4	0	2,5	1	2	1	0	2	0	2	95	0
18LE PNL 7	2,5	PYX	90	240	4	0	1	1	2	1	0	2	0	2	95	0
18LE PNL 7	3,5	PYX	90	240	4	0	1	1	2	1	0	2	0	2	95	0
21LW PNL 3	0,7	PYX	90	240	3	0	1	1	2	1	0	2	0	2	5	0
21LW PNL 2	1,8	PYX	90	256	2	0	14	1	2	1	0	2	0	2	5	0
21LW PNL 4	1,2	PYX	90	270	4	0	1	1	2	1	0	2	0	2	95	0
21LW PNL 4	5	PYX	90	270	4	0	1	1	2	1	0	2	0	2	95	0
21LW PNL 4	5,2	PYX	90	270	4	0	1	1	2	1	0	2	0	2	95	0
21LW PNL 4	0	PYX	90	276	4	0	1	1	2	1	0	2	0	2	95	0
21LW PNL 3 back	0,8	PYX	90	272	4	0	1	1	2	1	0	2	0	2	95	0
21LW PNL 3 back	1,1	PYX	90	272	4	0	1	1	2	1	0	2	0	2	95	0
21LW PNL 3 back	1,3	PYX	90	272	4	0	1	1	2	1	0	2	0	2	95	0
21LW PNL 3 back	2	PYX	90	272	4	0	1	1	2	1	0	2	0	2	95	0
21LW PNL 3 back	2,4	PEG VEIN	90	272	4	0	2,5	1	2	1	0	3	0	2	95	0
21LW PNL 3 back	0	PYX	90	330	3	0	1	1	2	1	0	2	0	2	5	0
21LW PNL 3 back	1,7	PEG VEIN	90	330	4	0	2,5	1	2	1	0	3	0	2	5	0
21LW PNL 4 back	5,5	PYX	90	240	4	0	1	1	2	1	0	2	0	2	5	0
21LW PNL 6	7,2	DYKE	90	240	4	0	1	1	2	1	0	3	0	2	5	0
21LW PNL 6	7,3	PYX	90	210	3	0	0,5	1	2	1	0	3	0	2	5	0
21LW PNL 7	0	PYX	90	260	4	0	1	1	2	1	0	2	0	2	95	0
21LW PNL 7	0,6	PYX	90	260	4	0	1	1	2	1	0	2	0	2	95	0
21LW PNL 7	10,3	PYX	90	260	4	0	1	1	2	1	0	2	0	2	95	0
21LW PNL 7	10,8	PYX	90	260	4	0	1	1	2	1	0	2	0	2	95	0
20LE PNL 2	0,4	PYX	90	256	4	0	1	1	2	1	0	2	0	2	95	0
20LE PNL 2	0,8	PYX	90	260	4	0	1	1	2	1	0	2	0	2	95	0
20LE PNL 2	1,2	PYX	90	260	4	0	1	1	2	1	0	2	0	2	95	0
20LE PNL 2	1,4	PYX	90	260	4	0	1	1	2	1	0	2	0	2	95	0
20LE PNL 3	0	PYX	90	256	4	0	1	1	2	1	0	2	0	2	95	0
20LE PNL 3	0,2	PYX	90	256	4	0	1	1	2	1	0	2	0	2	95	0
20LE PNL 3	0,3	PYX	90	256	4	0	1	1	2	1	0	2	0	2	95	0
20LE PNL 3	1,5	PYX	90	256	4	0	1	1	2	1	0	2	0	2	95	0
20LE PNL 3	1,8	PYX	90	256	4	0	1	1	2	1	0	2	0	2	95	0
20LE PNL 3	4,2	PYX	90	256	4	0	1	1	2	1	0	2	0	2	95	0
20LE PNL 3	4,6	PYX	90	256	4	0	1	1	2	1	0	2	0	2	95	0
20LE PNL 3	4,9	PYX	90	256	4	0	1	1	2	1	0	2	0	2	95	0
20LE PNL 3	5,2	PYX	90	256	4	0	1	1	2	1	0	2	0	2	95	0
20LE PNL 3	5,9	PYX	90	256	4	0	1	1	2	1	0	2	0	2	95	0
20LE PNL 3	7	PYX	90	256	4	0	1	1	2	1	0	2	0	2	95	0
20LE PNL 3	7,2	PYX	90	256	4	0	1	1	2	1	0	2	0	2	95	0
20LE PNL 3	7,8	PYX	90	256	4	0	1	1	2	1	0	2	0	2	95	0
20LE PNL 4	0	PYX	90	250	4	0	1	1	2	1	0	2	0	2	95	0
20LE PNL 4	1,7	PYX	90	250	4	0	1	1	2	1	0	2	0	2	95	0
20LE PNL 4	2,2	PYX	90	250	4	0	1	1	2	1	0	2	0	2	95	0
20LE PNL 4	2,7	PYX	90	250	4	0	1	1	2	1	0	2	0	2	95	0
20LE PNL 4	9,1	PYX	90	240	4	0	1	1	2	1	0	2	0	2	95	0
20LE PNL 4	0	DYKE	90	240	4	0	1	1	2	1	0	2	0	2	95	0
20LE PNL 4	0,7	DYKE	90	260	4	0	1	1	2	1	0	2	0	2	95	0
20LE PNL 4	2,1	DYKE	90	254	4	0	1	1	2	1	0	2	0	2	95	0
20LE PNL 4	2,3	DYKE	90	250	4	0	1	1	2	1	0	2	0	2	95	0
20LE PNL 5	0	PYX	90	240	4	0	1	1	2	1	0	2	0	2	95	0
20LE PNL 5	1,8	PEG VEIN	90	230	4	0	2,5	1	2	1	0	3	0	2	95	0
20LE PNL 5	2,3	PYX	90	262	4	0	1	1	2	1	0	2	0	2	95	0
20LE PNL 5	3,1	PYX	90	262	4	0	1	1	2	1	0	2	0	2	95	0
20LE PNL 5	8,1	PYX	90	262	4	0	1	1	2	1	0	2	0	2	95	0
20LE PNL 6	0	PYX	90	250	4	0	1	1	2	1	0	2	0	2	95	0
20LE PNL 6	0,8	PYX	90	244	4	0	1	1	2	1	0	2	0	2	95	0

Processed Data (from Dips)															
Panel Name	Distance	Rock	Dip	Azimuth	P	E	Jr	M	H	Ja	S	T	HL	Joint Set	Tape Azimuth	Tape Plunge
20LE PNL 6	1,5	PYX	90	250	4	0	1	1	2	1	0	2	0	2	95	0
20LE PNL 6	3,7	PYX	90	250	4	0	1	1	2	1	0	2	0	2	95	0
20LE PNL 6	5,2	PYX	90	250	4	0	1	1	2	1	0	2	0	2	95	0
20LE PNL 6	7,1	PYX	90	250	4	0	1	1	2	1	0	2	0	2	95	0
CHL Lateral west	0	PYX	90	236	4	0	1	1	2	1	0	2	0	2	95	0
CHL Lateral west	0,4	PYX	90	230	4	0	1	1	2	1	0	2	0	2	95	0
CHL Lateral west	1,7	PYX	90	236	4	0	1	1	2	1	0	2	0	2	95	0
CHL Lateral west	3,2	PYX	90	236	4	0	1	1	2	1	0	2	0	2	95	0
22 LE PNL 6 UP DIP 16D	0,8	PYX	90	280	4	0	1	1	2	1	0	2	0	2	95	0
22 LE PNL 6 UP DIP 16D	0,9	PYX	90	280	4	0	1	1	2	1	0	2	0	2	95	0
22 LE PNL 6 UP DIP 16D	1,2	PYX	90	280	4	0	1	1	2	1	0	2	0	2	95	0
22 LE PNL 6 UP DIP 16D	3	PYX	90	280	4	0	1	1	2	1	0	2	0	2	95	0
22 LE PNL 6 UP DIP 17D	3,6	PYX	90	280	4	0	1	1	2	1	0	2	0	2	95	0
22 LE PNL 6 UP DIP 17D	7,1	DYKE	90	270	4	0	1	1	2	1	0	2	0	2	95	0
22 LE PNL 7	0	PYX	90	260	4	0	1	1	2	1	0	2	0	2	95	0
22 LE PNL 7	0,5	PYX	90	260	4	0	1	1	2	1	0	2	0	2	95	0
22 LE PNL 7	0,9	PYX	90	260	4	0	1	1	2	1	0	2	0	2	95	0
22 LE PNL 7	3	PYX	90	260	4	0	1	1	2	1	0	2	0	2	95	0
22 LE PNL 7	3,5	PYX	90	260	4	0	1	1	2	1	0	2	0	2	95	0
22 LE PNL 8	0	PYX	90	264	2	0	1	1	2	1	0	2	0	2	95	0
22 LE PNL 8	1,6	PYX	90	264	2	0	1	1	2	1	0	2	0	2	95	0
22 LE PNL 8	3	PYX	90	264	2	0	1	1	2	1	0	2	0	2	95	0
21 LW PNL 6 Down-dip	0	PYX	90	262	4	0	1	1	2	1	0	2	0	2	95	0
21 LW PNL 6 Down-dip	1,5	PYX	90	262	4	0	1	1	2	1	0	2	0	2	95	0
21 LW PNL 6 Down-dip	2,1	PYX	90	262	4	0	1	1	2	1	0	2	0	2	95	0
21 LW PNL 6 Down-dip	4,2	PYX	90	262	4	0	1	1	2	1	0	2	0	2	95	0
21 LW PNL 6 Down-dip	4,9	PYX	90	262	4	0	1	1	2	1	0	2	0	2	95	0
21 LW PNL 6 Down-dip	5,7	PYX	90	262	4	0	1	1	2	1	0	2	0	2	95	0
21 LW PNL 6 Down-dip	6,8	PYX	90	262	4	0	1	1	2	1	0	2	0	2	95	0
21 LW PNL 6 Down-dip	7,4	PYX	90	270	4	0	1	1	2	1	0	2	0	2	95	0
21 LW PNL 6 Down-dip	8,3	PYX	90	272	4	0	1	1	2	1	0	2	0	2	95	0
21 LW PNL 7	0	PYX	90	260	4	0	1	1	2	1	0	2	0	2	95	0
21 LW PNL 7	2,1	PYX	90	260	4	0	1	1	2	1	0	2	0	2	95	0
21 LW PNL 7	3,2	PYX	90	260	4	0	1	1	2	1	0	2	0	2	95	0
21 LW PNL 7	4,5	PYX	90	260	4	0	1	1	2	1	0	2	0	2	95	0
22LW PNL 3	0	PYX	90	274	4	0	1	1	2	1	0	2	0	2	95	0
22LW PNL 3	0,5	PYX	90	274	4	0	1	1	2	1	0	2	0	2	95	0
22LW PNL 3	1,1	PYX	90	274	4	0	1	1	2	1	0	2	0	2	95	0
22LW PNL 3	1,6	PYX	90	274	4	0	1	1	2	1	0	2	0	2	95	0
22LW PNL 3	2,7	PYX	90	274	4	0	1	1	2	1	0	2	0	2	95	0
22LW PNL 3	3,6	PYX	90	274	4	0	1	1	2	1	0	2	0	2	95	0
22LW PNL 3	5,1	PYX	90	274	4	0	1	1	2	1	0	2	0	2	95	0
22LW PNL 3 DOWN-DIP	0	PYX	90	278	4	0	1	1	2	1	0	2	0	2	95	0
22LW PNL 3 DOWN-DIP	0,7	PYX	90	278	4	0	1	1	2	1	0	2	0	2	95	0
22LW PNL 3 DOWN-DIP	1,9	PYX	90	278	4	0	1	1	2	1	0	2	0	2	95	0
22LW PNL 3 DOWN-DIP	2,4	PYX	90	278	4	0	1	1	2	1	0	2	0	2	95	0
22LW PNL 3 DOWN-DIP	2,9	PYX	90	278	4	0	1	1	2	1	0	2	0	2	95	0
22LW PNL 3 DOWN-DIP	3,8	PYX	90	278	4	0	1	1	2	1	0	2	0	2	95	0
22LW PNL 3 DOWN-DIP	4,6	PYX	90	278	4	0	1	1	2	1	0	2	0	2	95	0
22LW PNL 3 DOWN-DIP	5,5	PYX	90	278	4	0	1	1	2	1	0	2	0	2	95	0
22LW PNL 3 DOWN-DIP	6,1	PYX	90	278	4	0	1	1	2	1	0	2	0	2	95	0
22LW PNL 7 UP-DIP	0	PYX	90	274	4	0	1	1	2	1	0	2	0	2	95	0
22LW PNL 7 UP-DIP	1,1	PYX	90	274	4	0	1	1	2	1	0	2	0	2	95	0
22LW PNL 7 UP-DIP	2,5	PYX	90	274	4	0	1	1	2	1	0	2	0	2	95	0
22LW PNL 7 UP-DIP	3	PYX	90	274	4	0	1	1	2	1	0	2	0	2	95	0
22LW PNL 7 UP-DIP	6	PYX	90	274	4	0	1	1	2	1	0	2	0	2	95	0
22LW PNL 7 UP-DIP	10	PYX	90	274	4	0	1	1	2	1	0	2	0	2	95	0
22LW PNL 7 UP-DIP 2	0	PYX	90	274	4	0	1	1	2	1	0	2	0	2	95	0
22LW PNL 7 UP-DIP 2	0,5	PYX	90	274	4	0	1	1	2	1	0	2	0	2	95	0
22LW PNL 7 UP-DIP 2	1,9	PYX	90	274	4	0	1	1	2	1	0	2	0	2	95	0
22LW PNL 7 UP-DIP 2	2,4	PYX	90	274	4	0	1	1	2	1	0	2	0	2	95	0
22LW PNL 7 UP-DIP 2	3	PYX	90	274	4	0	1	1	2	1	0	2	0	2	95	0
22LW PNL 7 UP-DIP 2	3,4	PYX	90	274	4	0	1	1	2	1	0	2	0	2	95	0
22LW PNL 7 UP-DIP 2	4,4	PYX	90	274	4	0	1	1	2	1	0	2	0	2	95	0
22LW PNL 7 UP-DIP 2	4,9	PYX	90	274	4	0	1	1	2	1	0	2	0	2	95	0
22LW PNL 7 UP-DIP 2	5,6	PYX	90	274	4	0	1	1	2	1	0	2	0	2	95	0
22LW PNL 7 UP-DIP 2	6,6	PYX	90	274	4	0	1	1	2	1	0	2	0	2	95	0
22LW PNL 7 UP-DIP 2	7,4	PYX	90	274	4	0	1	1	2	1	0	2	0	2	95	0
22LW PNL 7 UP-DIP 2	8,3	PYX	90	274	4	0	1	1	2	1	0	2	0	2	95	0
22LW PNL 7 UP-DIP 2	9,2	PYX	90	274	4	0	1	1	2	1	0	2	0	2	95	0

22LW PNL 7 UP-DIP 2	10,1	PYX	90	274	4	0	1	1	2	1	0	2	0	2	95	0
19LE PNL 7	0	PYX	90	246	4	0	1	1	2	1	0	2	0	2	95	0
19LE PNL 7	0,6	PYX	90	260	4	0	1	1	2	1	0	2	0	2	95	0
19LE PNL 7	0,8	PYX	90	260	4	0	1	1	2	1	0	2	0	2	95	0
19LE PNL 7	1,3	PYX	90	260	4	0	1	1	2	1	0	2	0	2	95	0
19LE PNL 7	2,1	PYX	90	260	4	0	1	1	2	1	0	2	0	2	95	0
19LE PNL 7	2,7	PYX	90	260	4	0	1	1	2	1	0	2	0	2	95	0
19LE PNL 7	4,2	PYX	20	260	4	0	1	1	2	1	0	2	0	2	95	0
19LE PNL 7	5,6	PYX	20	260	4	0	1	1	2	1	0	2	0	2	95	0
19LE PNL 6 up-dip	0	PYX	90	248	4	0	1	1	2	1	0	2	0	2	95	0
19LE PNL 6 up-dip	0,9	PYX	90	248	4	0	1	1	2	1	0	2	0	2	95	0
19LE PNL 6 up-dip	1,1	PYX	90	248	4	0	1	1	2	1	0	2	0	2	95	0
19LE PNL 6 up-dip	1,8	PYX	90	248	4	0	1	1	2	1	0	2	0	2	95	0
19LE PNL 6 up-dip	2,1	PYX	90	248	4	0	1	1	2	1	0	2	0	2	95	0
19LE PNL 6 up-dip	2,4	PYX	90	248	4	0	1	1	2	1	0	2	0	2	95	0
19LE PNL 6 up-dip	2,9	PYX	90	248	4	0	1	1	2	1	0	2	0	2	95	0
19LE PNL 6 up-dip	3,7	PYX	90	248	4	0	1	1	2	1	0	2	0	2	95	0
19LE PNL 6 up-dip	5,1	PYX	90	248	4	0	1	1	2	1	0	2	0	2	95	0
19LE PNL 6 up-dip	6	PYX	90	248	4	0	1	1	2	1	0	2	0	2	95	0
19LE PNL 6 up-dip	7,1	PYX	90	248	4	0	1	1	2	1	0	2	0	2	95	0
19LE PNL 6 up-dip	8,3	PYX	90	248	4	0	1	1	2	1	0	2	0	2	95	0
19LE PNL 5	0	PYX	90	240	4	0	1	1	2	1	0	2	0	2	95	0
19LE PNL 5	0,2	PYX	90	240	4	0	1	1	2	1	0	2	0	2	95	0
19LE PNL 5	0,5	PYX	90	240	4	0	1	1	2	1	0	2	0	2	95	0
19LE PNL 5	1,4	PYX	90	246	4	0	1	1	2	1	0	2	0	2	95	0
19LE PNL 5	2	PYX	90	246	4	0	1	1	2	1	0	2	0	2	95	0
19LE PNL 5	2,7	PYX	90	246	4	0	1	1	2	1	0	2	0	2	95	0
19LE PNL 5	3,4	PYX	90	246	4	0	1	1	2	1	0	2	0	2	95	0
19LE PNL 5	4,3	PYX	90	246	4	0	1	1	2	1	0	2	0	2	95	0
19LE PNL 5	5,1	PYX	90	246	4	0	1	1	2	1	0	2	0	2	95	0
19LE PNL 5	5,9	PYX	90	246	4	0	1	1	2	1	0	2	0	2	95	0
19LE PNL 5	6,7	PYX	90	246	4	0	1	1	2	1	0	2	0	2	95	0
19LE PNL 5	7,2	PYX	90	246	4	0	1	1	2	1	0	2	0	2	95	0
19LE PNL 5	9,5	PYX	90	246	4	0	1	1	2	1	0	2	0	2	95	0
19LE PNL 5	10,5	PYX	90	246	4	0	1	1	2	1	0	2	0	2	95	0
20 LE PNL 5	0	DYKE	40	230	3	0	1	1	2	1	0	2	0	2	95	0
20 LE PNL 5	1	DYKE	40	230	3	0	1	1	2	1	0	2	0	2	95	0
20 LE PNL 5	1,2	DYKE	40	230	3	0	1	1	2	1	0	2	0	2	95	0
20 LE PNL 5	1,4	DYKE	40	230	3	0	1	1	2	1	0	2	0	2	95	0
20 LE PNL 5	1,7	DYKE	40	230	3	0	1	1	2	1	0	2	0	2	95	0
20 LE PNL 5	2,3	DYKE	40	230	3	0	1	1	2	1	0	2	0	2	95	0
20 LE PNL 5	2,6	DYKE	40	230	3	0	1	1	2	1	0	2	0	2	95	0
20 LE PNL 5	2,9	DYKE	40	230	3	0	1	1	2	1	0	2	0	2	95	0
20 LE PNL 5	3,3	DYKE	40	230	3	0	1	1	2	1	0	2	0	2	95	0
20 LE PNL 5	4,2	DYKE	70	236	4	0	1	1	2	1	0	2	0	2	95	0
20 LE PNL 5	5,2	DYKE	70	236	4	0	1	1	2	1	0	2	0	2	95	0
20 LE PNL 5	5,8	DYKE	70	236	4	0	1	1	2	1	0	2	0	2	95	0
20 LE PNL 5	0	PYX	85	238	3	0	1	1	2	1	0	2	0	2	95	0
20 LE PNL 5	1,1	PYX	85	238	3	0	1	1	2	1	0	2	0	2	95	0
20 LE PNL 5	1,3	PYX	85	238	3	0	1	1	2	1	0	2	0	2	95	0
20 LE PNL 5	1,9	PYX	85	238	3	0	1	1	2	1	0	2	0	2	95	0
20 LE PNL 5	2,9	PYX	90	238	3	0	1	1	2	1	0	2	0	2	95	0
20 LE PNL 5	3,9	PYX	90	238	3	0	1	1	2	1	0	2	0	2	95	0
20 LE PNL 5	5,2	PYX	70	238	3	0	1	1	2	1	0	2	0	2	95	0
21LW PNL 4 DOWN-DIP	0	PYX	85	274	4	0	1	1	2	1	0	2	0	2	95	0

Processed Data (from Dips)																
Panel Name	Distance	Rock	Dip	Azimuth	P	E	Jr	M	H	Ja	S	T	HL	Joint Set	Tape Azimuth	Tape Plunge
21LW PNL 4 DOWN-DIP	0,8	PYX	85	274	4	0	1	1	2	1	0	2	0	2	95	0
21LW PNL 4 DOWN-DIP	1,1	PYX	85	274	4	0	1	1	2	1	0	2	0	2	95	0
21LW PNL 4 DOWN-DIP	1,4	PYX	85	274	4	0	1	1	2	1	0	2	0	2	95	0
21LW PNL 4 DOWN-DIP	1,7	PYX	85	274	4	0	1	1	2	1	0	2	0	2	95	0
21LW PNL 4 DOWN-DIP	2	PYX	85	274	4	0	1	1	2	1	0	2	0	2	95	0
21LW PNL 4 DOWN-DIP	2,2	PYX	85	274	4	0	1	1	2	1	0	2	0	2	95	0
21LW PNL 4 DOWN-DIP	3,1	PYX	85	274	4	0	1	1	2	1	0	2	0	2	95	0
21LW PNL 4 DOWN-DIP	3,8	PYX	85	274	4	0	1	1	2	1	0	2	0	2	95	0
21LW PNL 4 DOWN-DIP	4,1	PYX	85	274	4	0	1	1	2	1	0	2	0	2	95	0
21LW PNL 4 DOWN-DIP	4,6	PYX	85	274	4	0	1	1	2	1	0	2	0	2	95	0
21LW PNL 4 DOWN-DIP	5,3	PYX	85	274	4	0	1	1	2	1	0	2	0	2	95	0
23LW PNL 5	3,6	PYX	90	290	4	0	1	1	2	1	0	2	0	2	95	0
23LW PNL 5	6	PYX	70	286	4	0	1	1	2	1	0	2	0	2	95	0
23LW PNL 5	6,5	PYX	70	286	4	0	1	1	2	1	0	2	0	2	95	0
23LW PNL 5	6,8	PYX	70	286	4	0	1	1	2	1	0	2	0	2	95	0
23LW PNL 5	7,1	PYX	70	286	4	0	1	1	2	1	0	2	0	2	95	0
23LW PNL 7 DWN-DIP	0	PYX	90	260	4	0	1	1	2	1	0	2	0	2	95	0
23LW PNL 7 DWN-DIP	0,8	PYX	90	260	4	0	1	1	2	1	0	2	0	2	95	0
23LW PNL 7 DWN-DIP	1,8	PYX	90	260	4	0	1	1	2	1	0	2	0	2	95	0
23LW PNL 7 DWN-DIP	5,2	PYX	90	260	4	0	1	1	2	1	0	2	0	2	95	0
23LW PNL 7 DWN-DIP	6,1	PYX	90	260	4	0	1	1	2	1	0	2	0	2	95	0
21LE PNL 6 DWN DIP	0	PYX	90	266	4	0	1	1	2	1	0	2	0	2	95	0
21LE PNL 6 DWN DIP	0,5	PYX	90	266	4	0	1	1	2	1	0	2	0	2	95	0
21LE PNL 6 DWN DIP	0,7	PYX	90	266	4	0	1	1	2	1	0	2	0	2	95	0
21LE PNL 6 DWN DIP	1,7	PYX	90	266	4	0	1	1	2	1	0	2	0	2	95	0
21LE PNL 6 DWN DIP	2,2	PYX	90	266	4	0	1	1	2	1	0	2	0	2	95	0
21LE PNL 6 DWN DIP	3	PYX	90	266	4	0	1	1	2	1	0	2	0	2	95	0
21LE PNL 6 DWN DIP	3,6	PYX	90	266	4	0	1	1	2	1	0	2	0	2	95	0
21LE PNL 6 DWN DIP	4,9	PYX	90	266	4	0	1	1	2	1	0	2	0	2	95	0
21LE PNL 6 DWN DIP	5,8	PYX	90	266	4	0	1	1	2	1	0	2	0	2	95	0
21LE PNL 6 DWN DIP	6,2	PYX	90	266	4	0	1	1	2	1	0	2	0	2	95	0
21LE PNL 6 DWN DIP	6,7	PYX	90	266	4	0	1	1	2	1	0	2	0	2	95	0
21LE PNL 6 DWN DIP	7,7	PYX	90	266	4	0	1	1	2	1	0	2	0	2	95	0
21LE PNL 7 DWN DIP	0	PYX	85	274	4	0	1	1	2	1	0	2	0	2	95	0
21LE PNL 7 DWN DIP	0,5	PYX	85	274	4	0	1	1	2	1	0	2	0	2	95	0
21LE PNL 7 DWN DIP	0,8	PYX	85	274	4	0	1	1	2	1	0	2	0	2	95	0
21LE PNL 7 DWN DIP	1,7	PYX	85	274	4	0	1	1	2	1	0	2	0	2	95	0
21LE PNL 7 DWN DIP	2,7	PYX	85	274	4	0	1	1	2	1	0	2	0	2	95	0
21LE PNL 7 DWN DIP	3,4	PYX	85	274	4	0	1	1	2	1	0	2	0	2	95	0
21LE PNL 7 DWN DIP	4,3	PYX	85	274	4	0	1	1	2	1	0	2	0	2	95	0
21LE PNL 7 DWN DIP	4,8	PYX	85	274	4	0	1	1	2	1	0	2	0	2	95	0
21LE PNL 7 DWN DIP	5,4	PYX	85	274	4	0	1	1	2	1	0	2	0	2	95	0
21LE PNL 7 DWN DIP	6,3	PYX	85	274	4	0	1	1	2	1	0	2	0	2	95	0
21LE PNL 7 DWN DIP	6,8	PYX	85	274	4	0	1	1	2	1	0	2	0	2	95	0
21LE PNL 7 DWN DIP	7,9	PYX	85	274	4	0	1	1	2	1	0	2	0	2	95	0
21LE PNL 7 DWN DIP	9	PYX	85	274	4	0	1	1	2	1	0	2	0	2	95	0
21LE PNL 7 DWN DIP	10	PYX	85	274	4	0	1	1	2	1	0	2	0	2	95	0
23LE PNL 8 DWN-DIP	0	PYX	90	272	4	0	1	1	2	1	0	2	0	2	95	0
23LE PNL 8 DWN-DIP	0,8	PYX	90	272	4	0	1	1	2	1	0	2	0	2	95	0
23LE PNL 8 DWN-DIP	1,8	PYX	90	272	4	0	1	1	2	1	0	2	0	2	95	0
23LE PNL 8 DWN-DIP	2,2	PYX	90	272	4	0	1	1	2	1	0	2	0	2	95	0
23LE PNL 8 DWN-DIP	2,8	PYX	90	272	4	0	1	1	2	1	0	2	0	2	95	0
23LE PNL 8 DWN-DIP	3,9	PYX	90	272	4	0	1	1	2	1	0	2	0	2	95	0
23LE PNL 8 DWN-DIP	4,5	PYX	90	272	4	0	1	1	2	1	0	2	0	2	95	0
23LE PNL 8 DWN-DIP	5,2	PYX	90	272	4	0	1	1	2	1	0	2	0	2	95	0

Processed Data (from Dips)																
Panel Name	Distance	Rock	Dip	Azimuth	P	E	Jr	M	H	Ja	S	T	HL	Joint Set	Tape Azimuth	Tape Plunge
23LE PNL 8 DWN-DIP	6,2	PYX	90	272	4	0	1	1	2	1	0	2	0	2	95	0
23LE PNL 8 DWN-DIP	6,9	PYX	90	272	4	0	1	1	2	1	0	2	0	2	95	0
23LE PNL 8 DWN-DIP	7,8	PYX	90	272	4	0	1	1	2	1	0	2	0	2	95	0
23LE PNL 8 DWN-DIP	9,5	PYX	90	272	4	0	1	1	2	1	0	2	0	2	95	0
23LE PNL 8 DWN-DIP	10,3	PYX	90	272	4	0	1	1	2	1	0	2	0	2	95	0
19LE 3 down-dip	0	PYX	85	246	4	0	1	1	2	1	0	3	0	2	95	0
19LE 3 down-dip	0,6	PYX	85	246	4	0	1	1	2	1	0	3	0	2	95	0
19LE 3 down-dip	0,8	PYX	85	246	4	0	1	1	2	1	0	3	0	2	95	0
19LE 3 down-dip	2,5	PYX	85	246	4	0	1	1	2	1	0	3	0	2	95	0
19LE 3 down-dip	3,2	PYX	85	246	4	0	1	1	2	1	0	3	0	2	95	0
19LE 3 down-dip	4,3	PYX	85	246	4	0	1	1	2	1	0	3	0	2	95	0
19LE 3 down-dip	5,7	PYX	85	246	4	0	1	1	2	1	0	3	0	2	95	0
19LE 3 down-dip	6,6	PYX	85	246	4	0	1	1	2	1	0	3	0	2	95	0
19LE 3 down-dip	7,2	PYX	85	246	4	0	1	1	2	1	0	3	0	2	95	0
19LE 3 down-dip	8,1	PYX	85	246	4	0	1	1	2	1	0	3	0	2	95	0
19LE 3 down-dip	8,8	PYX	85	246	4	0	1	1	2	1	0	3	0	2	95	0
19LE 3 down-dip	10	PYX	85	246	4	0	1	1	2	1	0	3	0	2	95	0
19LE 4 UP-DIP	0	PYX	90	240	4	0	11	1	2	1	0	3	0	2	95	0
19LE 4 UP-DIP	0,8	PYX	90	240	4	0	1	1	2	1	0	3	0	2	95	0
19LE 4 UP-DIP	1,3	PYX	90	240	4	0	11	1	2	1	0	3	0	2	95	0
19LE 4 UP-DIP	3,1	PYX	90	240	4	0	1	1	2	1	0	3	0	2	95	0
19LE 4 UP-DIP	4,8	PYX	90	240	4	0	1	1	2	1	0	3	0	2	95	0
19LE 4 UP-DIP	6,2	PYX	90	240	4	0	11	1	2	1	0	3	0	2	95	0
19LE 4 UP-DIP	6,7	PYX	90	240	4	0	1	1	2	1	0	3	0	2	95	0
19LE 4 UP-DIP	7,7	PYX	90	240	4	0	1	1	2	1	0	3	0	2	95	0
19LE 4 UP-DIP	8,7	PYX	90	240	4	0	1	1	2	1	0	3	0	2	95	0
19LE 4 UP-DIP	9,5	PYX	90	240	4	0	1	1	2	1	0	3	0	2	95	0
19LE 4 UP-DIP	10	PYX	90	240	4	0	1	1	2	1	0	3	0	2	95	0
19LE 5 UP-DIP	0	PYX	90	260	4	0	1	1	2	1	0	3	0	2	95	0
19LE 5 UP-DIP	0,6	PYX	90	260	4	0	1	1	2	1	0	3	0	2	95	0
19LE 5 UP-DIP	1,1	PYX	90	260	4	0	1	1	2	1	0	3	0	2	95	0
19LE 5 UP-DIP	2,1	PYX	90	260	4	0	1	1	2	1	0	3	0	2	95	0
19LE 5 UP-DIP	3,3	PYX	90	260	4	0	1	1	2	1	0	3	0	2	95	0
19LE 5 UP-DIP	4,5	PYX	90	260	4	0	1	1	2	1	0	3	0	2	95	0
19LE 5 UP-DIP	6	PYX	90	260	4	0	1	1	2	1	0	3	0	2	95	0
19LE 5 UP-DIP	6,5	PYX	90	260	4	0	1	1	2	1	0	3	0	2	95	0
19LE 5 UP-DIP	7,5	PYX	90	260	4	0	1	1	2	1	0	3	0	2	95	0
19LE 5 UP-DIP	8,5	PYX	90	260	4	0	1	1	2	1	0	3	0	2	95	0
19LE 5 UP-DIP	9,5	PYX	90	260	4	0	1	1	2	1	0	3	0	2	95	0
19LE 7	0	PYX	90	248	4	0	1	1	2	1	0	3	0	2	95	0
19LE 7	0,2	PYX	90	248	4	0	1	1	2	1	0	3	0	2	95	0
19LE 7	0,4	PYX	90	248	4	0	1	1	2	1	0	3	0	2	95	0
19LE 7	0,7	PYX	90	248	4	0	1	1	2	1	0	3	0	2	95	0
19LE 7	1,1	PYX	90	248	4	0	1	1	2	1	0	3	0	2	95	0
19LE 7	1,7	PYX	90	248	4	0	1	1	2	1	0	3	0	2	95	0
19LE 7	2,2	PYX	90	248	4	0	1	1	2	1	0	3	0	2	95	0
19LE 7	2,8	PYX	90	248	4	0	1	1	2	1	0	3	0	2	95	0
19LE 7	3,3	PYX	90	248	4	0	1	1	2	1	0	3	0	2	95	0
19LE 7	3,9	PYX	90	248	4	0	1	1	2	1	0	3	0	2	95	0
19LE 7	4,4	PYX	90	248	4	0	1	1	2	1	0	3	0	2	95	0
19LE 7	5,3	PYX	90	248	4	0	1	1	2	1	0	3	0	2	95	0
19LE 7	5,8	PYX	90	248	4	0	1	1	2	1	0	3	0	2	95	0
19LE 7	6,7	PYX	90	248	4	0	1	1	2	1	0	3	0	2	95	0
19LE 7	7,5	PYX	90	248	4	0	1	1	2	1	0	3	0	2	95	0
19LE 7	8,4	PYX	90	248	4	0	1	1	2	1	0	3	0	2	95	0
19LE 7	9,1	PYX	90	248	4	0	1	1	2	1	0	3	0	2	95	0
19LE 7	10,2	PYX	90	248	4	0	1	1	2	1	0	3	0	2	95	0
19LE 7 UP-DIP	0	PYX	90	246	4	0	1	1	2	1	0	3	0	2	95	0
19LE 7 UP-DIP	0,2	PYX	90	246	4	0	1	1	2	1	0	3	0	2	95	0
19LE 7 UP-DIP	0,4	PYX	90	246	4	0	1	1	2	1	0	3	0	2	95	0
19LE 7 UP-DIP	1,5	PYX	90	246	4	0	1	1	2	1	0	3	0	2	95	0
19LE 7 UP-DIP	2,6	PYX	90	246	4	0	1	1	2	1	0	3	0	2	95	0
19LE 7 UP-DIP	3,2	PYX	90	246	4	0	1	1	2	1	0	3	0	2	95	0
19LE 7 UP-DIP	3,5	PYX	90	246	4	0	1	1	2	1	0	3	0	2	95	0
19LE 7 UP-DIP	4,1	PYX	90	246	4	0	1	1	2	1	0	3	0	2	95	0
19LE 7 UP-DIP	6,3	PYX	90	246	4	0	1	1	2	1	0	3	0	2	95	0
19LE 7 UP-DIP	6,7	PYX	90	246	4	0	1	1	2	1	0	3	0	2	95	0
19LE 7 UP-DIP	7,6	PYX	90	246	4	0	1	1	2	1	0	3	0	2	95	0
19LE 7 UP-DIP	8,3	PYX	90	246	4	0	1	1	2	1	0	3	0	2	95	0
19LE 7 UP-DIP	9	PYX	90	246	4	0	1	1	2	1	0	3	0	2	95	0

Processed Data (from Dips)																
Panel Name	Distance	Rock	Dip	Azimuth	P	E	Jr	M	H	Ja	S	T	HL	Joint Set	Tape Azimuth	Tape Plunge
19LE 7 UP-DIP	10,3	PYX	90	246	4	0	1	1	2	1	0	3	0	2	95	0
21 West 002	1,6	PYX	90	106	4	2	1	1	2	1	0	1	0	2	5	0
22E PNl 4E	0	PYX	85	246	3	1	1	1	2	1	1	1	0	2	95	0
22E PNl 4E	3,2	PYX	90	252	3	1	1	1	2	1	1	1	1	2	95	0
20E Up-dip	0,2	PYX	90	174	3	0	1	1	2	1	0	1	0	2	5	0
19E-5 up-dip	0,3	DYKE	70	248	4	1	1	1	2	1	0	2	0	3	95	0
19E-5 up-dip	0,7	DYKE	65	248	4	1	1	1	2	1	0	2	0	3	95	0
19E-5 up-dip	1,2	DYKE	65	248	4	1	1	1	2	1	0	2	0	3	95	0
19E-5 up-dip	2,2	DYKE	65	248	4	1	1	1	2	1	0	2	0	3	95	0
19E-5 up-dip	4,9	DYKE	65	250	4	1	1	1	2	1	0	2	0	3	95	0
19E-5 up-dip	6	DYKE	85	250	4	1	1	1	2	1	0	2	0	3	95	0
19LE PNL5	5,6	DYKE	70	166	4	0	1	1	2	1	0	2	0	3	5	0
21LW PNL 3	0	PYX	55	270	3	0	1	1	2	1	0	2	0	3	5	0
21LW PNL 4	3,2	PYX	45	252	4	0	1	1	2	1	0	2	0	3	95	0
21LW PNL 3 back	1,8	PYX	55	300	4	0	1	1	2	1	0	2	0	3	95	0
21LW PNL 6	4,5	DYKE	65	240	4	0	1	1	2	1	0	3	0	3	5	0
22 LE PNL 6 UP DIP 16D	0	PYX	30	268	4	0	1	1	2	1	0	2	0	3	95	0
22 LE PNL 6 UP DIP 16D	0,6	PYX	30	268	4	0	1	1	2	1	0	2	0	3	95	0
22 LE PNL 6 UP DIP 17D	0	DYKE	15	288	4	0	1	1	2	1	0	2	0	3	95	0
22 LE PNL 6 UP DIP 17D	1,2	DYKE	15	288	4	0	1	1	2	1	0	2	0	3	95	0
22 LE PNL 6 UP DIP 17D	1,8	DYKE	90	300	4	0	1	1	2	1	0	2	0	3	95	0
22 LE PNL 6 UP DIP 17D	2,5	DYKE	50	288	4	0	1	1	2	1	0	2	0	3	95	0
22 LE PNL 6 UP DIP 17D	4	DYKE	65	298	4	0	1	1	2	1	0	2	0	3	95	0
22 LE PNL 6 UP DIP 17D	10	DYKE	90	270	4	0	1	1	2	1	0	2	0	3	95	0
22LW PNL 4	0	PYX	50	210	4	0	1	1	2	1	0	2	0	3	5	0
22LW PNL 4	1,9	DYKE	50	210	4	0	1	1	2	1	0	2	0	3	5	0
22LW PNL 4	2,1	PYX	50	210	4	0	1	1	2	1	0	2	0	3	5	0
22LW PNL 4	2,5	PYX	50	210	4	0	1	1	2	1	0	2	0	3	5	0
22LW PNL 4	4	PYX	50	210	4	0	1	1	2	1	0	2	0	3	5	0
22LW PNL 4	5,4	PYX	50	210	4	0	1	1	2	1	0	2	0	3	5	0
22LW PNL 4	6,2	PYX	50	210	4	0	1	1	2	1	0	2	0	3	5	0
22LW PNL 4	6,6	PYX	45	210	4	0	1	1	2	1	0	2	0	3	5	0
22LW PNL 4	7,6	PYX	45	210	4	0	1	1	2	1	0	2	0	3	5	0
22LW PNL 4 DOWN DIP	0	PYX	30	246	4	0	1	1	2	1	0	2	0	3	95	0
22LW PNL 4 DOWN DIP	0,5	PYX	30	246	4	0	1	1	2	1	0	2	0	3	95	0
22LW PNL 4 DOWN DIP	2,6	PYX	30	246	4	0	1	1	2	1	0	2	0	3	95	0
22LW PNL 4 DOWN DIP	2,9	PYX	50	240	4	0	1	1	2	1	0	2	0	3	95	0
22LW PNL 4 DOWN DIP	3,8	PYX	50	240	4	0	1	1	2	1	0	2	0	3	95	0
21 West 002	5,4	PYX	45	340	4	0	14	1	2	1	0	1	0	3	5	0
21 West 003	2,3	PYX	60	234	4	0	0,5	1	2	1	0	2	0	3	5	0
21 West 003	9,1	PYX	55	108	1	1	0,5	1	2	1	1	0	3	3	5	0
22E PNl 4E	2,3	PYX	20	280	4	1	1	1	2	1	0	1	0	3	95	0
22E PNl 4E	4,7	PYX	45	182	4	1	1	1	2	1	1	1	1	3	95	0
20E Up-dip	0	PYX	60	272	4	1	1	1	2	1	0	1	0	3	5	0
20E Up-dip	2,1	DYKE	15	208	3	0	1	1	2	1	0	1	2	3	5	0

APPENDIX D. Dips Information

Document Name:
MSc Project 2

Document Title:

Document Setup:
Traverses: 0
Data is DIP/DIPDIRECTION format
Magnetic Declination (E pos): -17.85 degrees
Multiple Data Flag (Quantity) is OFF
1 Extra Data Columns
1113 Poles from 1113 Entries

Global Mean Vector:
Unweighted TREND/PLUNGE = 2.73166/2.9907
Weighted TREND/PLUNGE = 2.73166/2.9907
Unweighted DIP/DIPDIRECTION = 87.0093/182.732
Weighted DIP/DIPDIRECTION = 87.0093/182.732

Set Planes (via Add Set Options):

ID	*TREND/PLUNGE*	*DIP/DIPDIRECTION*	*LABEL*
2m	59.4/0.718476	89.2815/239.4	
2w	59.4/0.718476	89.2815/239.4	
3m	45.0116/45.9715	44.0285/225.012	
3w	45.0116/45.9715	44.0285/225.012	
1m	335.784/0.252107	89.7479/155.784	
1w	335.784/0.252107	89.7479/155.784	

Set Statistics
Set: 2m (UNWEIGHTED)
349 Poles from 349 Entries
Fisher's K = 41.0526
68.26% Variability Limit = 13.5793 degrees
95.44% Variability Limit = 22.3643 degrees
99.74% Variability Limit = 31.2393 degrees
68.26% Confidence Limit = 0.734161 degrees
95.44% Confidence Limit = 1.20429 degrees
99.74% Confidence Limit = 1.67205 degrees
Set: 2w (WEIGHTED)
349 Poles from 349 Entries
Fisher's Kw = 41.0526
68.26% Variability Limit = 13.5793 degrees
95.44% Variability Limit = 22.3643 degrees
99.74% Variability Limit = 31.2393 degrees
68.26% Confidence Limit = 0.734161 degrees
95.44% Confidence Limit = 1.20429 degrees
99.74% Confidence Limit = 1.67205 degrees

APPENDIX E. Sort Encapsulation Test

Sample Number	Pull-out Load (kN)	Encapsulated Length (mm)	Hole diameter	drill bit diameter	spin time
1	147.15	300	30.5	28	10
2	147.15	300	30.5	28	10
3	127.53	300	30.2	28	10
4	137.34	300	30.2	28	10
5	147.15	300	30.2	28	10
6	137.34	300	30.2	28	10
7	107.91	300	30.2	28	18
8	137.34	300	30.2	28	10
9	147.15	300	30.2	28	10
10	117.72	300	30.2	28	10

Sibanye Pt
we are one

A statistical analysis was done to quantify a load that can be allocated to the bolt/resin system with a 90% confidence that any given bolt installation will not fall below the design load. This statistical analysis was done based on a single tailed normal distribution curve. Samples tested were treated as samples and not a population. Table 2 shows that ***117.82 KN*** can be used as a design load if the resin/bolt system be used underground.

Table 2: Statistical Analysis

Unit	Value	Comment
Mean Load (kN)	135.378	
Std Dev (kN)	13.72	Sample deviation
Confidence level	1.28	90% Confidence 1.28 std deviations single tail normal distribution curve
300mm Design load (kN)	117.82	
kN/mm	0.39	
Critical bond length (mm)	299.75	Based on 12tonne 18mm rebar tensile strength (statistical strength)

Table 1: Short Encapsulation test results

Sample Number	Pullout Load (kN)	Encapsulated Length (mm)	Hole diameter	drill bit diameter	spin time
1	110	300	35.2	33	10
2	180	300	35.2	33	10
3	50	300	35.2	33	10
4	180	300	35.2	33	10
5	200	300	35.2	33	10
6	70	300	35.2	33	8
7	210	300	35.2	33	10
8	220	300	35.2	33	10
9	190	300	35.2	33	10
10	130	300	35.2	33	10

A statistical analysis was done to quantify a load that can be allocated to the bolt/resin system with a 90% confidence that any given bolt installation will not fall below the design load. This statistical analysis was done based on a single tailed normal distribution curve excluding outliers samples nr 3 and 6. These were excluded from the analysis because the resin was not confined to the intended 300mm encapsulation length and it is reasonably assumed that the bond was not full column. Samples tested were treated as samples and not a population. Table 2 shows that ***213.80 KN*** can be used as a design load for a 500mm bond length.

Table 2: Statistical Analysis

Mean Load (kN)	177.5	
Std Dev (kN)	38.45	Sample deviation
Confidence level	1.28	90% Confidence 1.28 std deviations single tail normal distribution curve
300mm Design load (kN)	128.28	
kN/mm	0.43	
500mm Design load (kN)	213.80	
Critical bond length (mm)	537.88	Based on 230kN 22mm rebar tensile strength

APPENDIX F. Company Specifications

High-tensile Rockfall Protection Netting DELTAX® G80/3

DELTAX® high-tensile rockfall protection netting

Mesh shape:	rhomboid
Diagonal:	x · y = 103 · 180 mm (+/-3%)
Mesh width:	D_i = 80 mm (+/-3%)
Angle of mesh:	ε ca. 49 degrees
Total height of mesh:	h_{tot} = 12.5 mm (+/-1.5 mm)
Clearance of mesh:	h_i = 6.5 mm (+/-1.5 mm)
No. of meshes longitudinal:	n_l = 5.6 pcs/m
No. of meshes transversal:	n_q = 9.7 pcs/m

Load capacity

Tensile strength of mesh longitudinal:	z_l = 110 kN/m'
Tensile strength of mesh transversal:	z_q = 45 kN/m'

DELTAX® steel wire

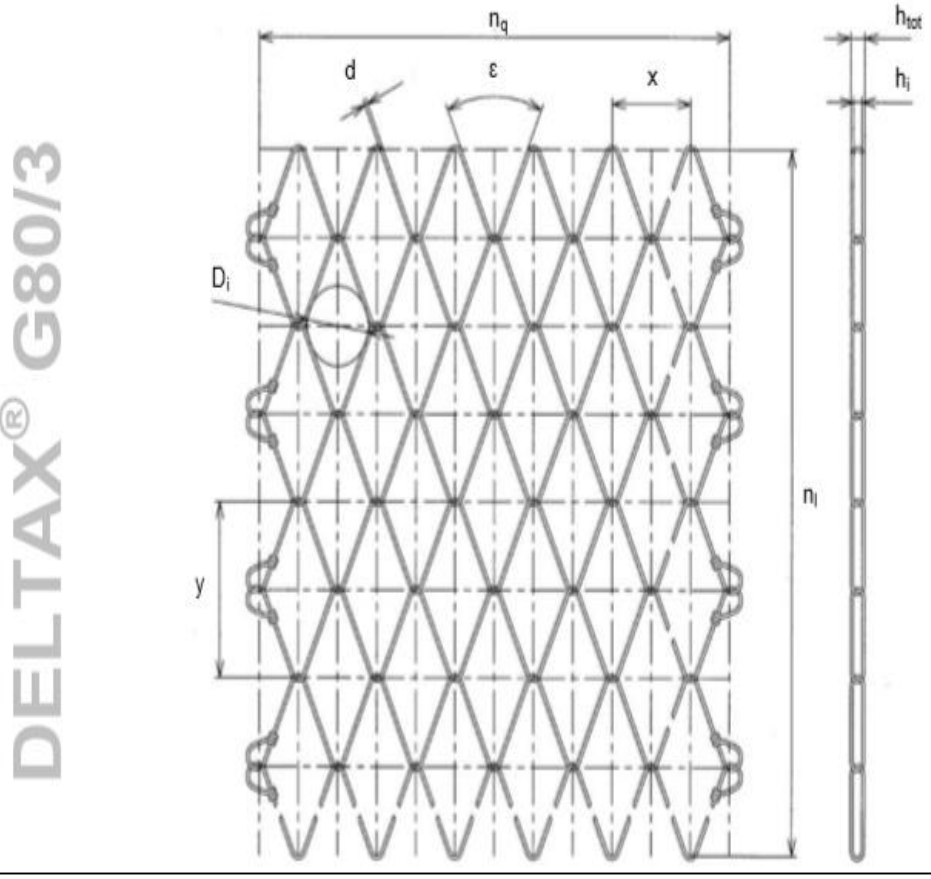
Wire diameter:	d = 3.0 mm
Tensile strength:	$f_t \geq$ 1'770 N/mm2
Material:	high-tensile steel wire
Tensile strength of a wire:	Z_w = 12.5 kN

DELTAX® corrosion protection

Corrosion protection:	GEOBRUGG ULTRACOATING®
Compound:	95% Zn / 5% Al + special add-on
Coating:	150 g/m²

DELTAX® mesh

Roll width:	b_{Roll} = 3.5 m
Roll length:	l_{Roll} = 30 m (on request until 100 m)
Total surface per roll:	A_{Roll} = 105 m²
Weight per m²:	g = 1.45 kg/m²
Weight per mesh roll:	G_{Roll} = 152 kg
Mesh edges:	mesh ends knotted

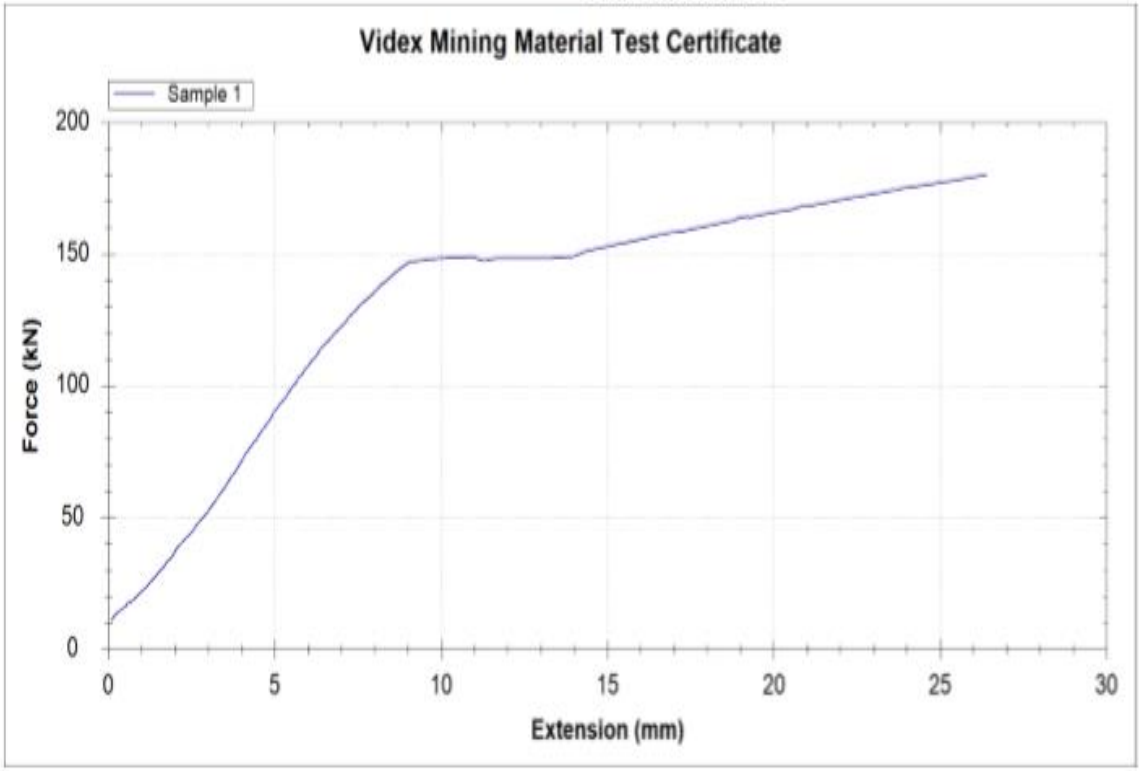


DELTAX® G80/3

Certificate No :V1801744

VIDEX MINING PRODUCTS
A Division of videx wire products (pty)Ltd
(Registration Number: 1984/09466/07)

REPORT No:V1801744
CUSTOMER:Aquarius
PRODUCT:1.5m Resin Bolt Y18 Din 20 LH +
PRODUCT+:DDE + Sw + S/Pin Nut
CAST NUMBER:192393 (040919N5)
TORQUE TEST:4.5mm pin breaks at 90Nm
TESTED BY:Onkgopotse Khwinana
COMMENT:Nut running freely after torque test
Specification:Tension test
Test Date:2019/09/04
Test Time:15:51:02
Finish Date:2019/09/04
Finish Time:15:52:40



Test Results

Diameter	**18** mm
Peak Force	**180.30152** kN
MaxStress1	**708.540201357586** mpa
GaugeLength	**956** mm
Extension@140kN	**8.33** mm
Extension@150kN	**14.13** mm



Figure 1. Roof bolt installed in the testing machine

3. TEST RESULTS

The results of the tensile tests carried out on roof bolts are summarised in Table 1.

Table 1. Maximum loads for the roof bolts (Ø18 mm x 1 m)

Specimen	Maximum load carried (kN)	Mode of failure
1	177	The bolts fractured as shown in Figure 2.
2	183	
3	182	
Mean	180.7	
Standard deviation	3.2	



Figure 1. TC bolt installed in the testing machine

3. TEST RESULTS

The results of the tensile tests carried out on TC bolts are summarised in Table 1.

Table 1. Maximum loads for the TC bolts (Ø22 mm x 1 m)

Specimen	Maximum load carried (kN)	Mode of failure
1	232	The bolts fractured as shown in Figure 2.
2	232	
3	233	
4	232	
5	230	
Mean	**231.8**	
Standard deviation	**1.1**	

TempRite

Yielding Temporary Prop





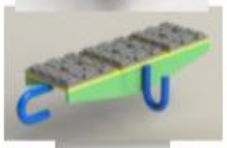
- *Steel prop*
- *Lightweight*
- *Very quick installation*
- *Remote release*
- *Rust indicator*
- *All components are durable*
- *Reliable yield loads, based on steel deformation*

- No pin holes are required in the prop barrel eliminating any stress points. the tube wall can therefore be thinner resulting in a lighter prop
- The Prop is easy to install in a one-man operation – no pins to find holes
- The prop is set using a conventional cam system – well known in the mining industry
- The prop can be removed remotely using a cable and spanner on the cams in a conventional manner.
- The prop can easily be retracted by turning up-side-down and giving a light tap to release the locking mechanism
- The TempRite can be supplied with a variety of headboards depending upon customer requirements. Netting hooks are included in headboard designs.
- The prop has a built in yield mechanism to protect the workforce during closure conditions. It will not buckle under closure resulting in loss of load. Yield loads are set between 80 to 100kN

The TempRite is backed up by Timrite's trained team of professional instructors, sales managers and technical managers



Steel Tri-headboard



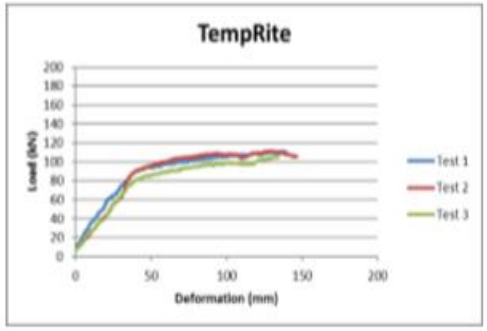
Steel 400 x 125cm headboard



Steel 125 x 125cm headboard



NAME	LENGTH (m)	
STICKER	Min (m)	Max (m)
TR1	0.65	1.0
TR2	0.9	1.35
TR3	1.1	1.55
TR3A	1.15	1.7
TR4	1.35	2.15
TR5	1.65	2.65
TR5A	1.65	2.65
TR6	2.15	3.0
TR7	3.15	4.0



www.timrite.co.za
info@timrite.co.za

Rockstop®

Description

The Rockstop range of safety nets are used as areal coverage to protect miners from falls of ground occurring between installed permanent and temporary support. The nets can be suspended from temporary supports adjacent to the work face, such as temporary mechanical jacks, and connected to previously installed rockbolts and elongates. The installation of the nets allows miners to move within the work area with the additional protection of the nets improving safety in the work area. Rockstop nets are made from webbing which is treated with a waterproof chemical ensuring that they remain lightweight and easy to handle even when wet. Rockstop nets are designed to safely arrest a 2 tonne mass dropped from a 300 mm height with minimal deflection. Installation accessories such as tensioners, S-hooks and hook installation tools are available to facilitate the safe installation of nets.





